

Accepted Manuscript

Purine-benzimidazole hybrids: Synthesis, single crystal determination and *in vitro* evaluation of antitumor activities

Alka Sharma, Vijay Luxami, Kamaldeep Paul



PII: S0223-5234(15)00132-4

DOI: [10.1016/j.ejmech.2015.02.036](https://doi.org/10.1016/j.ejmech.2015.02.036)

Reference: EJMECH 7718

To appear in: *European Journal of Medicinal Chemistry*

Received Date: 20 September 2014

Revised Date: 23 December 2014

Accepted Date: 19 February 2015

Please cite this article as: A. Sharma, V. Luxami, K. Paul, Purine-benzimidazole hybrids: Synthesis, single crystal determination and *in vitro* evaluation of antitumor activities, *European Journal of Medicinal Chemistry* (2015), doi: 10.1016/j.ejmech.2015.02.036.

This is a PDF file of an unedited manuscript that has been accepted for publication. As a service to our customers we are providing this early version of the manuscript. The manuscript will undergo copyediting, typesetting, and review of the resulting proof before it is published in its final form. Please note that during the production process errors may be discovered which could affect the content, and all legal disclaimers that apply to the journal pertain.

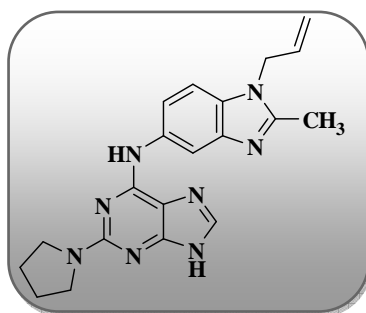
Purine-benzimidazole hybrids: Synthesis, single crystal determination and *in vitro* evaluation of antitumor activities

Alka Sharma, Vijay Luxami, Kamaldeep Paul*

School of Chemistry and Biochemistry, Thapar University, Patiala-147004 INDIA

** To whom corresponding should be addressed. Tel.: +91-94656-70595; Fax: +91-175-236-4498;*

E-mail address: kpaul@thapar.edu (K.Paul)



60 Human Cancer Cell Lines

GI₅₀ = 18.12 μM

Aurora-A Kinase Inhibitor

IC₅₀ = 0.01 μM

Purine-benzimidazole hybrids: Synthesis, single crystal determination and *in vitro* evaluation of antitumor activities

Alka Sharma, Vijay Luxami, Kamaldeep Paul*

School of Chemistry and Biochemistry, Thapar University, Patiala-147004 INDIA

**To whom corresponding should be addressed. Tel.: +91-94656-70595; Fax: +91-175-236-4498;*

E-mail address: kpaul@thapar.edu (K. Paul)

Abstract

In an effort to identify novel compounds for the treatment of cancer, a diverse array of potential bioactive hybrid, purine-benzimidazole was synthesized in good yields through nucleophilic substitution at C6 position of purine ring with versatile cyclic amines at C2 position. The structures of newly prepared compounds were confirmed by IR, ¹H, ¹³C NMR, mass spectroscopy and, in case of **19**, by single crystal X-ray diffraction analysis. The newly synthesized compounds were evaluated against 60 human tumour cell lines at one dose concentration level. Compound **6** exhibited significant growth inhibition and was evaluated as 60 cell panel at five dose concentration levels. Compound **6** proved to be 1.25 fold more active than the positive control 5-FU, with GI₅₀ value of 18.12 μM (MG-MID). Interaction of the compounds with Aurora-A enzyme involved in the process of propagation of cancer, has also been investigated. Compound **6** showed selectivity towards Aurora-A kinase inhibition with IC₅₀ value of 0.01 μM. Molecular docking studies in the active binding site provided theoretical support for the experimental biological data acquired.

Keywords: Purine, Benzimidazole, X-ray structure, Antitumor activity, Aurora kinase inhibitor, Molecular modeling

1. Introduction

Cancer is becoming a major health problem in developing and undeveloped countries [1,2]. Although major advances have been made in the chemotherapeutic management of some patients, the continued commitment to the laborious task of discovering new anticancer agents remains critically important. In the course of identifying various chemical substances which may serve as leads for designing novel antitumor agents, we are particularly interested in the present work of molecular hybridizations with purine and

benzimidazole derivatives which have been identified as a new class of cancer chemotherapeutic agents with significant therapeutic efficacy against solid tumors [3]. It is well known that purine derivatives are potent inhibitors of Aurora kinase [4], cyclin dependent kinase (CDK) [5], epidermal growth factor receptor (EGFR) and vascular endothelial growth factor receptor (VEGFR) [6]. Consequently, various approaches have been adopted to enhance the potency and selectivity of these inhibitors. These efforts led to discovery of many drugs such as Olomoucine, Roscovitine, R-CR8 and Dinaciclib (Figure 1) that have also maintained selectivity towards various kinases. Olomoucine and Roscovitine are first discovered CDK inhibitors while the optically pure R-enantiomer of Roscovitine (Seliciclib) is currently being evaluated as an oncology drug candidate in patient diagnosed with non small cell lung cancer and nasopharyngeal cancer [7] or other malignancies [8]. The anti-HIV/HBV drugs *abacavir* and *penciclovir* are some of the purine drugs, also available presently in the market [9]. Similarly, benzimidazole and its derivatives are categorized as the important pharmacophores and privileged sub-structures in medicinal chemistry owing to their involvement as a key component for various biological activities [10]. Benzimidazoles are among the important heterocyclic compounds that found in natural and non-natural products such as vitamin B12, marine alkaloid kealiquinone [11] etc. Some of their derivatives are marketed as anti-fungal agent such as Carbendazim [12], anti-helminthic agents such as Mebendazole and Thiabendazole [13] and anti-psychotic drug such as Pimozide [14].

Figure 1

In view of the previous rationale and in continuation of an ongoing program aiming at finding new structure leads with potential chemotherapeutic activities using molecular hybridization [15], new series of molecular hybrids using purine and benzimidazole have been synthesized and screened for *in vitro* antitumor activity as well as Aurora A kinase inhibitors. These series comprises the derived 2,6-disubstituted purine pharmacophore that are structurally related to Olomoucine and Roscovitine. In the present study, the substitution pattern at the 2,6-disubstituted purine and benzimidazole pharmacophore were selected so as to confer different electronic environment that would affect the activity of target molecules. SAR, QSAR and molecular modelling studies were used to identify the structural features required for the antitumor properties of these new hybrid series.

2. Results and Discussion

2.1. Chemistry

The synthetic strategy to prepare the purine-benzimidazole hybrids (**3a-d** and **4-19**) has been depicted in scheme 1. The target compounds were achieved in three steps using 3,4-dihydro-1*H*-purin-2,6-(5*H*,9*H*)-dione as starting material. Refluxing of 3,4-dihydro-1*H*-purin-2,6-(5*H*,9*H*)-dione with phosphorus oxychloride in the presence of triethylamine for 5 h afforded 2,6-dichloropurine (**1**). Treatment of compound **1** with **2a** [15] in the presence of isopropyl alcohol (IPA) at room temperature for 24 h gave **3a** in 79% yield. Similarly, compound **1** was also treated with **2b-d** under the same reaction conditions to give compounds **3b-d** with 47-94% yields. Refluxing of compounds **3a-d** with different secondary amines in ethanol for 48 h and after purification with column chromatography gave pure compounds **4-19** with moderate to excellent yields (Table-1). All the synthesized compounds were well characterized by IR, ¹H, ¹³C NMR, mass spectroscopy (supporting information) and in case of compound **19**, by single crystal X-ray diffraction analysis (Figure 2).

Scheme 1

Table 1

Figure 2

2.2. *In vitro* anticancer screening

All the synthesized compounds were submitted to National Cancer Institute (NCI) disease-oriented human cell lines for *in-vitro* evaluation as antitumor activities (Table S1). Fourteen compounds (**3a-d**, **4**, **6-11**, **16**, **18-19**) were evaluated against 60 cell lines at a single dose of 10 μ M concentration [16-19] and their outputs were reported as a mean graph of the percent growth of treated cells, and presented as percentage growth inhibition (GI %). Compound **6** exhibited significant growth inhibition and was evaluated for further 60 cell panel at five dose concentration levels.

Preliminary *in vitro* antitumor screening was revealed that only compounds belonging to the series **4-11** showed significant inhibition for most of cancer cell lines. The percentage of inhibition for cancer cells were more than 50% in a number of the tested derivatives. On the contrary, compounds **18** and **19** showed weak activities compared with other compounds and percentage of inhibition did not reach 30% except one or two cell lines. These variations

could be correlated to the difference in positions of allyl or butyl group on the benzimidazole moiety in which the distance between the core purine moiety and alkyl chains of benzimidazole are important factor for affecting antitumor activity. Compound **6** proved to be active towards lung cell NCI-H60 with GI value of 99.63%; colon cells HT29 and KM12 with GI values of 87.58% and 86.91%; melanoma cell MDA-MB-435 with GI value of 90.84%; renal cells A498, ACHN and TK-10 with GI values of 98.65%, 82.19% and 88.17% respectively. Meanwhile, compound **9** showed selectivity towards leukemia cell MOLT-4 with GI value of 90.95%; CNS cell SNB-75 with GI value of 88.56%; ovarian cell OVCAR-4 with GI value of 80.98% and breast cells BT-549 and T-47D with GI values of 82.04% and 93.22% respectively (Supporting Information).

From the above data, it is clear that compound **6** is the most active member of the series. Consequently, this active compound was carried over and tested against a panel of different tumor cell lines at five dose concentration level (Table S2). Compound **6** showed specificity towards colon, CNS and ovarian cancer cell lines with GI_{50} values of 3.16, 2.00 and 1.34 μM respectively. MG-MID revealed that compound **6** is 1.25 fold more active than 5-fluorouracil (5-FU), with GI_{50} value of 18.12 μM (Table-2).

Table 2

2.3. Aurora-A kinase inhibition of compounds

Based on the anti-cancer activities of the compounds, it was desirable to investigate some of the compounds for probable cellular targets. Interactions of compounds with Aurora-A enzyme involved in the process of propagation of cancer, has been investigated with the help of enzyme immunoassay using Aurora-A kinase inhibitor screening kit [20]. It has been shown that compounds **3a** and **5** displayed least activity towards Aurora A with IC_{50} values of 8.00 and 8.50 μM respectively. Amines substitution at C2 position of purine with morpholine and pyrrolidine resulted compounds **4** and **6** respectively that showed excellent inhibitory activity towards Aurora-A with IC_{50} values of 0.02 and 0.01 μM (Table-3). Substitution of **3a** with piperidine (compound **5**) decreased the inhibitory activity while substitution with 4-methylpiperazine increased the Aurora A inhibitory activity with IC_{50} value of 0.072 μM . Replacement of N-allyl group with N-butyl group (compound **3b**) of benzimidazole resulted in increase in potency with IC_{50} value of 0.075 μM . Substitution of **3b** at C2 position of purine with pyrrolidine resulted in almost 10 fold decrease in inhibitory activity. Therefore, it seems that the compound **6** under present investigation probably target

Aurora-A for exhibiting best anti-cancer activity. Ligand efficiency (LE) has also been determined for these compounds that indicated the higher efficiency of compound **6** with LE = 0.39 for binding to the enzyme. The partition coefficient of the molecules was also studied in octanol/water systems for the determination of log P values by shake-flask method [21] (Supporting Information). It has been indicated that compound **6** showed higher log P value that supported the dependency of lipophilicity with higher activity of this compound towards Aurora A inhibition and cancer cell lines.

Table 3

2.4. Quantitative structure-activity relationship (QSAR)

IC₅₀ values of purine-benzimidazole hybrid compounds were first calculated by Aurora-A kinase assay kit. Geometries of these compounds were refined by means of semi empirical method PM3 using QSARINS Software [22]. We have calculated q^2 , r^2 , RMSE_{cv}, RMSE_{tr} and F using log P, heat of formation, molar refractivity and steric energy to get equation 1. With the addition of each parameter, there is improvement of the correlation coefficient. So on collectively using these four parameters into a multiple linear regression analysis, we obtained much improved in the correlation coefficient (eq. 1)

$\log(\text{IC}_{50}) = 25.4623 + 14.2235 \log P + 0.1660 \text{ heat of formation} - 0.3082 \text{ molar refractivity} + 1.1124 \text{ steric energy}$

$n = 7 \quad q^2_{\text{LOO}} = 0.9185, r^2 = 0.994, \dots\dots\dots\text{eq.(1)}$

RMSE_{cv} = 1.0444, RMSE_{tr} = 0.2825, F = 83.3054

Here, n - number of samples, r^2 - correlation coefficient, q^2 - cross validated, obtained by leave one out method and F - fisher statistics.

Equation 1 appears to be the best QSAR model obtained by the multiple linear regression analysis, considered significant for the activity (Figure 3). Eq (1) showed the positive contribution of log P and steric energy indicating the importance of lipophilicity and steric hindrance of purine and benzimidazole rings for the activity of hybrid.

Figure 3

2.5. Structure-activity relationship (SAR)

Structure-activity correlation, based on the number of cancer cell lines and Aurora A kinase inhibitors revealed that the nature of the substituents at C2- and C6-positions of purine affected the biological functions. Regarding 60 human tumor cell line studies, compounds **4**,

6-11 showed comparatively higher activity than their isomers **16, 18-19** suggested that there is much difference in antitumor activity with orientations of alkyl chain of benzimidazole. In the first series of compounds, when the allyl group is replaced with butyl group, a comparable affinity is found (compare **3a** and **3b**), but when chloro of **3a** is constrained in a cyclic morpholine system (compound **4**), some activity is increased although other rings are well tolerated as illustrated by pyrrolidine (**6**) and 4-methylpiperazine (**7**) analogues and former showed higher activity than later. Similarly, substitution at C2-position of **3b** with piperidine leading to compound **9** that has increased the activity while decrease in activity was observed with morpholine, pyrrolidine and 4-methylpiperazine (**8, 10-11**). Another series of compounds **16, 18-19**, substitution of **3d** with morpholine (**16**) increases the activity while pyrrolidine (**18**) and 4-methylpiperazine (**19**) decreases the activity. SAR study of Aurora A kinase inhibitory activity was also demonstrated that substitution of **3a** with morpholine and pyrrolidine showed almost 400-fold and 800-fold increase in activity while replacement of these cyclic substituent with 4-methylpiperazine decreases the affinity slightly (compound **7**). These studies indicated that substitution of the purine heterocycle with various cyclic secondary amines leads to highly potency towards 60 human cancer cell line activities as well as Aurora A kinase inhibitions.

2.6. Molecular docking studies

Molecular docking studies were also carried out for compound **6**, which has been proved to be most active compound. Although the cellular targets were not defined in the experimental anticancer investigation of these molecules, to look into the possible interactions at the enzymatic level, we have carried out the docking studies [23] of compound **6** in the active sites of Aurora-A kinase (PDB ID 2WTV and 2XNE) using builder tool kit of software package ArgusLab 4.0.1 (www.arguslab.com) [24].

Docking of compound **6** in the active site of Aurora-A (2WTV) showed hydrogen bonding interaction of N atom of five membered purine moiety in the active site of His644 ($d = 2.48 \text{ \AA}$, $d = 2.09 \text{ \AA}$ and $d = 2.79 \text{ \AA}$) amino acid residue. Linker NH group of purine and benzimidazole showed H-bonding interaction with Asp622 ($d = 2.39 \text{ \AA}$) amino acid residue and nitrogen atom of benzimidazole moiety showed H-bonding interaction with Ser625 ($d = 2.59 \text{ \AA}$) amino acid residue. Pyrrolidine moiety also showed hydrogen bonding of N atom with active site of Arg626 ($d = 1.87 \text{ \AA}$) amino acid residue (Figure 4). Therefore, docking of compound **6** in the active site of these enzymes indicated the probable mode of action for anticancer activities.

The binding mode of purine-benzimidazole-based kinase inhibitors were also elucidated by co-crystallisation of Aurora-A (2XNE) and compared with isoform Aurora B/C. The N9 of purine in compound **6** showed hydrogen bonding with carbonyl group of Leu215 ($d = 2.60$ Å), amino groups of Leu 264 ($d = 2.81$ Å) and Gly216 ($d = 1.91$ Å) in the hinge region of the kinase. Purine N7 is hydrogen bonded to the amino group of Gly216 ($d = 2.36$ Å) and the nitrogen atom of pyrrolidine to the carbonyl and amino groups of Thr217 ($d = 2.39$ Å and $d = 2.32$ Å) as shown in figure 5. N1 atom of purine also showed hydrogen bonding with carbonyl group Thr217 ($d = 2.66$ Å). Linker NH group of benzimidazole and purine showed hydrogen bonding interaction with amino group of Thr217 ($d = 2.91$ Å). The benzimidazole with allyl chain of the inhibitor sits in a hydrophobic pocket formed the gatekeeper residues Val147, Glu211, Lys162 and Ala160. Importantly, the pyrrolidine moiety substituted at C2 position of purine resides in close proximity to Val218 of Aurora-A (3.3 Å closest contact), whereas the equivalent residue in Aurora-B/C is a leucine. This is one of the three active site sequence differences between Aurora-A and Aurora-B/C. The Arg220 side chain in Aurora-A (lysine in Aurora-B/C) points away from the active site. We exploited this observation in the design of compounds with substantially enhanced selectivity in inhibiting Aurora-A over isoforms -B and -C. It was envisaged that isoform selectivity for Aurora-A could be achieved by the introduction of a C2 purine and pyrrolidine moieties bearing an electron rich substituent capable of interacting with Leu215, Thr217 and Arg220 in Aurora-A, which would sterically clash with the equivalent residue in Aurora-B/C. It should be noted that Bavetsias et. al. and Coumar et al. recently reported respective imidazo[1,2-*a*]pyrazine and pyrazole-based Aurora-A selective inhibitor, and rationalised the selectivity for inhibition of Aurora-A over Aurora-B/C by proposing a similar argument, that is, hydrogen bonding interaction with the backbone NH of Thr217 in Aurora-A and steric clash with the equivalent residue in Aurora B/C [25].

Figure 4

Figure 5

3. Conclusion

The present work has led to the development of novel hybrids of purine-benzimidazole molecules and some of which shown promising antitumor activities. Compound **6** showed more active in most of the cancer cell lines at 10^{-5} M concentration and showed sensitivity towards colon cancer, CNS cancer and ovarian cancer with GI_{50} values of 3.16, 2.00 and 1.36

μM respectively at five dose concentration level. As per the results of enzyme immunoassays, compound **6** exhibited significant activity for inhibition of Aurora-A enzyme with IC_{50} value of $0.01 \mu\text{M}$. Subsequently, QSAR model for the affinity of this new series of Aurora A kinase inhibitors with physicochemical descriptors were developed with good predictive ability. Molecular modelling studies indicating considerable interactions of these compounds in the active site of amino acids of Aurora-A over Aurora B/C kinase enzyme that also favor the enzyme immunoassay results. The experimental (60 human cancer cell lines and Aurora A kinase enzyme) as well as theoretical studies (QSAR and molecular modelling) clearly predicted activity of purine-benzimidazole hybrids. These preliminary encouraging results of biological screening could offer an excellent framework in this field and may lead to discovery of potent antitumour agents.

4. Experimental Section

4.1. Chemistry

All chemicals and solvents of commercial grade were used without further purification and were supplied by loba, spectrochemicals and Sigma-Aldrich. Melting points were determined in open capillaries and are uncorrected. ^1H and ^{13}C NMR spectra were recorded on Jeol ECS 400 (^1H , 400 MHz; ^{13}C , 100 MHz) NMR spectrometer respectively, using CDCl_3 and $\text{DMSO-}d_6$ as solvents. The chemical shifts were expressed in parts per million with TMS as internal reference and J values are given in hertz. Mass Spectra of the synthesized compounds were recorded at Waters Micromass Q-ToF Micro. The crystal structure was collected on Bruker AXS KAPPA APEX II CCD diffractometer. Reactions were monitored by thin layer chromatography (TLC) with silica plate coated with silica gel HF-254 and column chromatography was performed with silica gel 60-120 mesh. Ethylacetate: hexane and chloroform: methanol were adopted solvent systems.

4.2. General procedure for the preparation of 1/3-butyl-2-methyl-1H/3H-benzo[d]imidazole-5-ylamine (**2b**, **2d**)

1/3-Butyl-2-methyl-5-nitro-1H/3H-benzimidazole was synthesized by previous reported method by the alkylation of 2-methyl-5-nitro-benzimidazole (0.05 mol) with butyl bromide (0.075 mol) in the presence of NaH (0.126 mol) in THF at room temperature for 8h. To a suspension of $\text{SnCl}_2 \cdot 2\text{H}_2\text{O}$ (135 mmol) in 2N HCl (95.2 ml), 1/3-butyl-2-methyl-5-nitro-1H/3H-benzimidazole (36.4 mmol) was heated at 110°C for 7 h. After the completion of the reaction (monitored by TLC), the suspension was neutralized with 2N NaOH and diluted with

ethanol. Filtered the solid product and extracted the filtrate with chloroform, dried over Na_2SO_4 , filtered and concentrated to get mixture of products which were separated through column chromatography using ethylacetate:methanol (9.5:0.5) to get pure solid compounds **2b** and **2d**.

4.2.1. *N*-(1-butyl-2-methyl-1*H*-benzo[d]imidazol-5-yl)amine (**2b**)

Brownish powder (450 mg, 52% yield) m.p. 138-140 °C. IR ν_{max} (KBr, cm^{-1}); 3314, 3184, 2955, 2921, 1624, 1465, 1401, 1211. ^1H NMR (CDCl_3); δ 7.46 (d, $J = 8.72$ Hz, 1H, CH), 7.08 (d, $J = 8.24$ Hz, 1H, ArH), 6.67-6.61 (m, 1H, ArH), 4.04-3.96 (m, 2H, N- CH_2), 2.55 (s, 3H, CH_3), 1.77-1.72 (m, 2H, CH_2), 1.39-1.34 (m, 2H, CH_2), 0.97 (t, $J = 3.66$ Hz, 3H, CH_3). EIMS, m/z ; 203.4 ($\text{M}^+ + 1$).

4.2.2. *N*-(3-butyl-2-methyl-3*H*-benzo[d]imidazol-5-yl)amine (**2d**)

Brownish powder (750 mg, 86% yield) m.p. 138-140 °C. IR ν_{max} (KBr, cm^{-1}); 3349, 3198, 2956, 2926, 1624, 1454, 1406, 1213. ^1H NMR (CDCl_3); δ 7.44 (d, $J = 8.24$ Hz, 1H, CH), 6.62 (dd, $^2J = 8.64$ Hz, $^3J = 2.28$ Hz, 1H, ArH), 6.56 (d, $J = 2.28$ Hz, 1H, ArH), 3.98 (t, $J = 7.32$ Hz, 2H, N- CH_2), 2.52 (s, 3H, CH_3), 1.76-1.69 (m, 2H, CH_2), 1.41-1.32 (m, 2H, CH_2), 0.96 (t, $J = 7.36$ Hz, 3H, CH_3). EIMS, m/z ; 203.4 ($\text{M}^+ + 1$).

4.3. General procedure for the preparation of **3a-d**

To a solution of **2a-d** (5.34 mmol) and isopropyl alcohol (25 ml), 2,6-dichloropurine (5.29 mmol) was added and stirred at room temperature for 24 h. After washing the crude solid with IPA, dried to obtain pure white solid of **3a-d**.

4.3.1. *N*-(1-allyl-2-methyl-1*H*-benzo[d]imidazol-5-yl)-2-chloro-9*H*-purin-6-amine (**3a**)

White powder (1.4 g, 79% yield) m.p. 270 °C (d). IR ν_{max} (KBr, cm^{-1}); 3354, 3305, 3199, 1637, 1596, 1496, 1302, 1250, 1166. ^1H NMR ($\text{DMSO-}d_6$); δ 13.36 (bs, 1H, NH), 10.58 (bs, 1H, NH), 8.66 (s, 1H, CH), 8.60 (s, 1H, CH), 7.97 (d, $J = 9.16$ Hz, 1H, ArH), 7.80 (d, $J = 8.68$ Hz, 1H, ArH), 6.08-6.04 (m, 1H, CH), 5.36 (d, $J = 10.52$ Hz, 1H, CH_2), 5.29 (d, $J = 16.96$ Hz, 1H, CH_2), 5.11 (d, $J = 5.04$ Hz, 2H, N- CH_2), 2.56 (s, 3H, CH_3). ^{13}C NMR ($\text{DMSO-}d_6$); δ 152.5, 151.5, 151.2, 137.6, 132.1, 131.2, 128.3, 119.0, 112.6, 46.9, 12.2. EIMS, m/z ; 340.1 ($\text{M}^+ + 1$).

4.3.2. *N*-(1-butyl-2-methyl-1*H*-benzo[d]imidazol-5-yl)-2-chloro-9*H*-purin-6-amine (**3b**)

White powder (0.9 g, 47% yield) m.p. 260 °C (d). IR ν_{\max} (KBr, cm^{-1}); 3380, 2958, 1648, 1498, 1433, 1232, 1109. ^1H NMR (DMSO- d_6); δ 10.62 (bs, 1H, NH), 8.72 (bs, 1H, NH), 8.59 (s, 1H, CH), 8.32 (s, 1H, ArH), 7.87 (d, $J = 1.46$ Hz, 1H, ArH), 7.75 (d, $J = 9.16$ Hz, 1H, ArH), 4.36 (t, $J = 7.32$ Hz, 2H, N-CH₂), 2.82 (s, 3H, CH₃), 1.92-1.85 (m, 2H, CH₂), 1.51-1.41 (m, 2H, CH₂), 1.01 (t, $J = 7.36$ Hz, 3H, CH₃). ^{13}C NMR (DMSO- d_6); δ 152.6, 151.1, 150.3, 137.4, 136.7, 132.9, 117.3, 115.2, 101.0, 46.8, 25.1, 19.5, 13.6, 12.2. EIMS, m/z ; 356.1 ($\text{M}^+ + 1$).

4.3.3. *N*-(3-allyl-2-methyl-3*H*-benzo[*d*]imidazol-5-yl)-2-chloro-9*H*-purin-6-amine (**3c**)

White powder (1.7 g, 94% yield) m.p. 285 °C (d). IR ν_{\max} (KBr, cm^{-1}); 3341, 3122, 2964, 1646, 1559, 1422, 1230, 1128. ^1H NMR (DMSO- d_6); δ 10.54 (bs, 1H, NH), 8.69 (bs, 1H, NH), 8.48 (s, 1H, CH), 8.27 (d, $J = 11.92$ Hz, 1H, ArH), 7.82 (s, 1H, ArH), 7.71 (d, $J = 9.16$ Hz, 1H, ArH), 6.05-5.98 (m, 1H, CH), 5.40 (t, $J = 16.52$ Hz, 2H, CH₂), 4.97 (d, $J = 6.40$ Hz, 2H, N-CH₂), 2.77 (s, 3H, CH₃). ^{13}C NMR (DMSO- d_6); δ 152.4, 151.4, 136.6, 130.8, 119.9, 119.8, 119.4, 115.1, 114.9, 103.8, 46.9, 12.0. EIMS, m/z ; 340.1 ($\text{M}^+ + 1$).

4.3.4. *N*-(3-butyl-2-methyl-3*H*-benzo[*d*]imidazol-5-yl)-2-chloro-9*H*-purin-6-amine (**3d**)

White powder (1.6 g, 86% yield) m.p. 280 °C (d). IR ν_{\max} (KBr, cm^{-1}); 3350, 2959, 1649, 1500, 1432, 1235, 1112. ^1H NMR (DMSO- d_6); δ 10.65 (bs, 1H, NH), 8.78 (bs, 1H, NH), 8.53 (s, 1H, CH), 8.35 (s, 1H, ArH), 7.82 (d, $J = 8.72$ Hz, 1H, ArH), 7.75 (d, $J = 8.68$ Hz, 1H, ArH), 4.34 (t, $J = 7.36$ Hz, 2H, N-CH₂), 2.79 (s, 3H, CH₃), 1.89-1.80 (m, 2H, CH₂), 1.46-1.37 (m, 2H, CH₂), 0.96 (d, $J = 7.32$ Hz, 3H, CH₃). ^{13}C NMR (TFA+CDCl₃); δ 156.5, 150.6, 149.3, 147.8, 139.5, 135.2, 131.7, 127.1, 121.5, 109.3, 105.4, 45.5, 30.4, 19.6, 12.4, 10.7. EIMS, m/z ; 356.4 ($\text{M}^+ + 1$).

4.4. General procedure for the preparation of compounds **4-19**

(1/3-allyl/butyl-2-methyl-1*H*/3*H*-benzo[*d*]imidazol-5-yl)-2-chloro-9*H*-purin-6-amine (0.29 mmol) was refluxed with amines (0.73 mmol) in ethanol (20 ml) for 2-3 days. Reaction was monitored by TLC, crude solid obtained with evaporation of the solvent under vacuum that was purified by column chromatography using chloroform : methanol as eluents to give pure compounds **4-19**.

4.4.1. *N*-(1-allyl-2-methyl-1*H*-benzo[*d*]imidazol-5-yl)-2-morpholino-9*H*-purin-6-amine (**4**)

White powder (65 mg, 75% yield) m.p. 239-240 °C. IR ν_{\max} (KBr, cm^{-1}); 3322, 3066, 2975, 1626, 1588, 1478, 1424, 1293, 1168, 1110. ^1H NMR (DMSO- d_6); δ 10.03 (bs, 1H,

NH), 8.20 (s, 1H, CH), 7.83 (s, 1H, ArH), 7.66 (s, 1H, ArH), 7.46 (d, $J = 8.28$ Hz, 1H, ArH), 5.96-5.93 (m, 1H, CH), 5.24 (d, $J = 10.56$ Hz, 1H, CH₂), 4.99 (d, $J = 17.44$ Hz, 1H, CH₂), 4.72 (d, $J = 2.76$ Hz, 2H, N-CH₂), 3.80 (s, 8H, _{mor}CH₂), 2.59 (s, 3H, CH₃). ¹³C NMR (DMSO-*d*₆); δ 159.2, 151.9, 142.5, 134.1, 133.4, 131.7, 131.1, 116.9, 115.9, 110.1, 108.9, 66.7, 45.6, 45.1, 29.4, 13.6. EIMS, *m/z*; 391.0 ($M^+ + 1$).

4.4.2. *N*-(1-allyl-2-methyl-1*H*-benzo[*d*]imidazol-5-yl)-2-(piperidin-1-yl)-9*H*-purin-6-amine (5)

White powder (60 mg, 53% yield) m.p. 242-244 °C. IR ν_{\max} (KBr, cm⁻¹); 3312, 2929, 1604, 1581, 1475, 1302, 1255, 1174. ¹H NMR (CDCl₃); δ 10.10 (bs, 1H, NH), 8.22 (d, $J = 1.96$ Hz, 1H, CH), 7.97 (s, 1H, ArH), 7.53 (dd, $^2J = 8.68$ Hz, $^3J = 2.28$ Hz, 1H, ArH), 7.22 (d, $J = 8.68$ Hz, 1H, ArH), 5.98-5.91 (m, 1H, CH), 5.24 (d, $J = 10.52$ Hz, 1H, CH₂), 4.99 (d, $J = 16.92$ Hz, 1H, CH₂), 4.72 (d, $J = 5.04$ Hz, 2H, N-CH₂), 3.80 (s, 4H, _{pip}CH₂), 2.58 (s, 3H, CH₃), 1.82 (s, 2H, _{pip}CH₂), 1.67 (s, 4H, _{pip}CH₂). ¹³C NMR (CDCl₃); δ 159.4, 152.2, 152.1, 142.8, 135.0, 134.2, 131.7, 131.5, 117.4, 116.1, 110.6, 109.0, 50.9, 46.0, 45.9, 25.9, 25.0, 13.8. EIMS, *m/z*; 389.0 ($M^+ + 1$).

4.4.3. *N*-(1-allyl-2-methyl-1*H*-benzo[*d*]imidazol-5-yl)-2-(pyrrolidin-1-yl)-9*H*-purin-6-amine (6)

White powder (66 mg, 60% yield) m.p. 260 °C (d). IR ν_{\max} (KBr, cm⁻¹); 3388, 2969, 1642, 1589, 1478, 1344, 1282, 1172. ¹H NMR (DMSO-*d*₆); δ 10.21 (bs, 1H, NH), 9.05 (s, 1H, CH), 8.47 (d, $J = 1.84$ Hz, 1H, ArH), 7.66 (t, $J = 4.60$ Hz, 1H, ArH), 7.28 (d, $J = 8.68$ Hz, 1H, ArH), 6.02-5.95 (m, 1H, CH), 5.21 (d, $J = 11.00$ Hz, 1H, CH₂), 4.95 (d, $J = 16.96$ Hz, 1H, CH₂), 4.79 (d, $J = 4.84$ Hz, 2H, N-CH₂), 3.61 (s, 4H, N-_{pyr}CH₂), 2.55 (s, 3H, CH₃), 2.00 (t, $J = 6.40$ Hz, 4H, _{pyr}CH₂). ¹³C NMR (DMSO-*d*₆); δ 157.9, 152.0, 142.5, 135.4, 132.6, 130.8, 116.9, 115.7, 109.6, 109.3, 47.1, 45.8, 25.7, 13.7. EIMS, *m/z*; 375.0 ($M^+ + 1$).

4.4.4. *N*-(1-allyl-2-methyl-1*H*-benzo[*d*]imidazol-5-yl)-2-(4-methylpiperazin-1-yl)-9*H*-purin-6-amine (7)

White powder (44 mg, 74% yield) m.p. 70-72 °C. IR ν_{\max} (KBr, cm⁻¹); 3412, 2971, 1638, 1598, 1461, 1307, 1263, 1101. ¹H NMR (CDCl₃); δ 10.01 (bs, 1H, NH), 8.16 (d, $J = 1.84$ Hz, 1H, CH), 7.78 (s, 1H, ArH), 7.65 (s, 1H, ArH), 7.50 (dd, $^2J = 8.72$ Hz, $^3J = 1.84$ Hz, 1H, ArH), 5.95-5.92 (m, 1H, CH), 5.25 (d, $J = 11.00$ Hz, 1H, N-CH₂), 5.00 (d, $J = 16.96$ Hz, 1H, CH₂), 4.73 (d, $J = 4.60$ Hz, 2H, N-CH₂), 3.90 (s, _{piperazine}CH₂, 4H), 2.59 (s, 3H, CH₃), 2.38 (s, 3H, CH₃), 1.25 (s, _{piperazine}CH₂, 4H). ¹³C NMR (CDCl₃); δ 153.7, 152.2, 134.9, 131.3, 117.4, 116.3, 116.2, 110.7, 108.9, 54.8, 46.6, 45.8, 29.6, 13.7. EIMS, *m/z*; 404.3 ($M^+ + 1$).

4.4.5. *N*-(1-butyl-2-methyl-1*H*-benzo[d]imidazol-5-yl)-2-morpholino-9*H*-purin-6-amine (**8**)

White powder (72 mg, 63% yield) m.p. 228-232 °C. IR ν_{\max} (KBr, cm^{-1}); 3317, 3060, 2962, 1589, 1480, 1428, 1292, 1261, 1170, 1107. ^1H NMR (DMSO- d_6); δ 12.23 (bs, 1H, NH), 8.76 (s, 1H, NH), 8.17 (s, 1H, CH), 7.83 (d, $J = 2.72$ Hz, 1H, ArH), 7.69 (s, 1H, ArH), 7.62 (d, $J = 7.36$ Hz, 1H, ArH), 4.17 (t, $J = 7.32$ Hz, 2H, N-CH₂), 3.90 (t, $J = 4.82$ Hz, 4H, morCH₂), 2.62 (s, 3H, CH₃), 2.61 (t, $J = 1.84$ Hz, 4H, morCH₂), 1.85-1.77 (m, 2H, CH₂), 1.45-1.37 (m, 2H, CH₂), 1.01 (t, $J = 7.32$ Hz, 3H, CH₃). ^{13}C NMR (DMSO- d_6); δ 158.7, 151.2, 141.7, 133.9, 130.5, 115.6, 109.5, 108.6, 66.2, 63.3, 48.9, 44.7, 43.1, 42.9, 31.2, 19.5, 13.3. EIMS, m/z; 407.5 ($\text{M}^+ + 1$).

4.4.6. *N*-(1-butyl-2-methyl-1*H*-benzo[d]imidazol-5-yl)-2(piperidin-1-yl)-9*H*-purin-6-amine (**9**)

White powder (82 mg, 72% yield) m.p. 218-220 °C. IR ν_{\max} (KBr, cm^{-1}); 3206, 2979, 1643, 1558, 1500, 1421, 1230, 1113. ^1H NMR (DMSO- d_6); δ 12.00 (bs, 1H, NH), 8.11 (s, 1H, CH), 7.59 (d, $J = 11.92$ Hz, 2H, ArH), 7.25 (d, $J = 8.72$ Hz, 1H, ArH), 4.11 (t, $J = 7.32$ Hz, 2H, N-CH₂), 3.78 (s, 4H, pipCH₂), 2.58 (s, 3H, CH₃), 1.80-1.73 (m, 2H, CH₂), 1.61 (s, 6H, pipCH₂), 1.40-1.35 (m, 2H, CH₂), 0.96 (t, $J = 7.32$ Hz, 3H, CH₃). ^{13}C NMR (DMSO- d_6); δ 158.7, 151.2, 142.1, 133.8, 130.6, 115.2, 109.4, 108.4, 45.3, 43.1, 31.2, 25.1, 24.4, 19.5, 13.4, 13.2. EIMS, m/z; 405.5 ($\text{M}^+ + 1$).

4.4.7. *N*-(1-butyl-2-methyl-1*H*-benzo[d]imidazol-5-yl)-2(pyrrolidin-1-yl)-9*H*-purin-6-amine (**10**)

White powder (87 mg, 80% yield) m.p. 280 °C (d). IR ν_{\max} (KBr, cm^{-1}); 3340, 2957, 1626, 1580, 1450, 1339, 1277, 1112. ^1H NMR (DMSO- d_6); δ 12.42 (bs, 1H, NH), 9.32 (s, 1H, NH), 8.70 (s, 1H, CH), 8.24 (s, 1H, ArH), 7.75 (s, 1H, ArH), 7.50 (d, $J = 8.72$ Hz, 1H, ArH), 4.12 (t, $J = 7.32$ Hz, 2H, N-CH₂), 3.61 (s, 4H, pyrCH₂), 2.56 (s, 3H, CH₃), 2.01 (t, $J = 6.44$ Hz, 4H, pyrCH₂), 1.77-1.73 (m, 2H, CH₂), 1.41-1.35 (m, 2H, CH₂), 0.97 (t, $J = 7.32$ Hz, 3H, CH₃). ^{13}C NMR (TFA+CDCl₃); δ 151.1, 150.9, 149.6, 149.4, 140.6, 138.3, 135.0, 134.7, 131.7, 127.9, 122.9, 105.8, 49.6, 47.4, 30.8, 19.6, 13.1, 12.4, 11.5. EIMS, m/z; 391.2 ($\text{M}^+ + 1$).

4.4.8. *N*-(1-butyl-2-methyl-1*H*-benzo[d]imidazol-5-yl)-2(4-methylpiperazine-1-yl)-9*H*-purin-6-amine (**11**)

White powder (65 mg, 55% yield) m.p. 225-228 °C. IR ν_{\max} (KBr, cm^{-1}); 3350, 2935, 1583, 1470, 1426, 1366, 1253, 1147. ^1H NMR (DMSO- d_6); δ 12.45 (bs, 1H, NH), 9.47 (bs, 1H, NH), 8.21 (s, 1H, CH), 8.05 (s, 1H, ArH), 7.83 (s, 1H, ArH), 7.43 (d, $J = 8.72$ Hz, 1H, ArH), 4.08-4.02 (m, 2H, N-CH₂), 3.68 (s, 4H, piperazineCH₂), 2.47 (s, 3H, CH₃), 2.45 (s, 4H, piperazineCH₂), 2.36 (s, 3H, CH₃), 1.69-1.63 (m, 2H, CH₂), 1.28-1.22 (m, 2H, CH₂), 0.87 (t, $J = 7.36$ Hz, 3H, CH₃). ^{13}C NMR (DMSO- d_6); δ 158.7, 152.4, 152.3, 151.9, 151.7, 151.3, 138.8, 137.8, 137.0, 134.9, 133.2, 117.9, 116.2, 115.4, 113.5, 103.2, 101.2, 54.5, 45.9, 44.3, 43.1, 31.3, 19.8, 13.6, 13.6. EIMS, m/z ; 420.5 ($\text{M}^+ + 1$).

4.4.9. *N*-(3-allyl-2-methyl-3H-benzo[d]imidazol-5-yl)-2-morpholino-9H-purin-6-amine (**12**)

White powder (120 mg, 96% yield) m.p. 260 °C (d). IR ν_{\max} (KBr, cm^{-1}); 3394, 2958, 1626, 1583, 1458, 1309, 1101. ^1H NMR (DMSO- d_6); δ 12.29 (bs, 1H, NH), 9.19 (bs, 1H, NH), 8.28 (s, 1H, CH), 8.01 (s, 1H, ArH), 7.69 (s, 1H, ArH), 7.49 (d, $J = 8.72$ Hz, 1H, ArH), 6.03-5.97 (m, 1H, CH), 5.20 (d, $J = 10.52$ Hz, 1H, CH₂), 4.86 (d, $J = 16.96$ Hz, 1H, CH₂), 4.75 (s, 2H, N-CH₂), 3.73 (s, 4H, morCH₂), 2.57 (s, 4H, morCH₂), 2.53 (s, 3H, CH₃). ^{13}C NMR (DMSO- d_6); δ 158.6, 151.7, 151.2, 150.8, 137.5, 135.9, 134.7, 134.5, 131.4, 117.8, 116.0, 114.9, 113.4, 100.6, 66.2, 44.9, 44.7, 30.4, 13.1. EIMS, m/z ; 391.4 ($\text{M}^+ + 1$).

4.4.10. *N*-(3-allyl-2-methyl-3H-benzo[d]imidazol-5-yl)-2-(piperidin-1-yl)-9H-purin-6-amine (**13**)

White powder (98 mg, 85% yield) m.p. 243-245 °C. IR ν_{\max} (KBr, cm^{-1}); 3275, 2925, 1623, 1583, 1437, 1425, 1305, 1255, 1191. ^1H NMR (DMSO- d_6); δ 12.21 (bs, 1H, NH), 9.02 (bs, 1H, NH), 8.40 (s, 1H, CH), 7.93 (s, 1H, ArH), 7.64 (s, 1H, ArH), 7.49 (d, $J = 8.72$ Hz, 1H, ArH), 6.01-5.97 (m, 1H, CH), 5.20 (d, $J = 10.52$ Hz, 1H, CH₂), 4.88 (d, $J = 16.96$ Hz, 1H, CH₂), 4.74 (s, 2H, N-CH₂), 3.80 (t, $J = 5.52$ Hz, 4H, pipCH₂), 2.54 (s, 3H, CH₃), 1.67 (s, 2H, pipCH₂), 1.61 (s, 4H, pipCH₂). ^{13}C NMR (DMSO- d_6); δ 158.5, 150.9, 150.7, 137.2, 135.8, 134.8, 134.7, 131.4, 117.7, 116.0, 114.7, 100.2, 45.2, 44.9, 25.2, 24.4, 13.2. EIMS, m/z ; 389.5 ($\text{M}^+ + 1$).

4.4.11. *N*-(3-allyl-2-methyl-3H-benzo[d]imidazol-5-yl)-2-(pyrrolidin-1-yl)-9H-purin-6-amine (**14**)

White powder (60 mg, 55% yield) m.p. 240 °C (d). IR ν_{\max} (KBr, cm^{-1}); 3320, 2964, 1633, 1578, 1460, 1337, 1275, 1204, 1113. ^1H NMR (DMSO- d_6); δ 12.36 (bs, 1H, NH), 9.26 (bs, 1H, NH), 8.63 (s, 1H, CH), 8.15 (s, 1H, ArH), 7.68 (s, 1H, ArH), 7.47 (d, $J = 5.28$ Hz,

1H, ArH), 6.04-5.96 (m, 1H, CH), 5.16 (d, $J = 10.08$ Hz, 1H, CH₂), 4.82 (s, 1H, CH₂), 4.78 (d, $J = 9.16$ Hz, 2H, N-CH₂), 3.57 (s, 4H, N-pyrCH₂), 2.52 (s, 3H, CH₃), 1.99 (t, $J = 6.44$ Hz, 4H, pyrCH₂). ¹³C NMR (DMSO-*d*₆); δ 156.8, 150.8, 150.4, 136.2, 135.1, 134.3, 131.8, 131.7, 117.1, 116.9, 115.4, 114.4, 102.2, 100.2, 46.3, 44.6, 24.7, 12.7. EIMS, m/z ; 375.5 ($M^+ + 1$).

4.4.12. *N*-(3-allyl-2-methyl-3H-benzo[*d*]imidazol-5-yl)-2-(4-methylpiperazin-1-yl)-9H-purin-6-amine (**15**)

White powder (70 mg, 62% yield) m.p. 159-162 °C. IR ν_{\max} (KBr, cm⁻¹); 3313, 2936, 1629, 1601, 1583, 1476, 1440, 1364, 1257, 1139. ¹H NMR (DMSO-*d*₆); δ 12.38 (bs, 1H, NH), 9.38 (bs, 1H, NH), 8.30 (s, 1H, CH), 8.14 (s, 1H, ArH), 7.75 (s, 1H, ArH), 7.45 (d, $J = 8.68$ Hz, 1H, ArH), 6.05-5.98 (m, 1H, CH), 5.17 (d, $J = 10.52$ Hz, 1H, CH₂), 4.80 (s, 1H, CH₂), 4.75 (s, 2H, N-CH₂), 3.73 (s, 4H, piperazineCH₂), 2.52 (s, 3H, CH₃), 2.49 (s, 3H, CH₃), 2.27 (s, 4H, piperazineCH₂). ¹³C NMR (DMSO-*d*₆); δ 158.5, 152.0, 151.4, 150.9, 137.5, 136.3, 134.4, 132.2, 117.7, 115.8, 115.1, 100.9, 54.5, 45.8, 45.0, 44.2, 13.2. EIMS, m/z ; 404.5 ($M^+ + 1$).

4.4.13. *N*-(3-butyl-2-methyl-3H-benzo[*d*]imidazol-5-yl)-2-morpholino-9H-purin-6-amine (**16**)

White powder (74 mg, 65% yield) m.p. 218 °C (d). IR ν_{\max} (KBr, cm⁻¹); 3353, 2931, 1600, 1585, 1471, 1431, 1382, 1254, 1124. ¹H NMR (DMSO-*d*₆); δ 12.46 (s, 1H, NH), 9.42 (s, 1H, NH), 8.25 (s, 1H, CH), 7.80 (s, 1H, ArH), 7.50 (d, $J = 8.72$ Hz, 1H, ArH), 7.43 (d, $J = 9.04$ Hz, 1H, ArH), 4.12 (t, $J = 7.32$ Hz, 2H, N-CH₂), 3.73 (s, 4H, morCH₂), 2.54 (d, $J = 2.28$ Hz, 4H, morCH₂), 2.53 (s, 3H, CH₃), 1.77-1.72 (m, 2H, CH₂), 1.39-1.32 (m, 2H, CH₂), 0.99 (t, $J = 7.32$ Hz, 3H, CH₃). ¹³C NMR (DMSO-*d*₆); δ 158.6, 137.7, 136.5, 134.7, 134.6, 117.6, 115.2, 101.0, 99.4, 66.1, 48.6, 44.9, 31.2, 30.6, 25.3, 19.6, 13.6. EIMS, m/z ; 407.5 ($M^+ + 1$).

4.4.14. *N*-(3-butyl-2-methyl-3H-benzo[*d*]imidazol-5-yl)-2-(piperidin-1-yl)-9H-purin-6-amine (**17**)

Light brown (78 mg, 72% yield) m.p. 278 °C (d). IR ν_{\max} (KBr, cm⁻¹); 3328, 2924, 1627, 1603, 1583, 1480, 1307, 1252, 1126. ¹H NMR (DMSO-*d*₆); δ 12.37 (bs, 1H, NH), 9.38 (bs, 1H, NH), 8.27 (s, 1H, CH), 7.80 (s, 1H, ArH), 7.40 (d, $J = 8.72$ Hz, 1H, ArH), 7.36 (d, $J = 8.24$ Hz, 1H, ArH), 4.04 (t, $J = 7.36$ Hz, 2H, N-CH₂), 3.71 (t, $J = 5.04$ Hz, 4H, pipCH₂), 2.45 (s, 3H, CH₃), 1.69-1.61 (m, 2H, CH₂), 1.56 (s, 2H, pipCH₂), 1.49 (s, 4H, pipCH₂), 1.29-1.21 (m, 2H, CH₂), 0.89 (t, $J = 7.36$ Hz, 3H, CH₃). ¹³C NMR (DMSO-*d*₆); δ 158.5, 152.4,

151.6, 150.9, 137.8, 136.5, 134.8, 117.8, 115.2, 113.1, 100.9, 45.2, 42.9, 31.3, 25.3, 24.5, 19.6, 13.7, 13.6. EIMS, m/z; 405.5 ($M^+ + 1$).

4.4.15. *N*-(3-butyl-2-methyl-3*H*-benzo[*d*]imidazol-5-yl)-2-(pyrrolidin-1-yl)-9*H*-purin-6-amine (**18**)

White powder (77 mg, 70% yield) m.p. 260 °C (d). IR ν_{\max} (KBr, cm^{-1}); 3321, 2956, 1581, 1521, 1467, 1382, 1274, 1198, 1115. ^1H NMR (DMSO- d_6); δ 12.39 (bs, 1H, NH), 9.27 (bs, 1H, NH), 8.67 (s, 1H, CH), 8.22 (s, 1H, ArH), 7.48 (d, $J = 7.80$ Hz 1H, ArH), 7.37 (d, $J = 8.68$ Hz 1H, ArH), 4.09 (t, $J = 10.08$ Hz, 2H, N-CH₂), 3.59 (s, 4H, pyr-CH₂), 2.52 (s, 3H, CH₃), 1.98 (t, $J = 5.96$ Hz, 4H, pyr-CH₂), 1.78-1.68 (m, 2H, CH₂), 1.40-1.31 (m, 2H, CH₂), 0.94 (t, $J = 7.32$ Hz, 3H, CH₃). ^{13}C NMR (DMSO- d_6); δ 157.2, 152.2, 150.3, 137.2, 135.3, 134.7, 131.6, 121.9, 119.0, 117.5, 114.5, 100.1, 62.0, 48.6, 46.6, 43.0, 31.4, 25.3, 19.6, 13.6, 13.4. EIMS, m/z; 391.5 ($M^+ + 1$).

4.4.16. *N*-(3-butyl-2-methyl-3*H*-benzo[*d*]imidazol-5-yl)-2-(4-methylpiperazin-1-yl)-9*H*-purin-6-amine (**19**)

White powder (96 mg, 82% yield) m.p. 238-240 °C. IR ν_{\max} (KBr, cm^{-1}); 3393, 2955, 1624, 1583, 1442, 1355, 1252, 1136. ^1H NMR (DMSO- d_6); δ 12.29 (bs, 1H, NH), 9.08 (bs, 1H, NH), 8.30 (s, 1H, CH), 7.96 (d, $J = 3.20$ Hz, 1H, ArH), 7.48 (d, $J = 5.88$ Hz, 1H, ArH), 7.46 (s, 1H, ArH), 4.12-4.08 (m, 2H, N-CH₂), 3.82 (s, 4H, piperazine-CH₂), 2.58 (s, 3H, CH₃), 2.49 (t, $J = 4.6$ Hz, 4H, piperazine-CH₂), 2.32 (s, 3H, CH₃), 1.85-1.75 (m, 2H, CH₂), 1.40-1.36 (m, 2H, CH₂), 0.96 (t, $J = 6.84$ Hz, 3H, CH₃). ^{13}C NMR (DMSO- d_6); δ 158.5, 150.5, 137.5, 134.6, 134.5, 117.7, 114.9, 100.5, 56.3, 54.4, 45.7, 44.1, 43.0, 31.2, 25.0, 19.6, 18.1, 13.4. EIMS, m/z; 420.5 ($M^+ + 1$).

4.5. Procedure for *in vitro* anticancer screening

The human tumor cell lines of the cancer screening panel are grown in RPMI 1640 medium containing 5% fetal bovine serum and 2 mM L-glutamine. Cells are inoculated into 96 well microtiter plates in 100 μl at plating densities ranging from 5,000 to 40,000 cells/well depending on the doubling time of individual cell lines. The microtiter plates are then incubated at 37 °C, 5% CO₂, 95% air and 100% relative humidity for 24 h.

After 24 h, two plates of each cell line are fixed *in situ* with TCA, to represent a measurement of the cell population for each cell line. Experimental drugs are solubilized in DMSO at 400-fold the desired final maximum test concentration and stored frozen prior to

use. At the time of drug addition, an aliquot of frozen concentrate is thawed and diluted to twice the desired final maximum test concentration with complete medium containing 50 µg/ml gentamicin. Additional four, 10-fold or ½ log serial dilutions are made to provide a total of five drug concentrations plus control. Aliquots of 100 µL of these different drug dilutions are added to the appropriate microtiter wells, resulting in the required final drug concentrations. Following drug addition, the plates are incubated for an additional 48 h at 37 °C, 5% CO₂, 95% air, and 100% relative humidity. For adherent cells, the assay is terminated by the addition of cold TCA. Cells are fixed in situ by the gentle addition of 50 µL of cold 50% (w/v) TCA and incubated for 60 min at 4 °C. The supernatant is discarded, and the plates are washed five times with tap water and air dried. Sulforhodamine B (SRB) solution (100 µL) at 0.4% (w/v) in 1% acetic acid is added to each well, and plates are incubated for 10 min at room temperature. After staining, unbound dye is removed by washing five times with 1% acetic acid and the plates are air dried and then subsequently solubilized with 10 mM trizma base, and the absorbance is read on an automated plate reader at a wavelength of 515 nm. Using the seven absorbance measurements [time zero (T_z), control growth (C), and test growth in the presence of drug at the five concentration levels (T_i)], the percentage growth is calculated at each of the drug concentration levels. Percentage growth inhibition is calculated as:

$[(T_i - T_z)/(C - T_z)] \times 100$ for concentrations for which $T_i \geq T_z$; $[(T_i - T_z)/T_z] \times 100$ for concentrations for which $T_i < T_z$.

Three dose response parameters are calculated for each experimental agent. Growth inhibition of 50% (GI₅₀) is calculated from $[(T_i - T_z)/(C - T_z)] \times 100 = 50$. The drug concentration resulting in total growth inhibition (TGI) is calculated from $T_i = T_z$. The LC₅₀ is calculated from $[(T_i - T_z)/T_z] \times 100 = 50$ [16,19, 26].

Acknowledgment

We wish to thank to UGC, New Delhi (41-322/2012, SR) and CSIR, New Delhi (02(0034)/11/EMR-II) for providing funds. Sincere thank to Prof. Sanjay Saxena and Mahiti Gupta, department of biotechnology for helping Aurora kinase activities. NCI, USA is gratefully acknowledged for investigating antitumor activities.

References

- [1] R.V. Kumara, S. Bhasker, *J. Cancer Policy* 2 (2014) 63. [2] M.N. Noolvi, H.M. Patel, V. Bhardwaj, A. Chauhan, *Eur. J. Med. Chem.* 46 (2011) 2327. [3] W.B. Parker, *Chem. Rev.* 109 (2009) 2880.
- [4] A.M. D'Alise, G. Amabile, M. Iovino, F.P.D. Giorgio, M. Bartiromo, F. Sessa, F. Villa, A. Musacchio, R. Cortese, *Mol. Cancer Ther.* 7 (2008) 1140.
- [5] M. Legraverend, P. Tunnah, M. Noble, P. Ducrot, O. Ludwig, D.S. Grierson, M. Leost, L. Meijer, *J. Endicott, J. Med. Chem.* 43 (2000) 1282.
- [6] C. Peifer, S. Buhler, D. Hauser, K. Kinkel, F. Totzke, C. Schachtele, S. Laufer, *Eur. J. Med. Chem.* 44 (2009) 1788.
- [7] W.S. Hsieh, R. Soo, B.K. Peh, T. Loh, D. Dong, D. Soh, L.S. Wong, S. Green, J. Chiao, C.Y. Cui, Y.F. Lai, S.C. Lee, B. Mow, R. Soong, M. Salto-Tellez, B.C. Goh, *Clin. Cancer Res.* 15 (2009) 1435.
- [8] C.L. Tourneau, S. Faivre, V. Laurence, C. Delbaldo, K. Vera, V. Girre, J. Chiao, S. Armour, S. Frame, S.R. Green, A. Gianella-Borradori, V. Dieras, E. Raymond, *Eur. J. Cancer* 46 (2010) 3243.
- [9] M. Ferrero, V. Gotor, *Chem. Rev.* 100 (2000) 4319.
- [10] (a) G. Singh, M. Kaur, C. Mohan, *Int. J. Pharm.* 4 (2013) 82. (b) Y. Bansal, O. Silakari, *Bioorg. Med. Chem.* 20 (2012) 6208. (c) P. Singla, V. Luxami, K. Paul *RSC Adv.* 4 (2014) 12422.
- [11] S. Nakamura, N. Tsuno, M. Yamashita, I. Kawasaki, S. Ohta, Y. Ohishi, *J. Chem. Soc. Perkin Trans.1* (2001) 429.
- [12] E.S. Park, H.J. Lee, H. Park, M.N. Kim, K.H. Chung, J.S. Yoon, *J. Appl. Poly. Sci.* 80 (2001) 728.
- [13] (a) J.C. Hazelton, B. Iddon, H. Suschitzky, L.H. Woolley, *Tetrahedron* 51 (1995) 10771. (b) C.S. Labaw, R.L. Webb, U.S 4285878, 1981; *Chem. Abstr.* 95 (1981) 168837. (c) P. Kohler, *Int. J. Parasitol.* 31 (2001) 336.
- [14] P. Meisel, H.J. Heidrich, H.J. Jaensch, E. Kretzschmar, S. Henker, G. Laban, DD 243284, 1987; *Chem. Abstr.* 107 (1987) 217629. (b) D. Kyle, R.R. Goehring, B. Shao, WO 001,039775; *Chem. Abstr.* 135 (2001) 33477.
- [15] (a) A. Sharma, V. Luxami, K. Paul, *Bioorg. Med. Chem. Lett.* 23 (2013) 3288. (b) K. Paul, A. Sharma, V. Luxami, *Bioorg. Med. Chem. Lett.* 24 (2014) 624.
- [16] M.R. Grever, S.A. Sehepartz, B.A. Chabners, *Semin. Oncol.* 19 (1992) 622.

- [17] A. Monks, D. Scudiero, P. Skehan, R. Shoemaker, K. Paull, D. Vistica, C. Hose, J. Langley, P. Cronise, A. Vaigro-Wolff, M. Gray-Goodrich, H. Campbell, J. Mayo, M. Boyd, *J. Natl. Cancer Inst.* 83 (1991) 757.
- [18] M.R. Boyd, K.D. Paull, *Drug Dev. Res.* 34 (1995) 91.
- [19] P. Skehan, R. Storeng, D. Scudiero, A. Monks, J. McMahon, D. Vistica, J.T. Warren, H. Bokesch, S. Kenney, M.R. Boyd, *J. Natl. Cancer Inst.* 82 (1990) 1107.
- [20] CycLex Aurora-A kinase Assay/Inhibitor Screening kit Cat# CY-1165.
- [21] A.I. Caco, L.C. Tome, R. Dohrn, I.M. Marrucho, *J. Chem. Eng. Data* 55 (2010) 3160 and references therein.
- [22] QSARINS (QSAR-INSubria): QSARINS, software for QSAR MLR model Development and validation, version 2.1- 2014, QSAR Research Unit in Environmental Chemistry and Ecotoxicology, Department of theoretical and applied sciences (DiSTA), University of Insubria, Via J.H. Dunant 3, Varese, Italy. <http://www.qsar.it>.
- [23] M.M. Neaz, M. Muddassar, F.A. Pasha, S.J. Cho, *Acta Pharmacol. Sin.* 31 (2010) 244.
- [24] Compounds were constructed and docked with builder toolkit of the software package ArgusLab 4.0.1 (www.arguslab.com).
- [25] (a) N. Bouloc, J. M. Large, M. Kosmopoulou, C. Sun, A. Faisal, M. Matteucci, J. Reynisson, N. Brown, B. Atrash, J. Blagg, E. McDonald, S. Linardopoulos, R. Bayliss, V. Bavetsias, *Bioorg. Med. Chem. Lett.* 20 (2010) 5988, (b) M. S. Coumar, J.-S. Leou, P. Shukla, J.-S. Wu, A. K. Dixit, W.-H. Lin, C.-Y. Chang, T.-W. Lien, U.-K. Tan, C.-H. Chen, J. T.-A. Hsu, Y.-S. Chao, S.-Y. Wu, H.-P. Hsieh, *J. Med. Chem.* 52 (2009) 1050.
- [26] M.C. Alley, D.A. Scudiero, A. Monks, M.L. Hursey, M.J. Czerwinski, D.L. Fine, B.J. Abbott, J.G. Mayo, R.H. Shoemaker, M.R. Boyd, *Cancer Res.* 48 (1988) 589.

Figures Captions

Figure 1. Purine related drugs

Figure 2. ORTEP diagram of compound **19** (CCDC No. 1022534)

Figure 3. Plot of observed vs predicted Aurora A kinase inhibitory activity (expressed as log (IC₅₀) values for compounds **3a-3b**, **4-7** and **10** using eq 1). Predicted values were obtained with a leave-one-out cross-validation procedure.

Figure 4. Compound **6** docked in active site of Aurora-A (2WTV). H-bonds of compound **6** with different amino acids residues are visible. Carbon atoms are given in green colour.

Figure 5. Compound **6** docked in active site of Aurora-A (2XNE). H-bonds of compound **6** with different amino acids residues are visible. Carbon atoms are given in green colour.

Scheme 1. Synthetic route for the preparation of target compounds **4-19**

Table 1. Physicochemical properties of the newly synthesized compounds **3a-d** and **4-19**

Table 2. Compound **6** and **5-FU** median growth inhibitory (GI_{50} , μM), total growth inhibitory (TGI, μM) and median lethal concentrations (LC_{50} , μM) of *in vitro* subpanel tumour cell lines.

Table 3. IC_{50} , ligand efficiency and experimental log P values of tested compounds

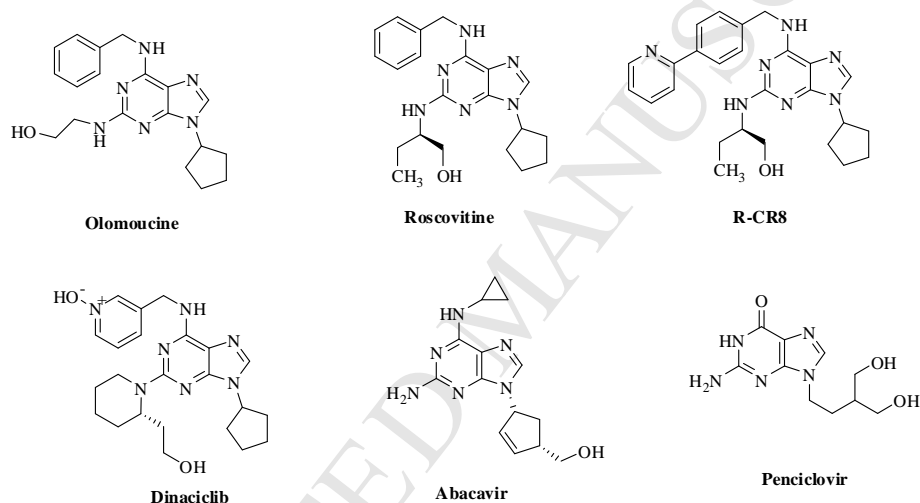


Figure 1. Purine related drugs

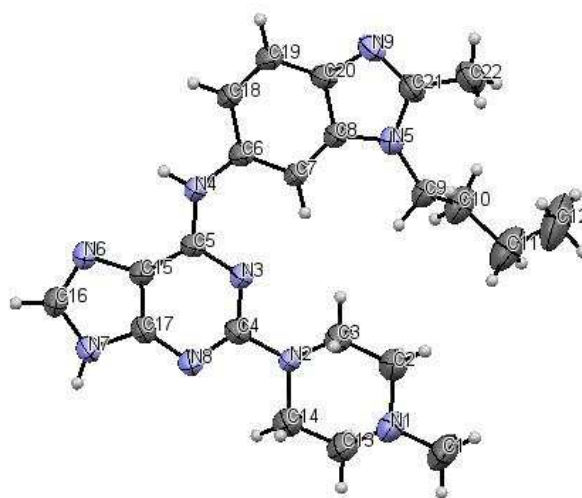


Figure 2. ORTEP diagram of compound **19** (CCDC No. 1022534)

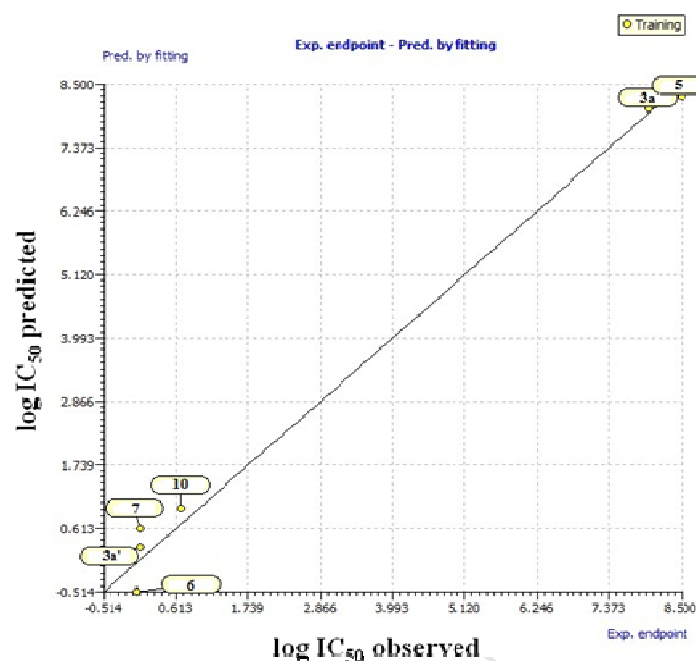


Figure 3 Plot of observed vs predicted Aurora A kinase inhibitory activity (expressed as log (IC_{50}) values for compounds **3a-3b**, **4-7** and **10** using eq 1). Predicted values were obtained with a leave-one-out cross-validation procedure.

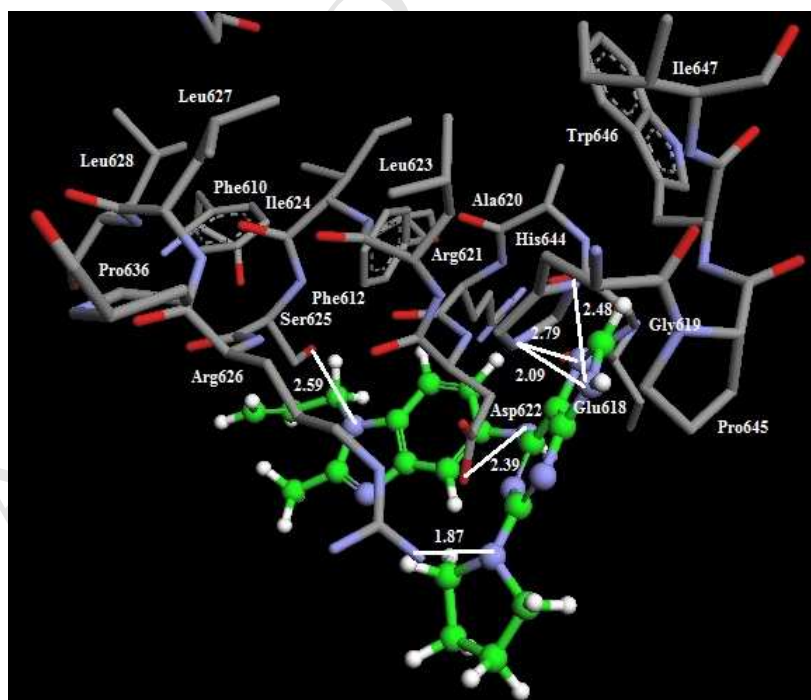


Figure 4. Compound **6** docked in active site of Aurora-A (2WTV). H-bonds of compound **6** with different amino acids residues are visible. Carbon atoms are in given green colour.

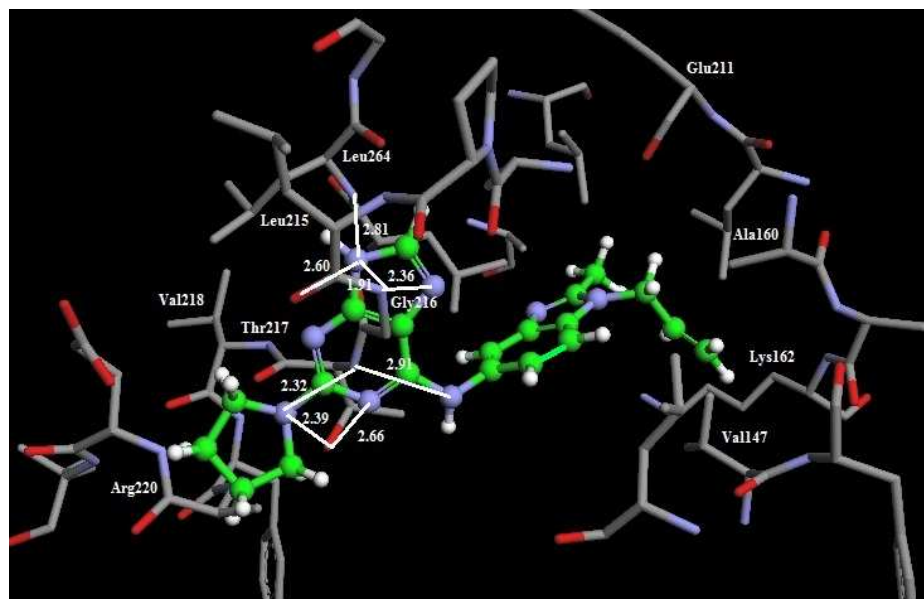
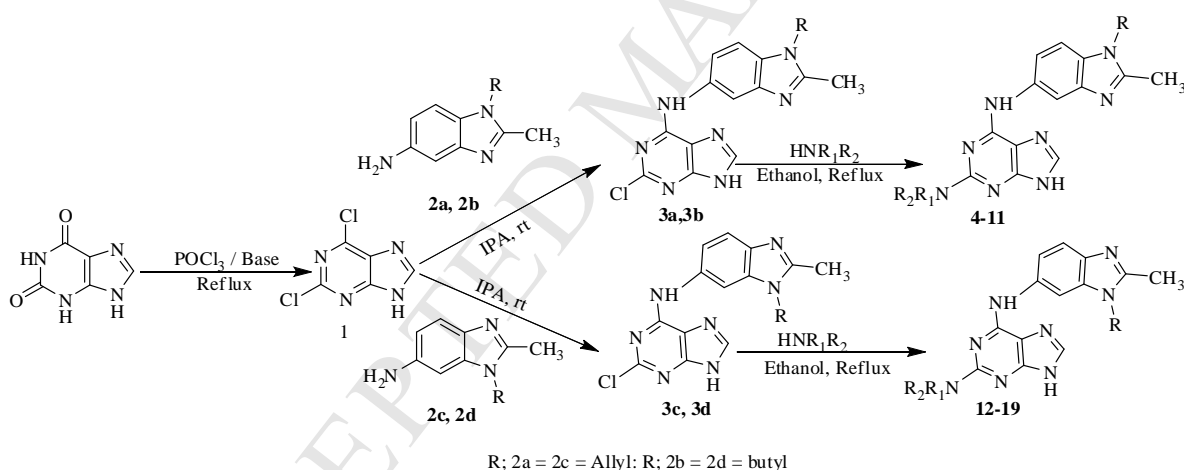


Figure 5. Compound **6** docked in active site of Aurora-A (2XNE). H-bonds of compound **6** with different amino acids residues are visible. Carbon atoms are given in green colour.



Scheme 1 Synthetic route for the preparation of target compounds **4-19**

Table 1. Physicochemical properties of the newly synthesized compounds **3a-d** and **4-19**

Compds	Starting Material	NHR ₁ R ₂	% yields	M.pt. (°C)	Molecular formulae
3a	2a	--	79	270 (d)	C ₁₆ H ₁₄ N ₇ Cl
3b	2b	--	47	260 (d)	C ₁₇ H ₁₈ N ₇ Cl
3c	2c	--	94	285(d)	C ₁₆ H ₁₄ N ₇ Cl
3d	2d	--	86	280 (d)	C ₁₇ H ₁₈ N ₇ Cl
4	3a	morpholin-4-yl	75	239-240	C ₂₀ H ₂₂ N ₈ O
5	3a	piperidin-1-yl	53	242-244	C ₂₁ H ₂₄ N ₈
6	3a	pyrrolidin-1-yl	60	260(d)	C ₂₀ H ₂₂ N ₈
7	3a	4-methylpiperazin-1-yl	74	70-72	C ₂₁ H ₂₅ N ₉

8	3b	morpholin-4-yl	63	228-232	C ₂₁ H ₂₆ N ₈ O
9	3b	piperidin-1-yl	72	218-220	C ₂₂ H ₂₈ N ₈
10	3b	pyrrolidin-1-yl	80	280 (d)	C ₂₁ H ₂₆ N ₈
11	3b	4-methylpiperazin-1-yl	55	225-228	C ₂₂ H ₂₉ N ₉
12	3c	morpholin-4-yl	96	260(d)	C ₂₀ H ₂₂ N ₈ O
13	3c	piperidin-1-yl	85	243-245	C ₂₁ H ₂₄ N ₈
14	3c	pyrrolidin-1-yl	55	240(d)	C ₂₀ H ₂₂ N ₈
15	3c	4-methylpiperazin-1-yl	62	159-162	C ₂₁ H ₂₅ N ₉
16	3d	morpholin-4-yl	65	218 (d)	C ₂₁ H ₂₆ N ₈ O
17	3d	piperidin-1-yl	72	278 (d)	C ₂₂ H ₂₈ N ₈
18	3d	pyrrolidin-1-yl	70	260 (d)	C ₂₁ H ₂₆ N ₈
19	3d	4-methylpiperazin-1-yl	82	238-240	C ₂₂ H ₂₉ N ₉

Table 2. Compound **6** and **5-FU** median growth inhibitory (GI₅₀, μM), total growth inhibitory (TGI, μM) and median lethal concentrations (LC₅₀, μM) of *in vitro* subpanel tumour cell lines.

Comps	Activity	I	II	III	IV	V	VI	VII	VIII	IX	MG-MID ^a
6	GI ₅₀	54.5	b	3.16	2.00	29.6	1.34	b	b	b	18.12
	TGI	b	b	b	b	b	b	b	b	b	b
	LC ₅₀	b	b	b	b	b	b	b	b	b	b
5-FU	GI ₅₀	15.1	b	8.4	72.1	70.6	61.4	45.6	22.7	76.4	22.60
	TGI	b	b	b	b	b	b	b	b	b	b
	LC ₅₀	b	b	b	b	b	b	b	b	b	b

I, Leukemia; II, non-small cell lung cancer; III, colon cancer; IV, CNS cancer; V, melanoma; VI, ovarian cancer; VII, renal cancer; VIII, prostate cancer; IX, breast cancer.

^a Full panel mean-graph midpoint (μM).

^b Compounds showed values >100 μM.

Table 3. IC₅₀, ligand efficiency and experimental log P values of tested compounds

Compounds	IC ₅₀ (μM)	Ligand efficiency ^a	Experimental log P
3a	8.00	0.29	2.48
3b	0.07	0.38	1.28
4	0.02	0.24	1.59
5	8.50	0.35	1.55
6	0.01	0.39	2.53
7	0.07	0.29	1.25
10	0.70	0.33	1.36

^a Calculated using the formula: LE = [-1.4 × log₁₀(IC₅₀ (M))]/(number of non hydrogen atoms).

Highlights

- A new series of regioisomeric purine-benzimidazole hybrids.
- Single X-ray determination of compound **19**
- *In vitro* evaluation of synthesized compounds for their antitumor activity.
- *In vitro* evaluation of Aurora kinase inhibitors
- Molecular modeling in active sites of Aurora A kinase.

Supporting Information

Purine-benzimidazole hybrids: Synthesis, single crystal determination and *in vitro* evaluation of antitumor activities

Alka Sharma, Vijay Luxami, Kamaldeep Paul*

School of Chemistry and Biochemistry, Thapar University, Patiala-147004, India.

Tel.: +91-94656-70595; fax: +91-175-236-4498;

E-mail: kpaul@thapar.edu

Table of Contents

S. No.	Contents	Page No.
1	¹ H and ¹³ C NMR spectra of compounds	S2-S22
2	60 human tumor cell line (one dose results)	S23-S24
3	Five dose results of compound 6	S25
4	Aurora A kinase studies	S25-S26
5	Shake Flask Method for lipophilicity determination	S26-S27
6	X-ray crystallographic data of compound 19	S27-S36
7	Docking of compound 6	S36

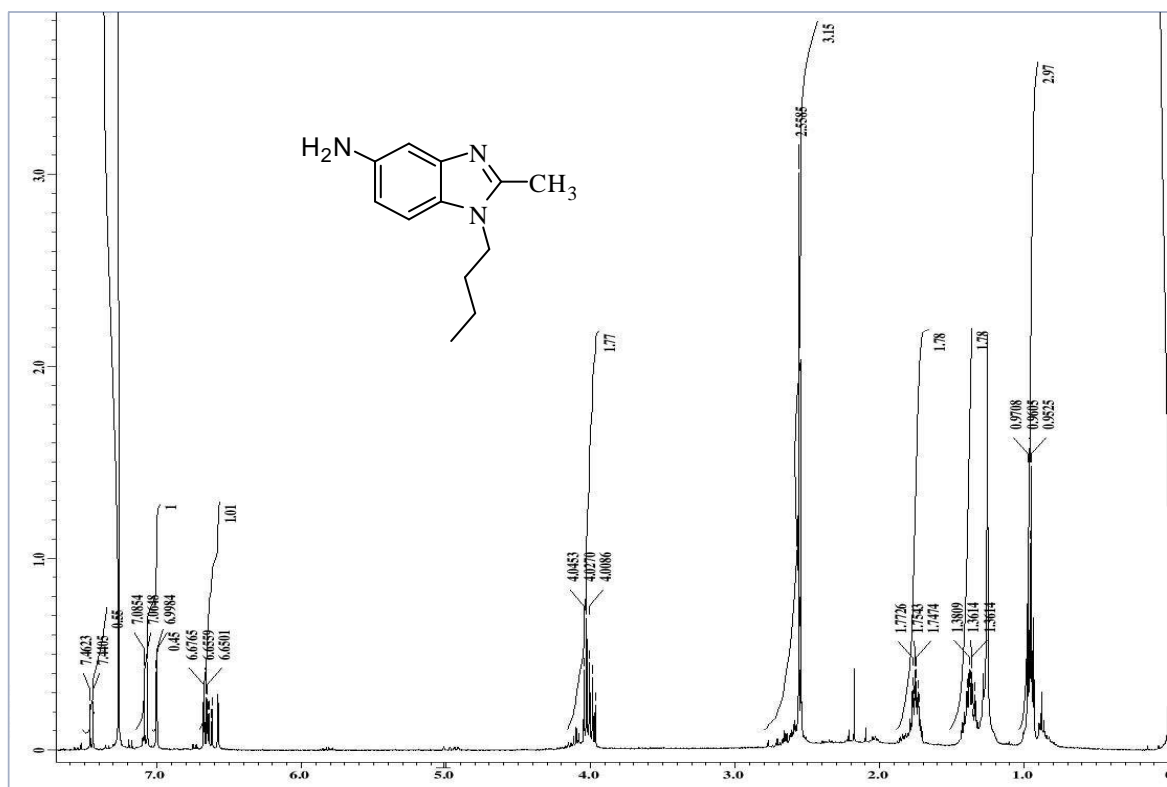


Figure S1. ^1H NMR spectrum of compound **2b** in CDCl_3

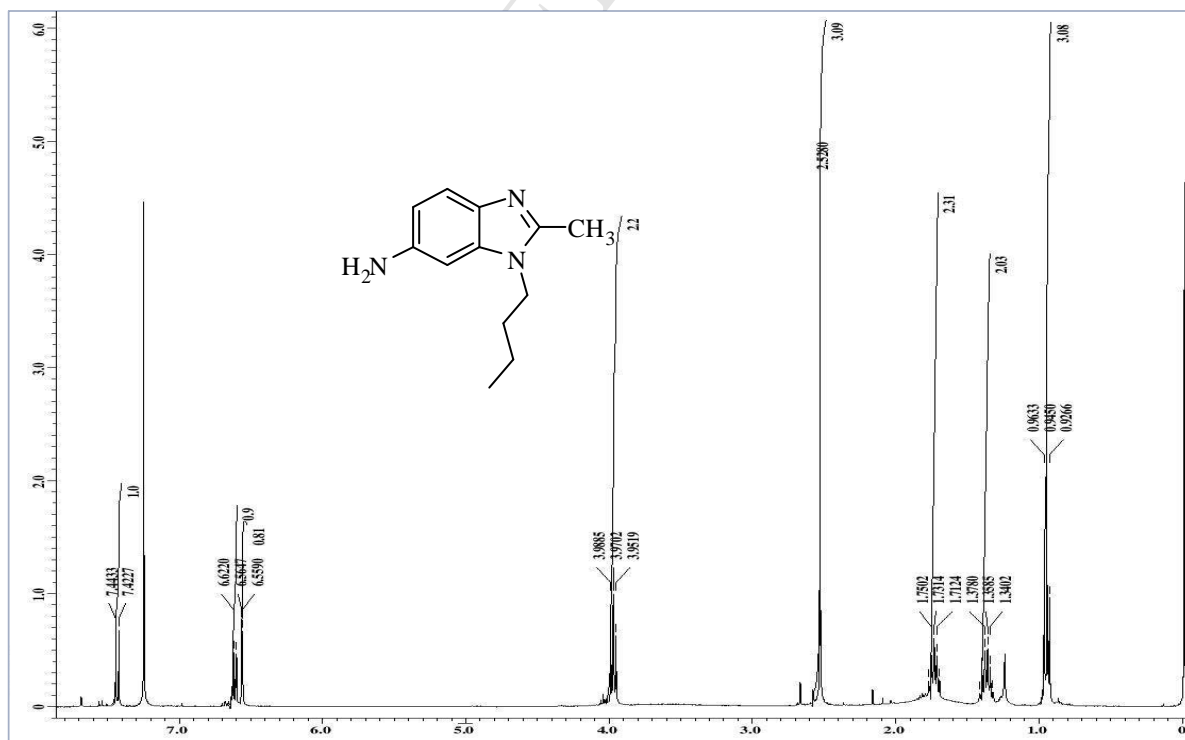


Figure S2. ^1H NMR spectrum of compound **2d** in CDCl_3 .

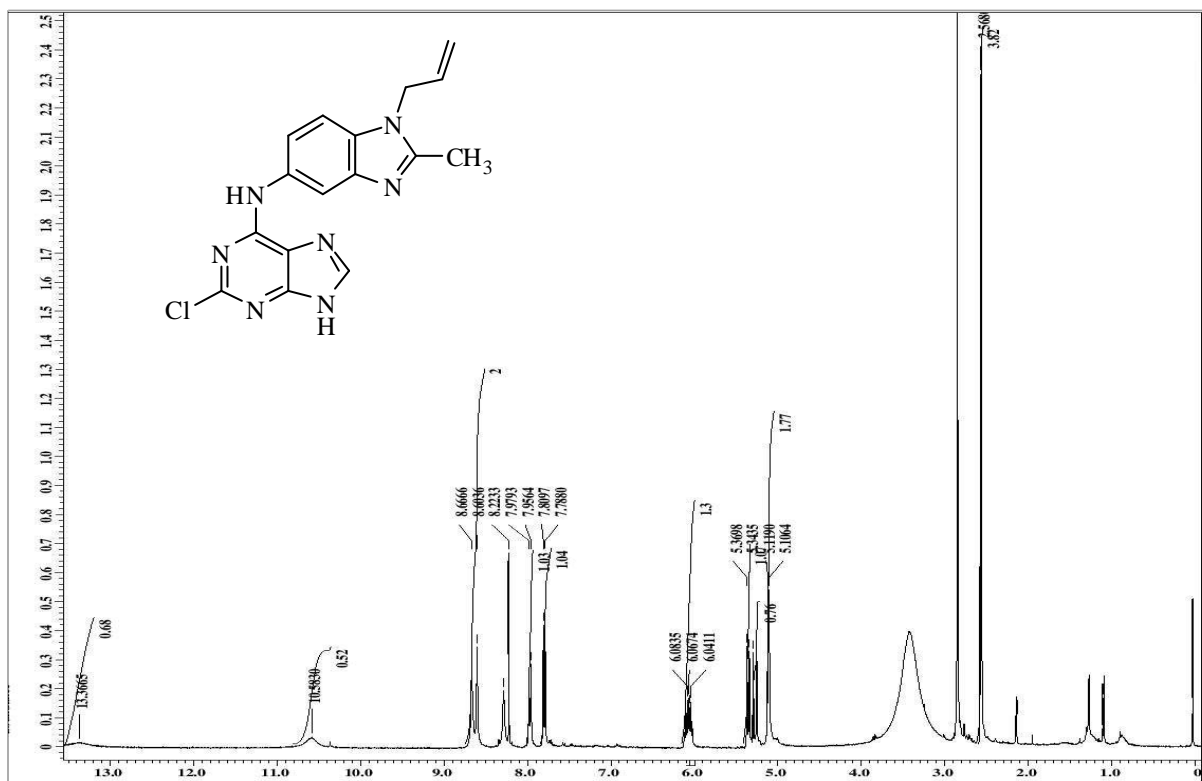


Figure S3. ¹H NMR spectrum of compound 3a in DMSO-*d*₆.

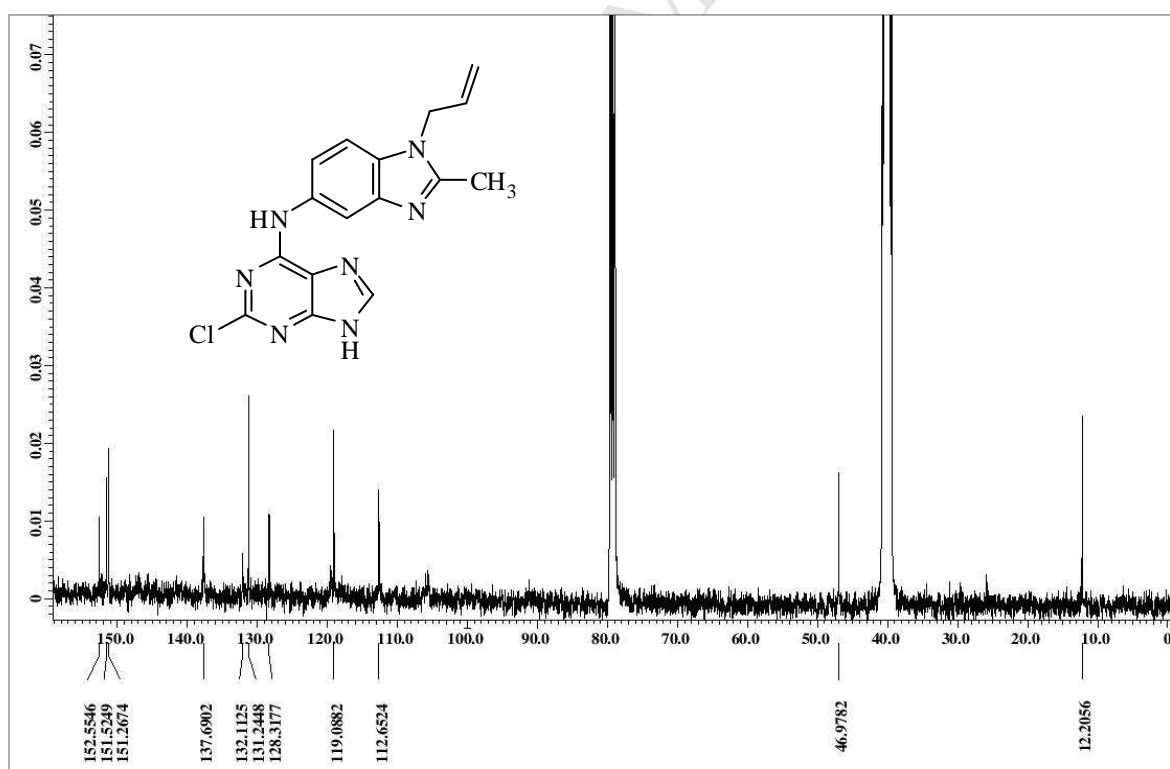
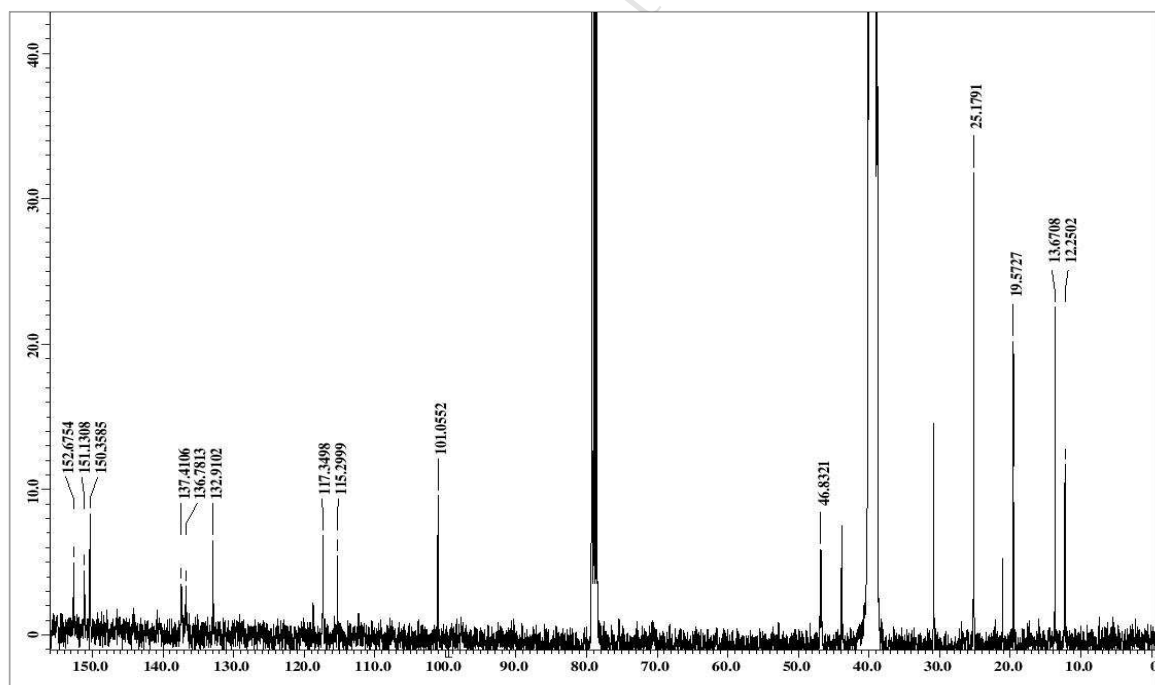
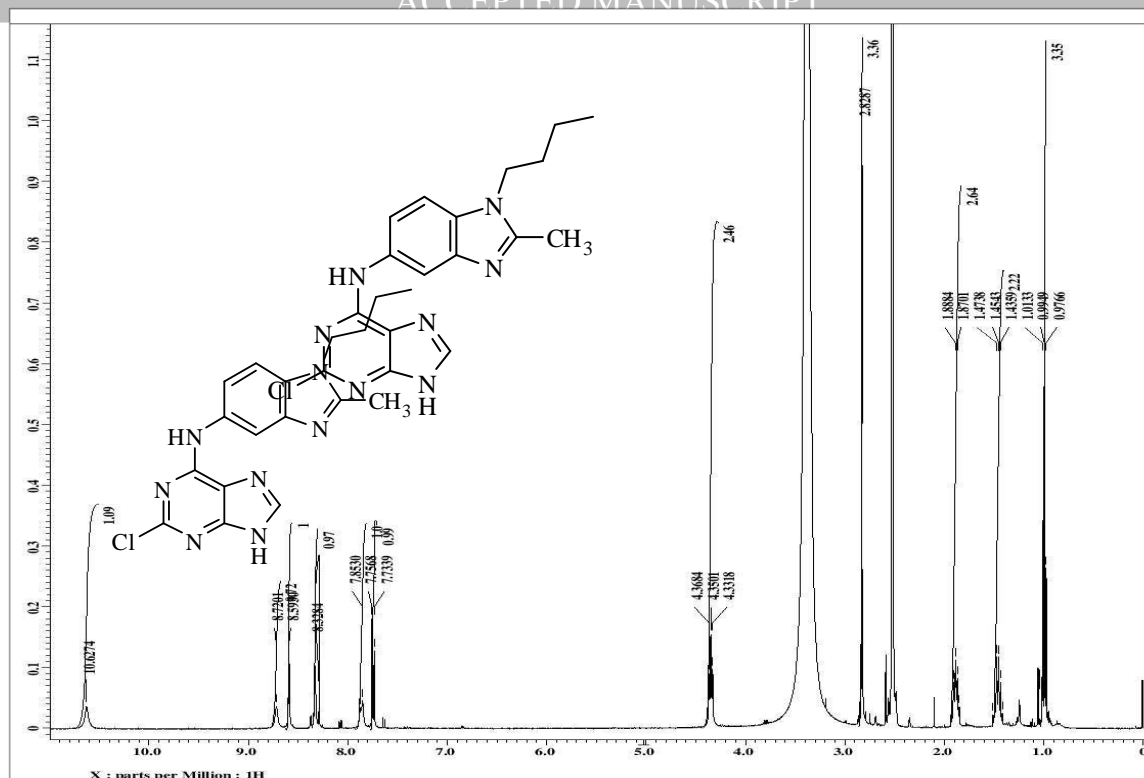


Figure S4. ¹³C NMR spectrum of compound 3a in DMSO-*d*₆.



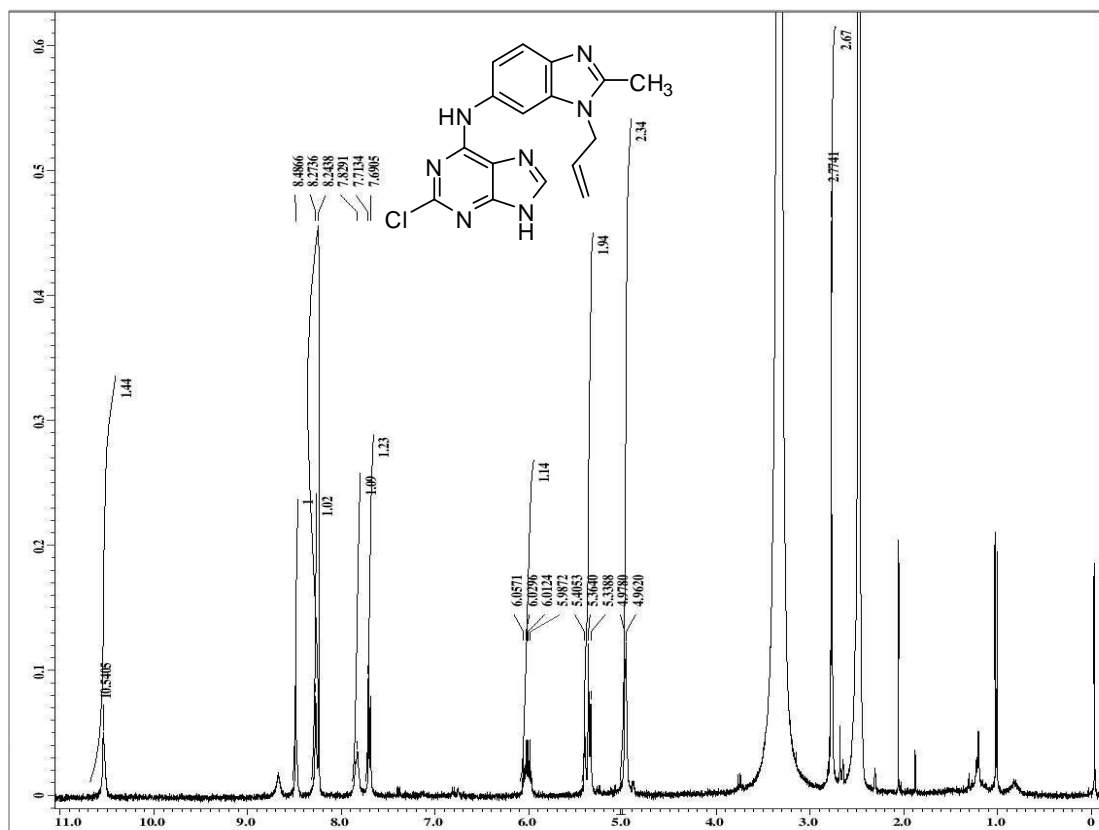


Figure S7. $^1\text{H NMR}$ spectrum of compound 3c in $\text{DMSO-}d_6$.

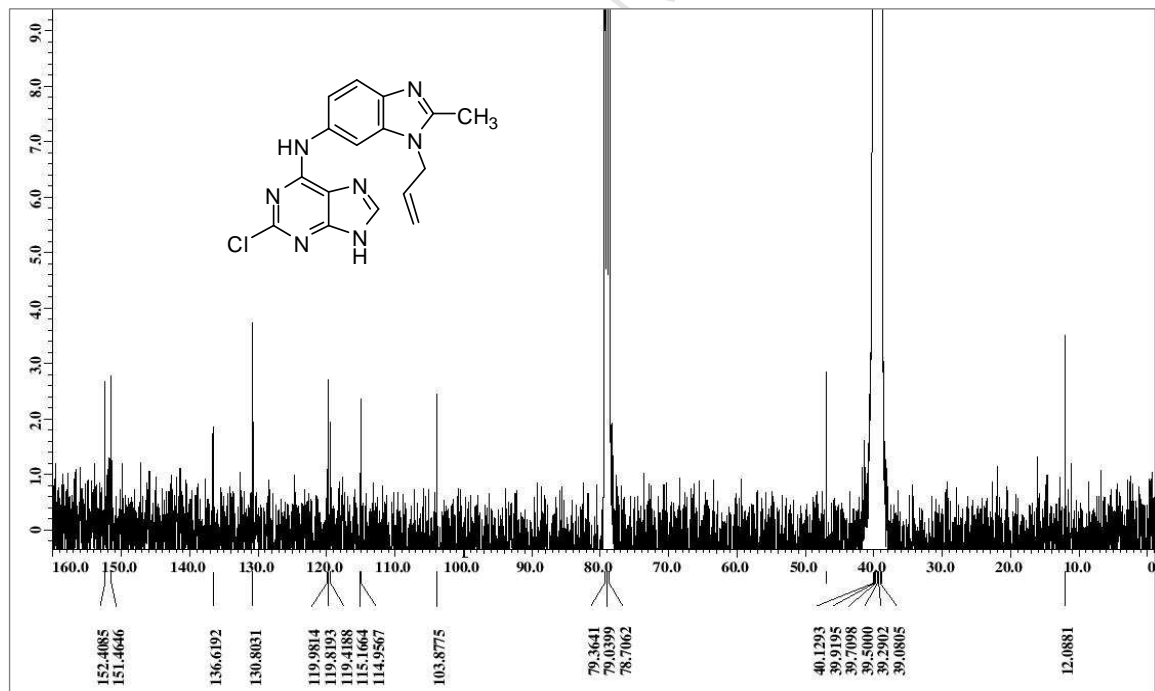


Figure S8. $^{13}\text{C NMR}$ spectrum of compound 3c in $\text{DMSO-}d_6$.

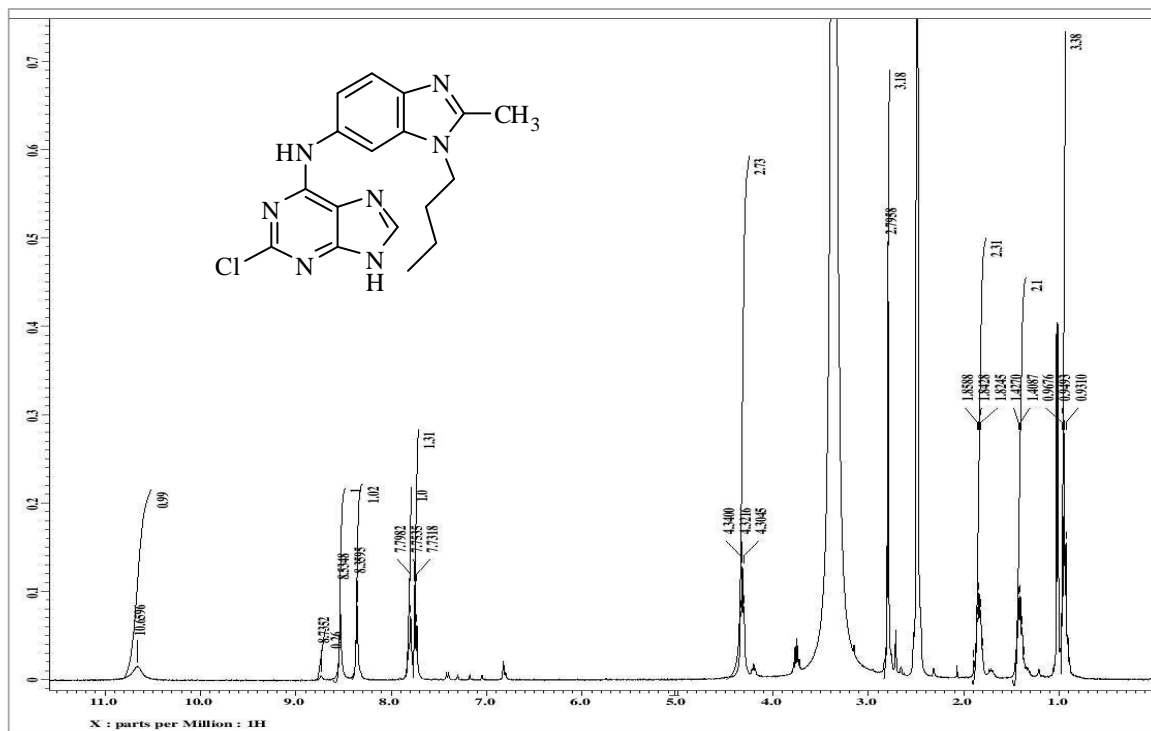


Figure S9. ^1H NMR spectrum of compound **3d** in $\text{DMSO-}d_6$.

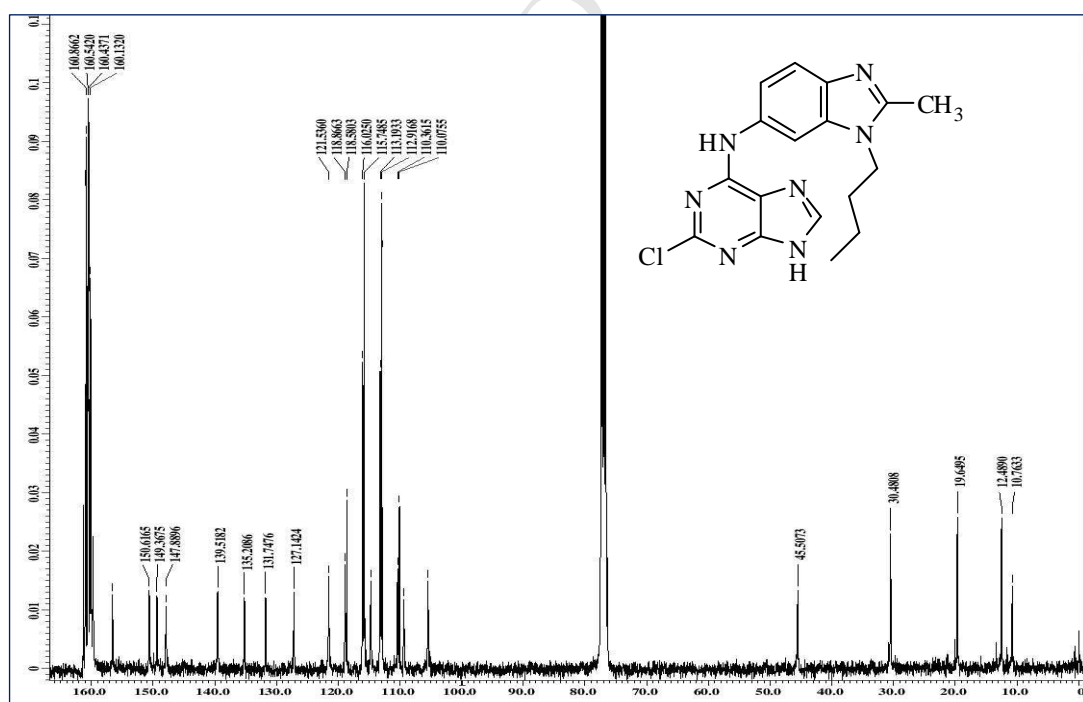


Figure S10. ^{13}C NMR spectrum of compound **3d** in TFA+CDCl_3 .

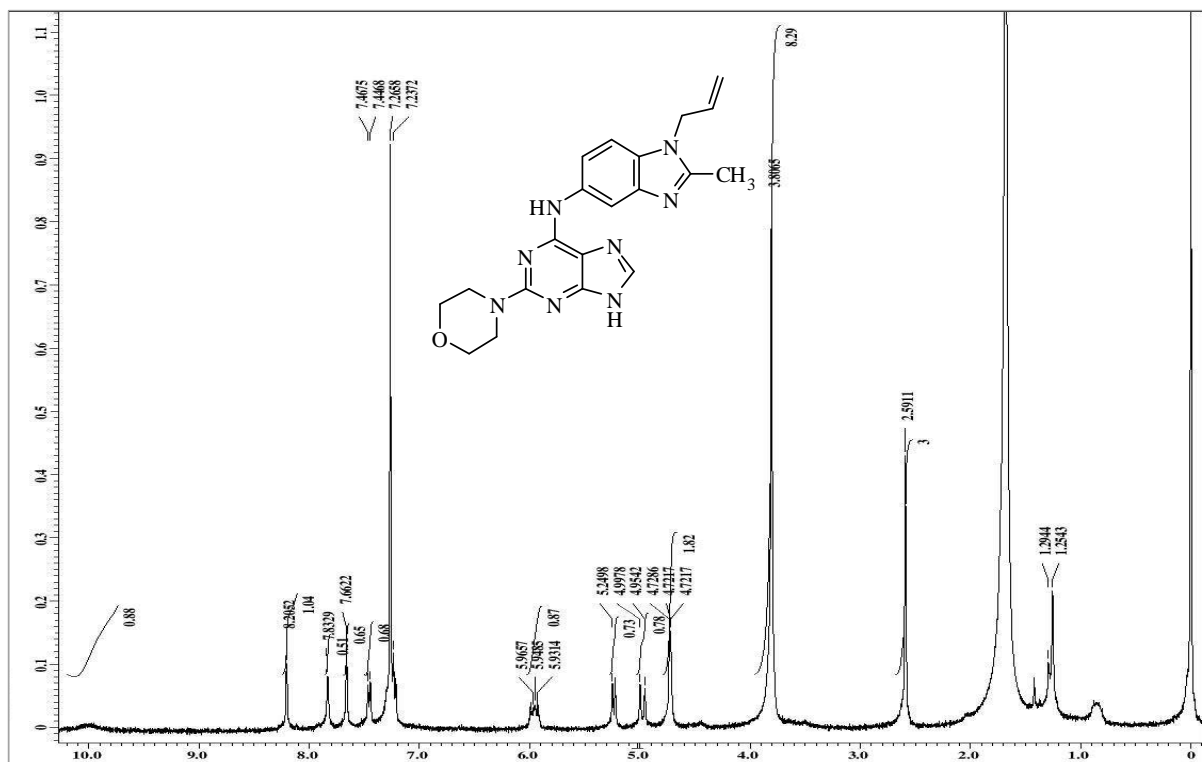


Figure S11. ^1H NMR spectrum of compound 4 in $\text{DMSO-}d_6$.

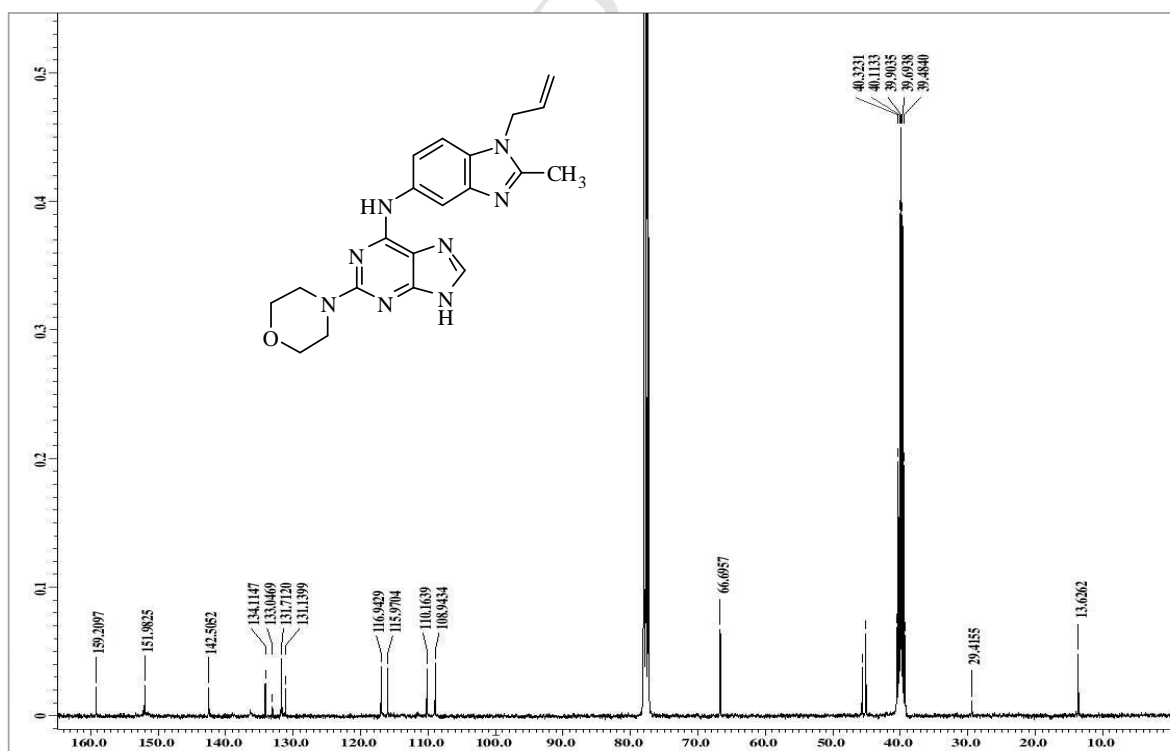


Figure S12. ^{13}C NMR spectrum of compound 4 in $\text{DMSO-}d_6$.

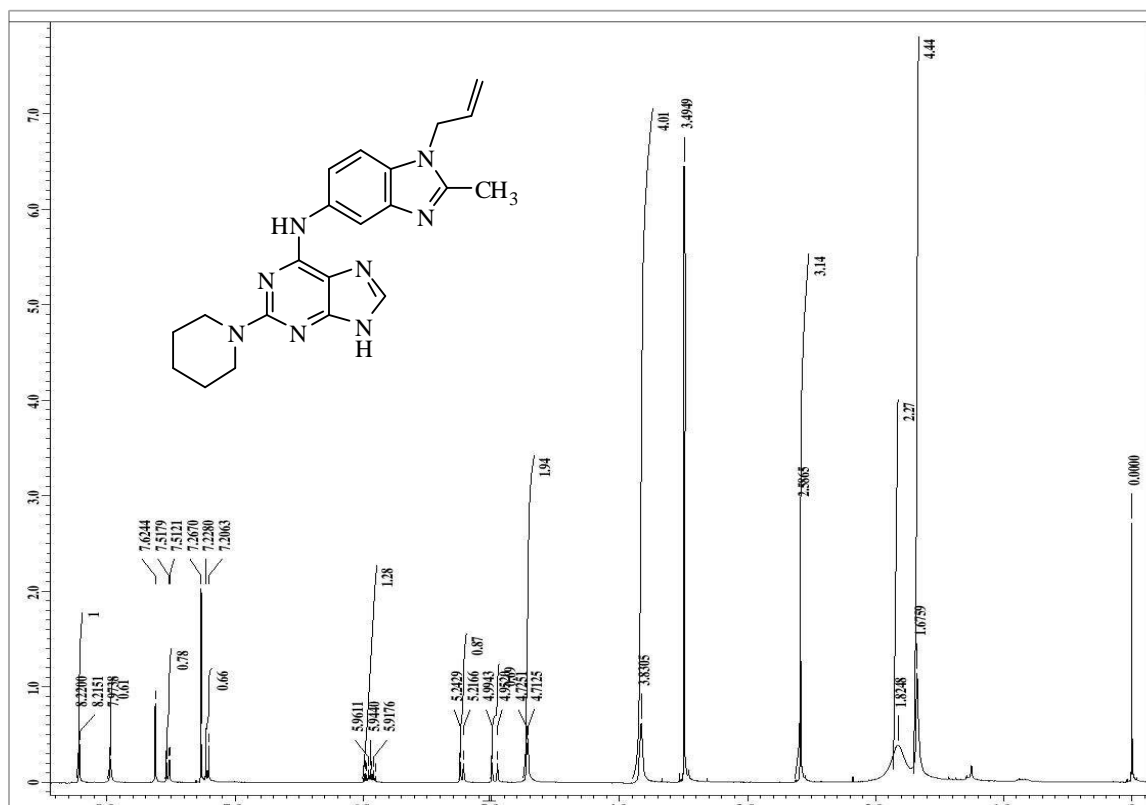


Figure S13. ¹H NMR spectrum of compound 5 in CDCl₃.

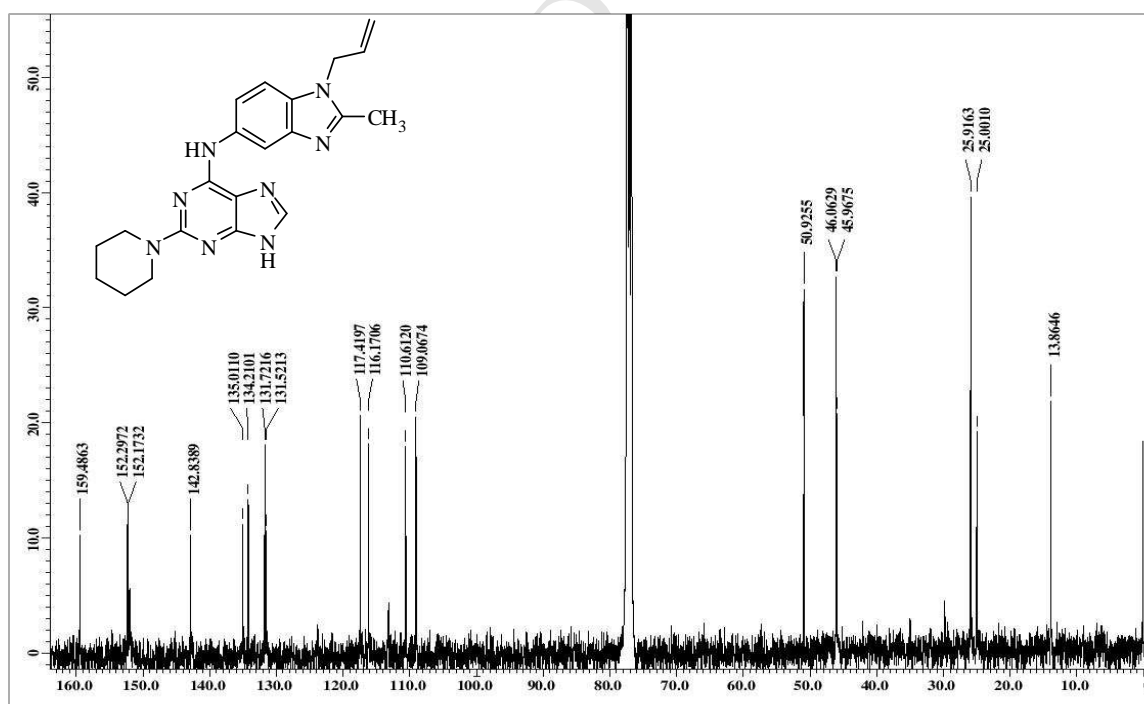


Figure S14. ¹³C NMR spectrum of compound 5 in CDCl₃.

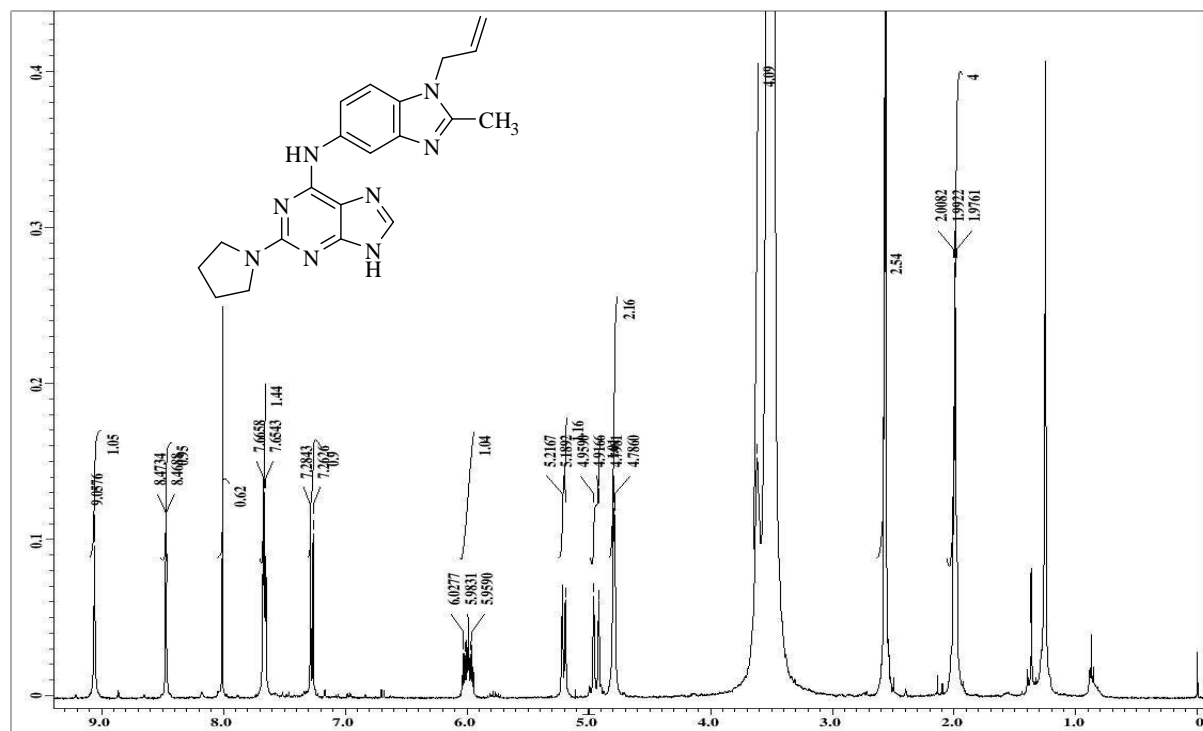


Figure S15. ¹H NMR spectrum of compound 6 in DMSO-*d*₆.

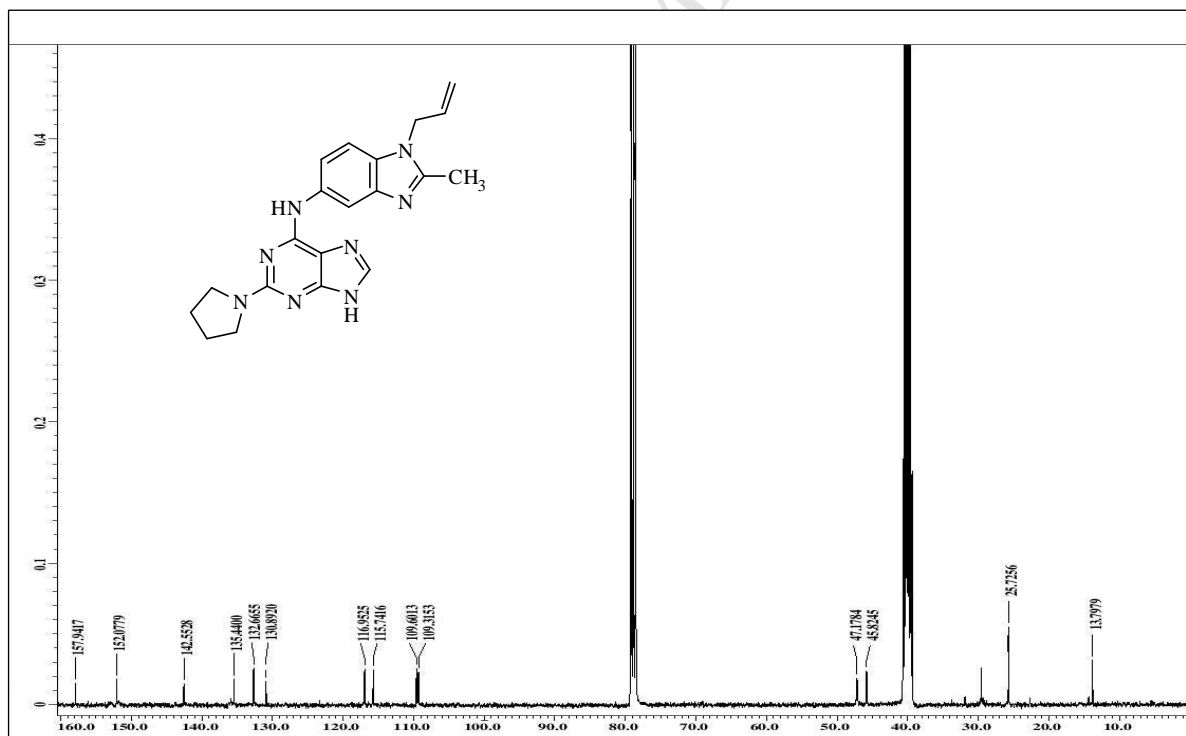


Figure S16. ¹³C NMR spectrum of compound 6 in DMSO-*d*₆.

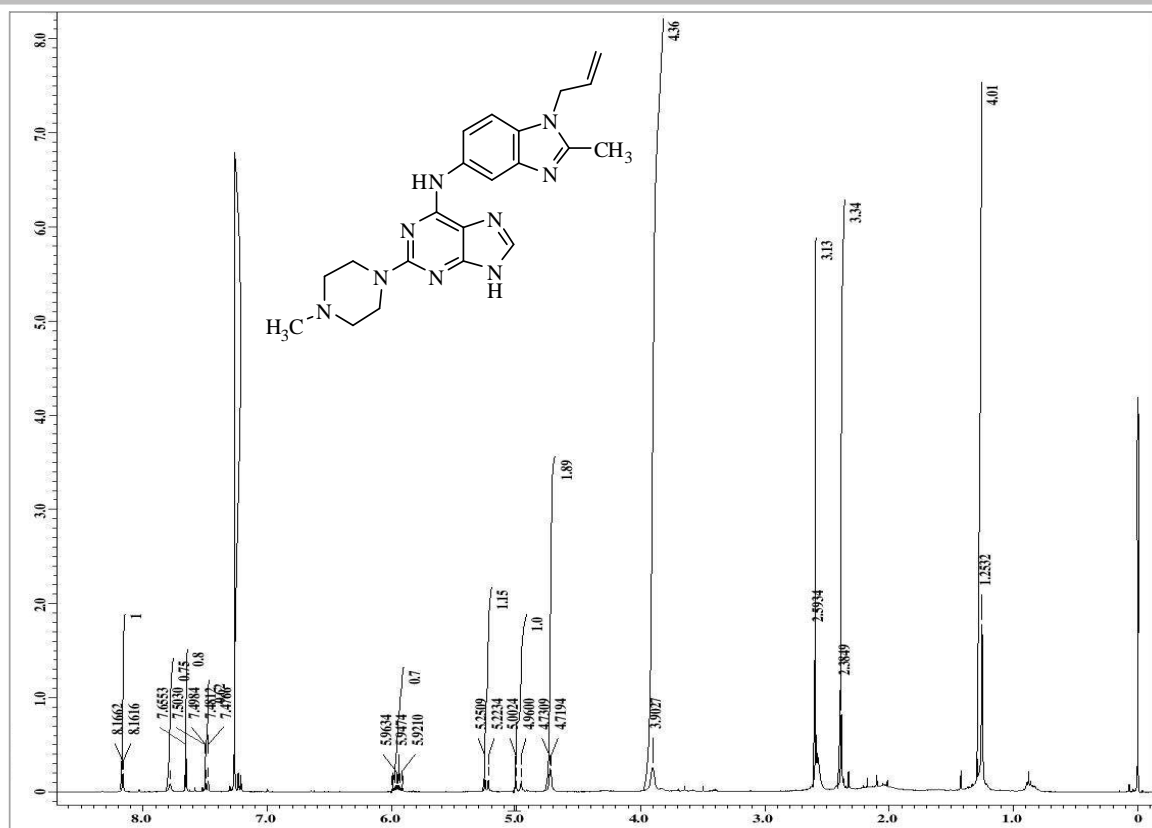


Figure S17. ^1H NMR spectrum of compound **7** in CDCl_3 .

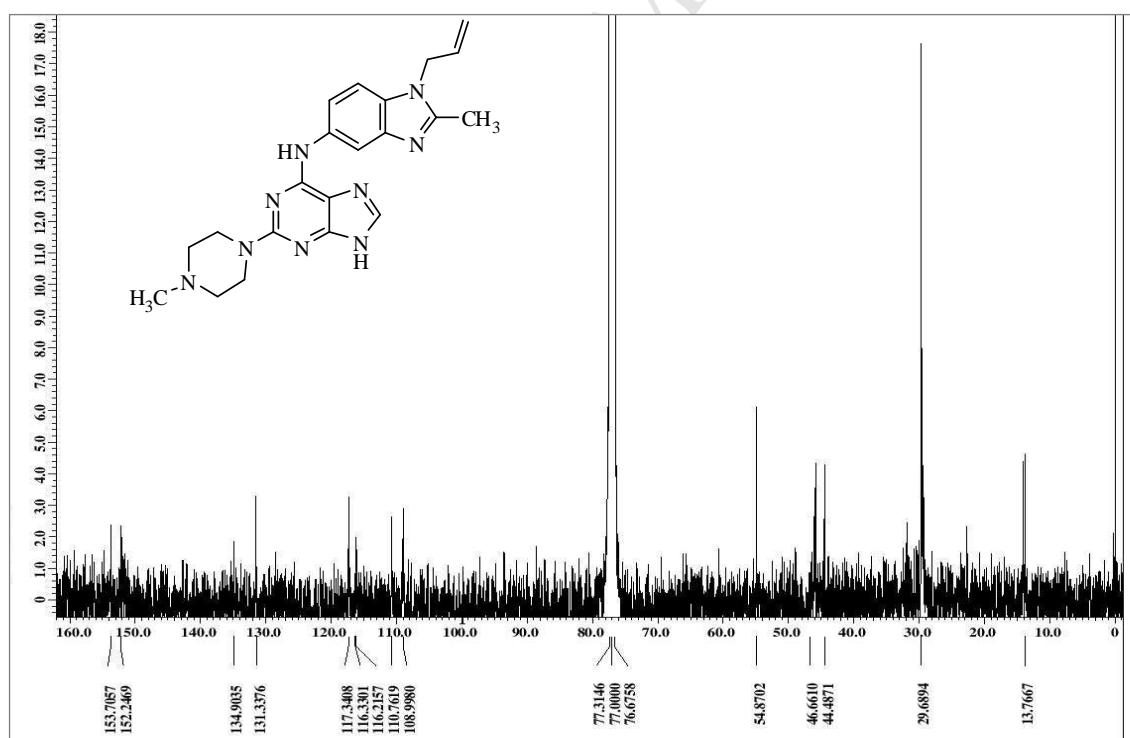


Figure S18. ^{13}C NMR spectrum of compound **7** in CDCl_3 .

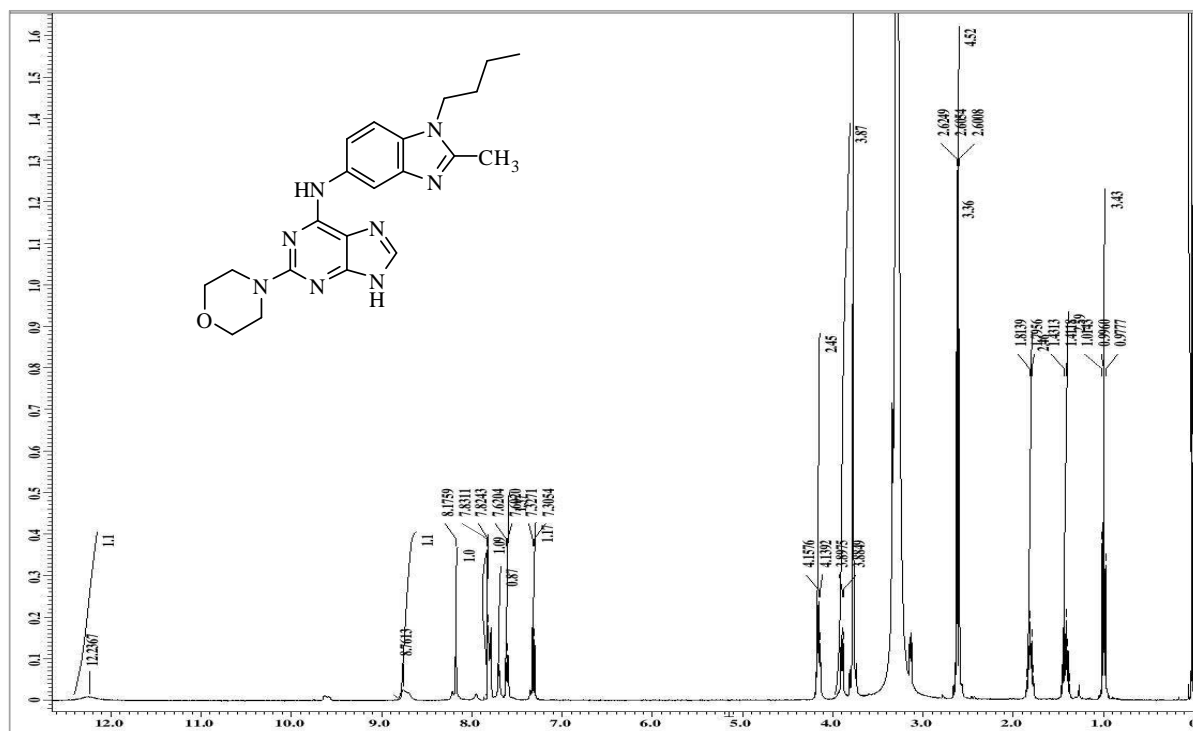


Figure S19. ^1H NMR spectrum of compound **8** in $\text{DMSO-}d_6$.

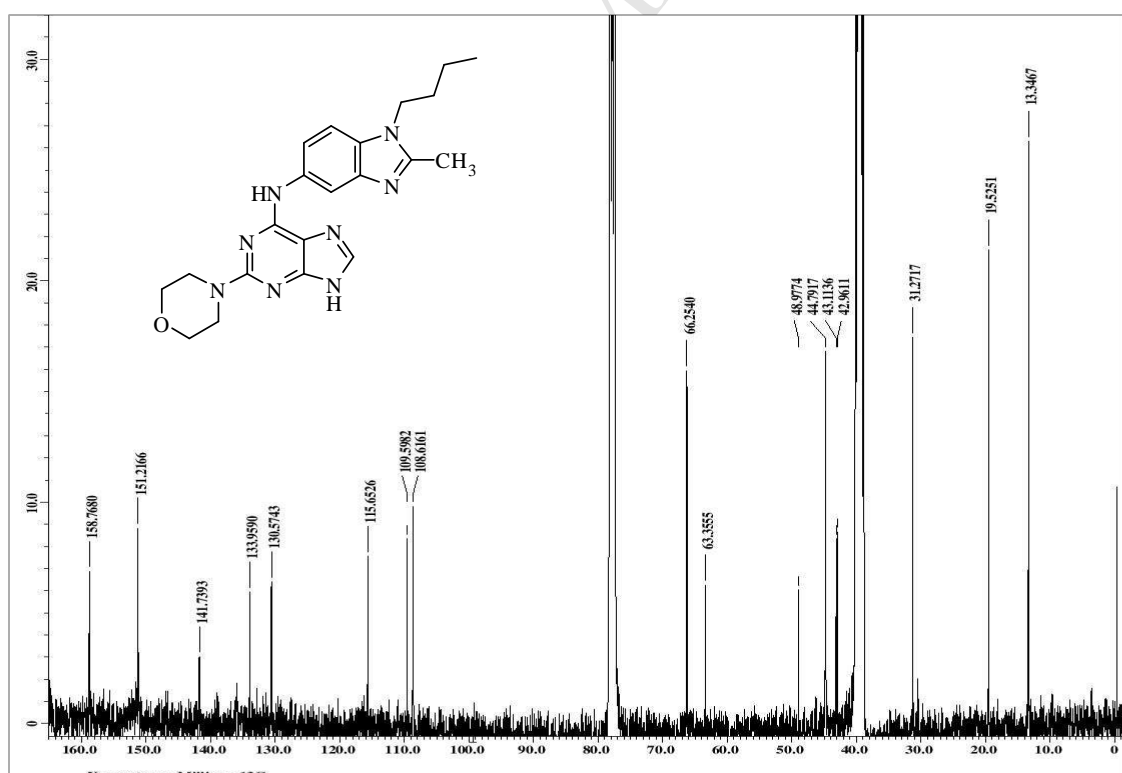


Figure S20. ^{13}C NMR spectrum of compound **8** in $\text{DMSO-}d_6$.

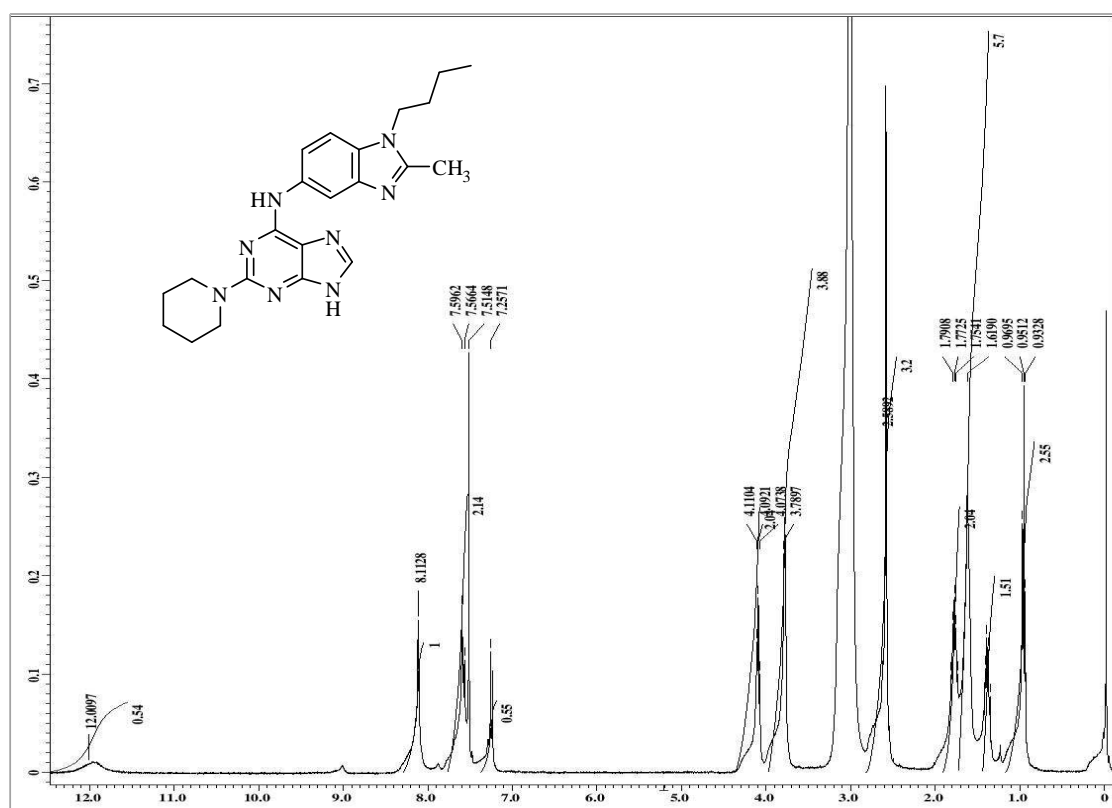


Figure S21. ¹H NMR spectrum of compound 9 in DMSO-*d*₆.

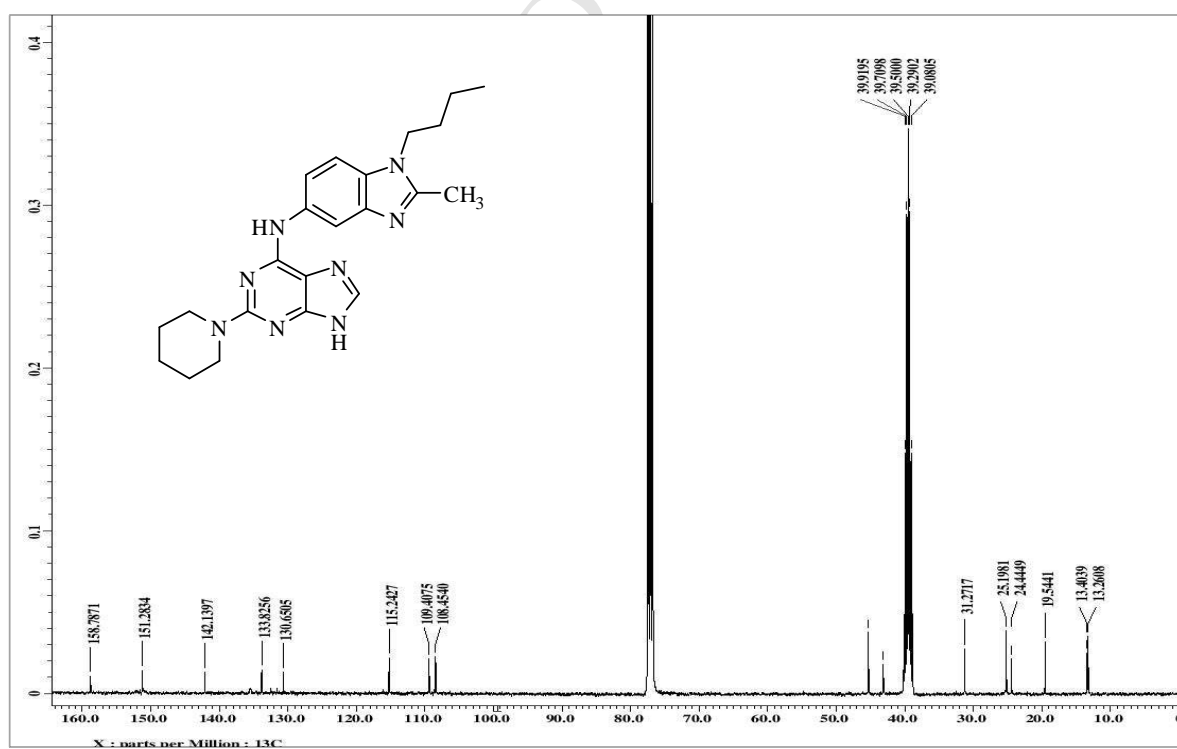


Figure S22. ¹³C NMR spectrum of compound 9 in DMSO-*d*₆.

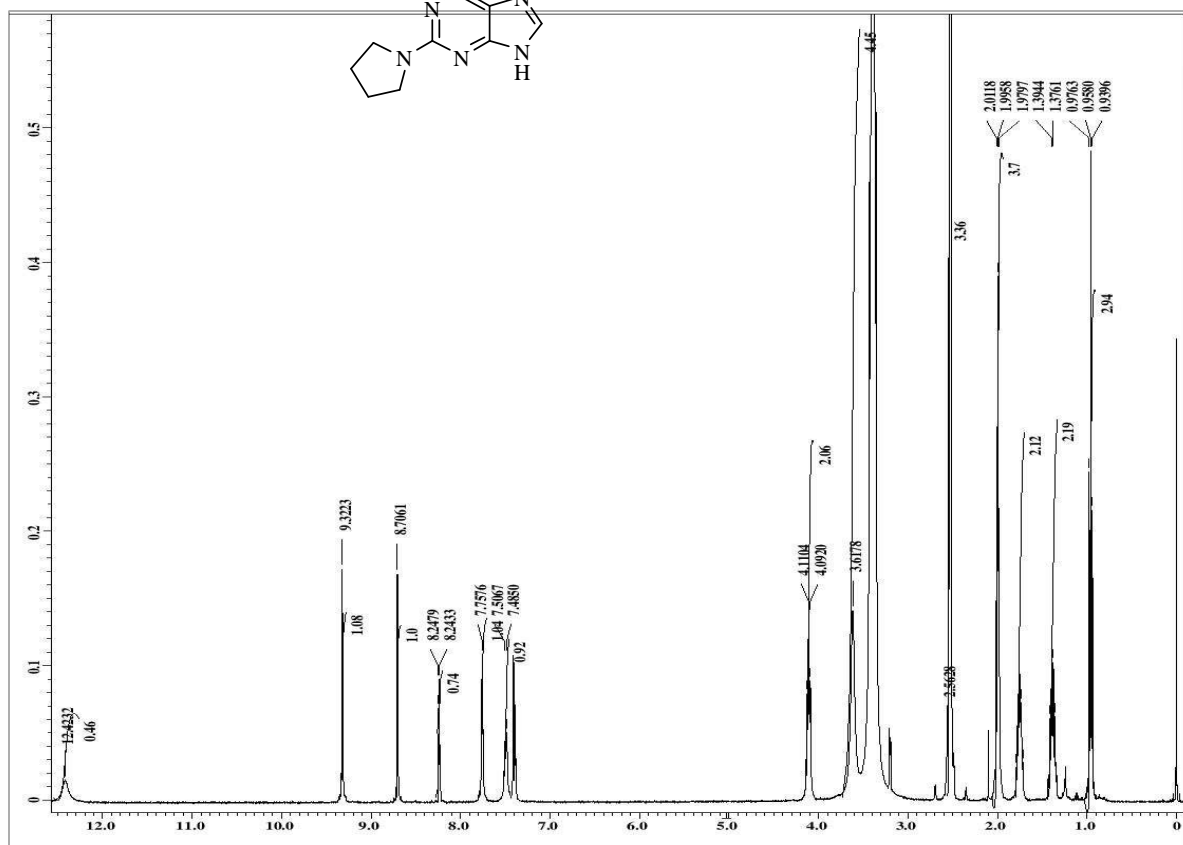


Figure S23. ¹H NMR spectrum of compound 10 in DMSO-*d*₆.

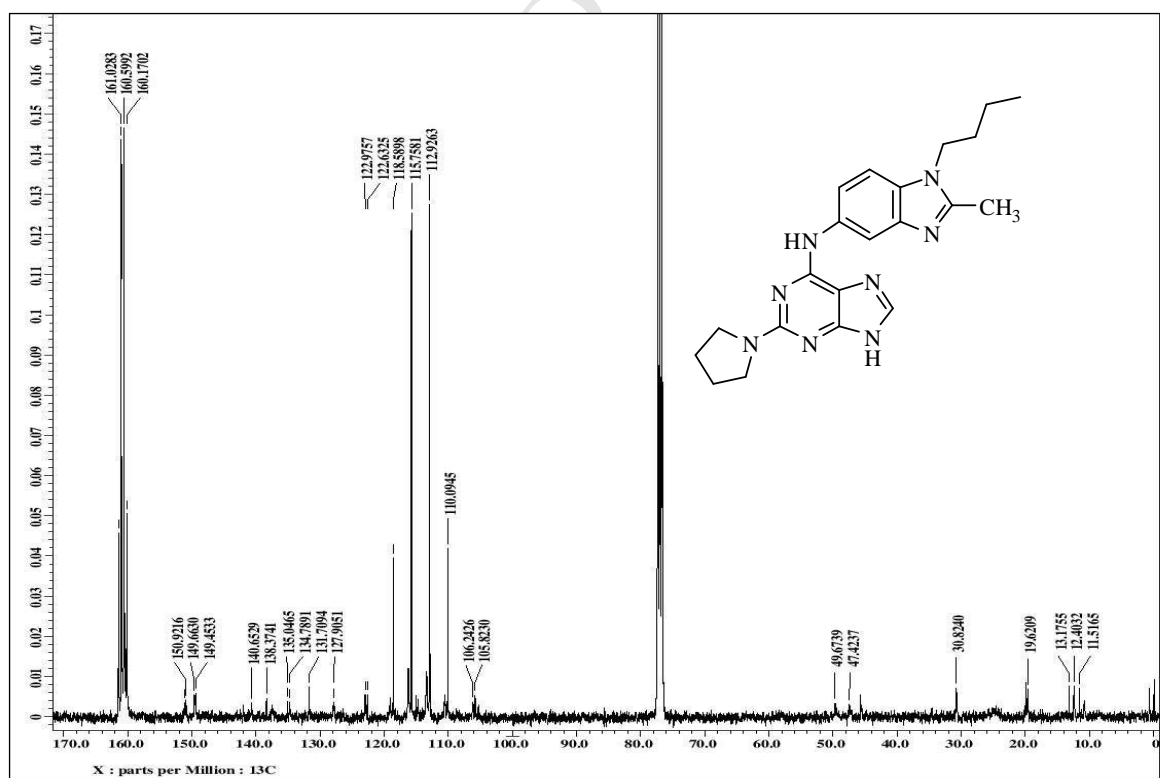


Figure S24. ¹³C NMR spectrum of compound 10 in TFA+CDCl₃.

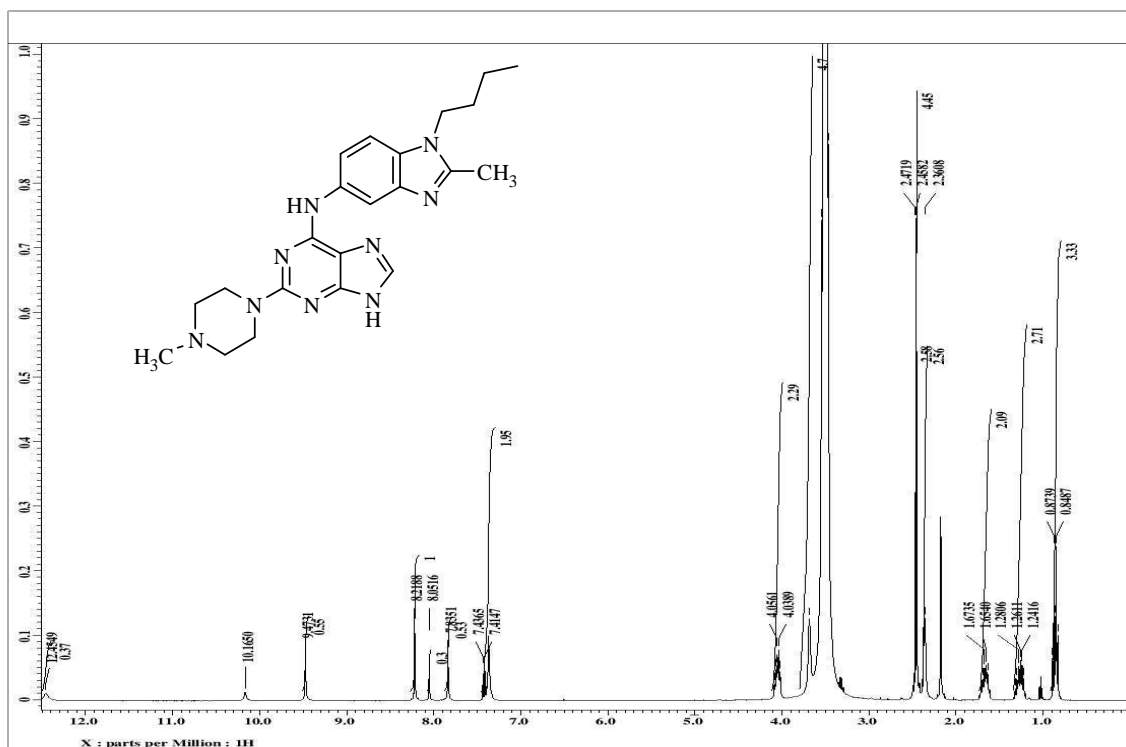


Figure S25. ^1H NMR spectrum of compound 11 in $\text{DMSO-}d_6$.

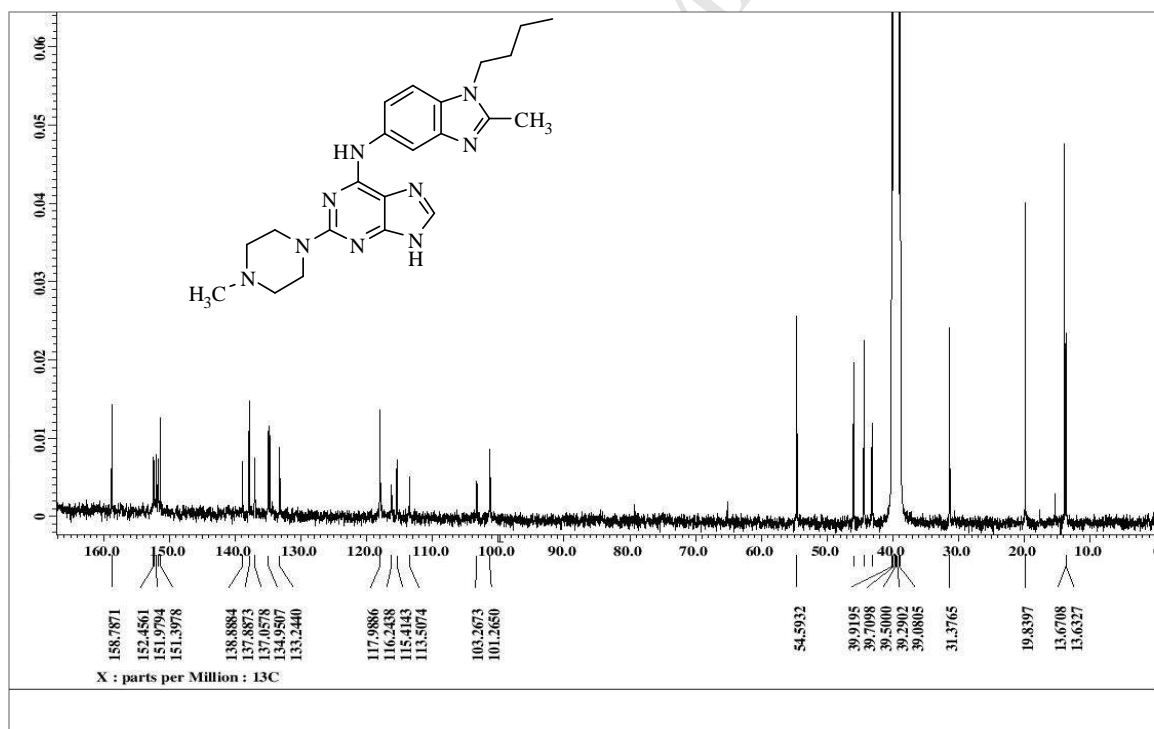


Figure S26. ^{13}C NMR spectrum of compound 11 in $\text{DMSO-}d_6$.

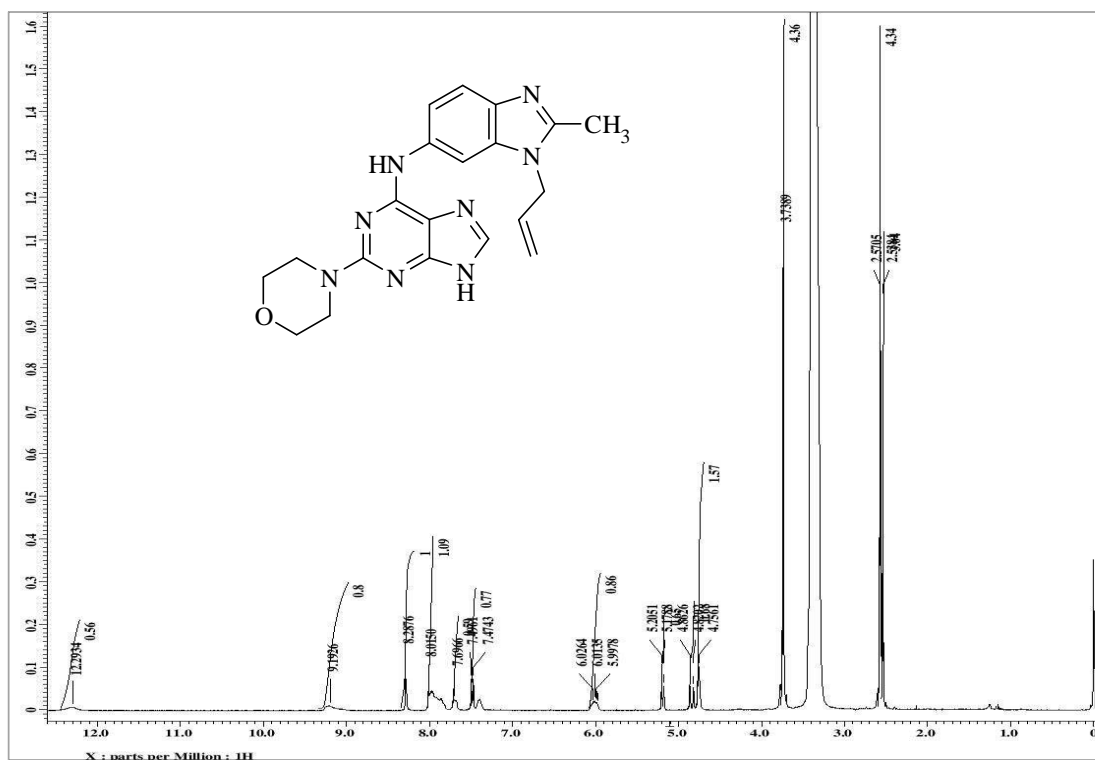


Figure S27. ¹H NMR spectrum of compound 12 in DMSO-*d*₆.

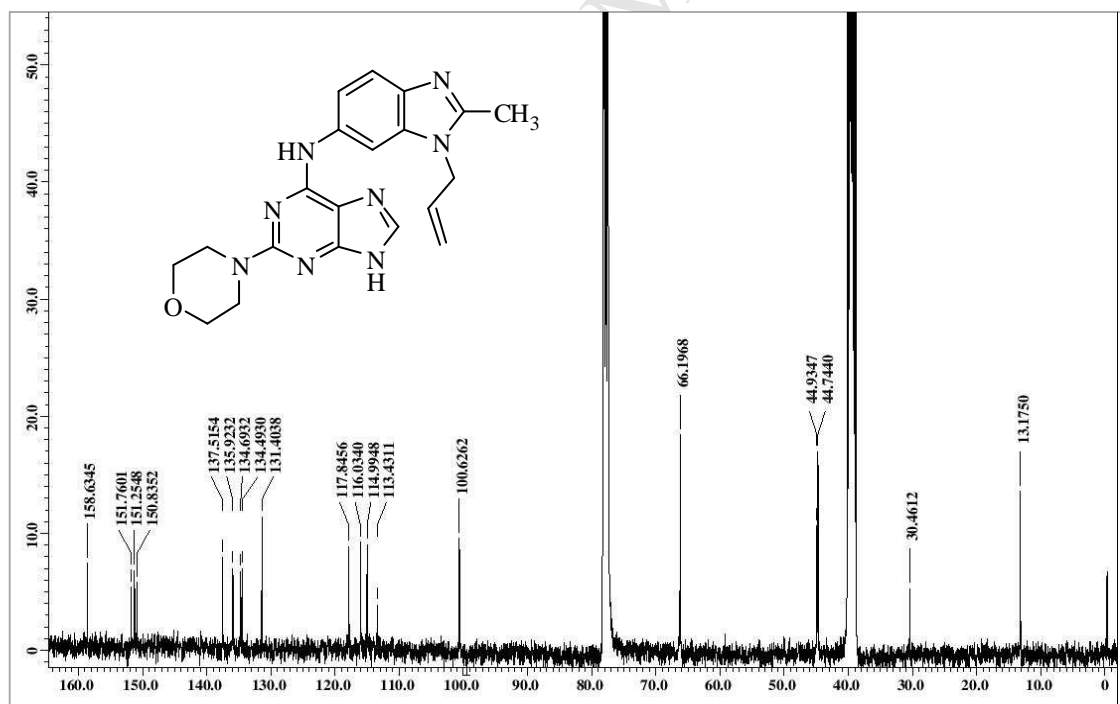


Figure S28. ¹³C NMR spectrum of compound 12 in DMSO-*d*₆.

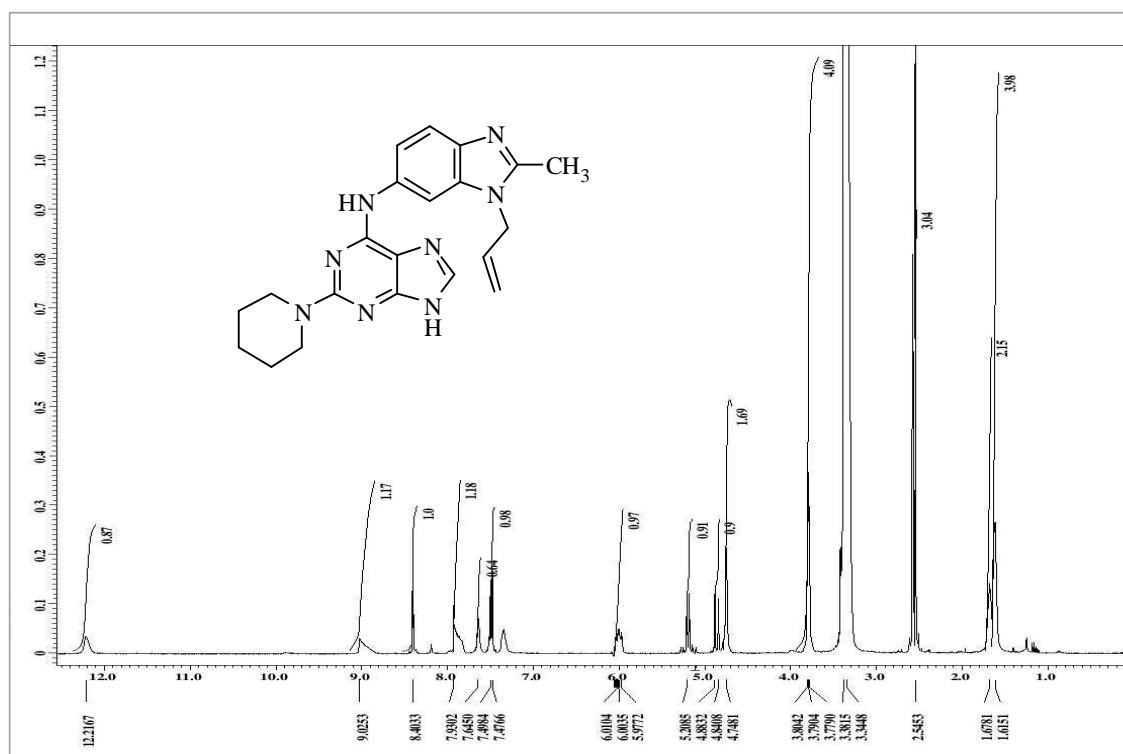


Figure S29. ^1H NMR spectrum of compound **13** in $\text{DMSO-}d_6$.

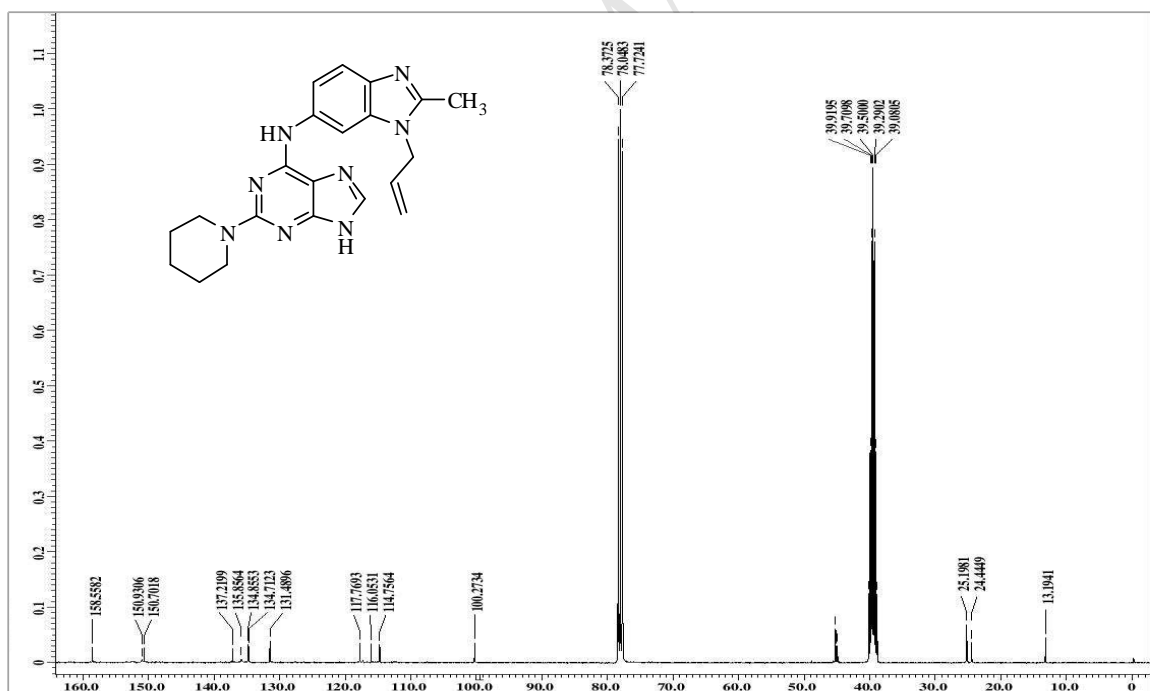


Figure S30. ^{13}C NMR spectrum of compound **13** in $\text{DMSO-}d_6$.

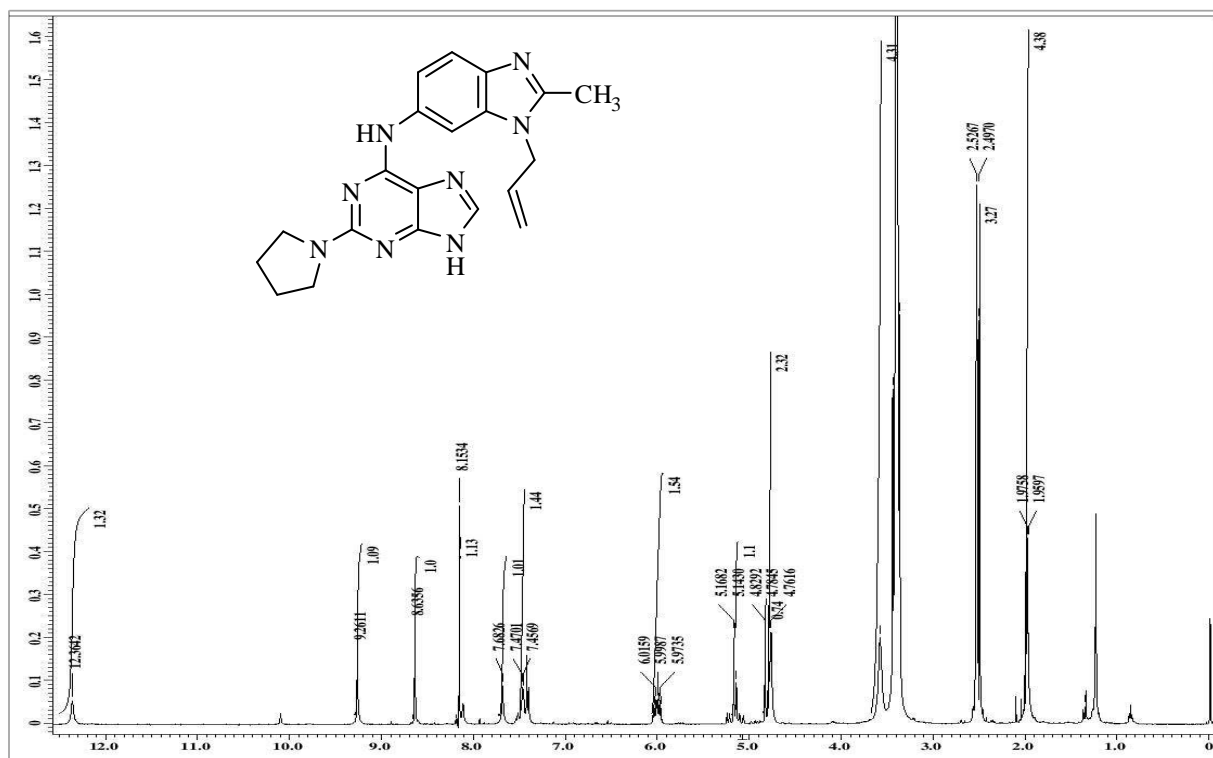


Figure S31. ^1H NMR spectrum of compound 14 in $\text{DMSO-}d_6$.

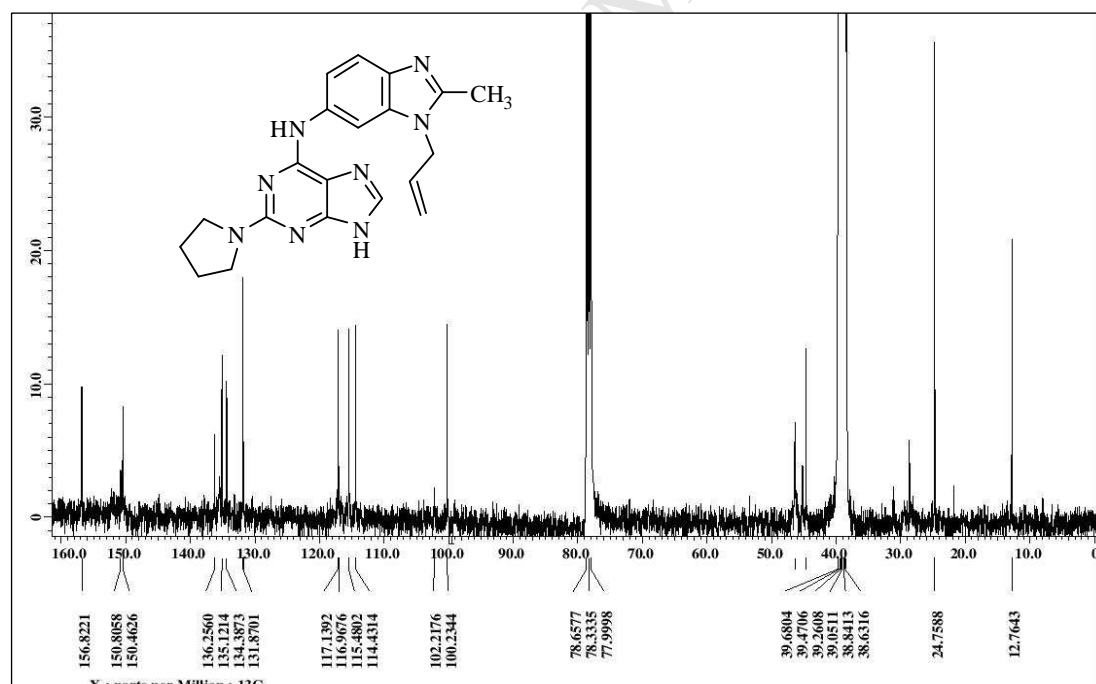


Figure S32. ^{13}C NMR spectrum of compound 14 in $\text{DMSO-}d_6$.

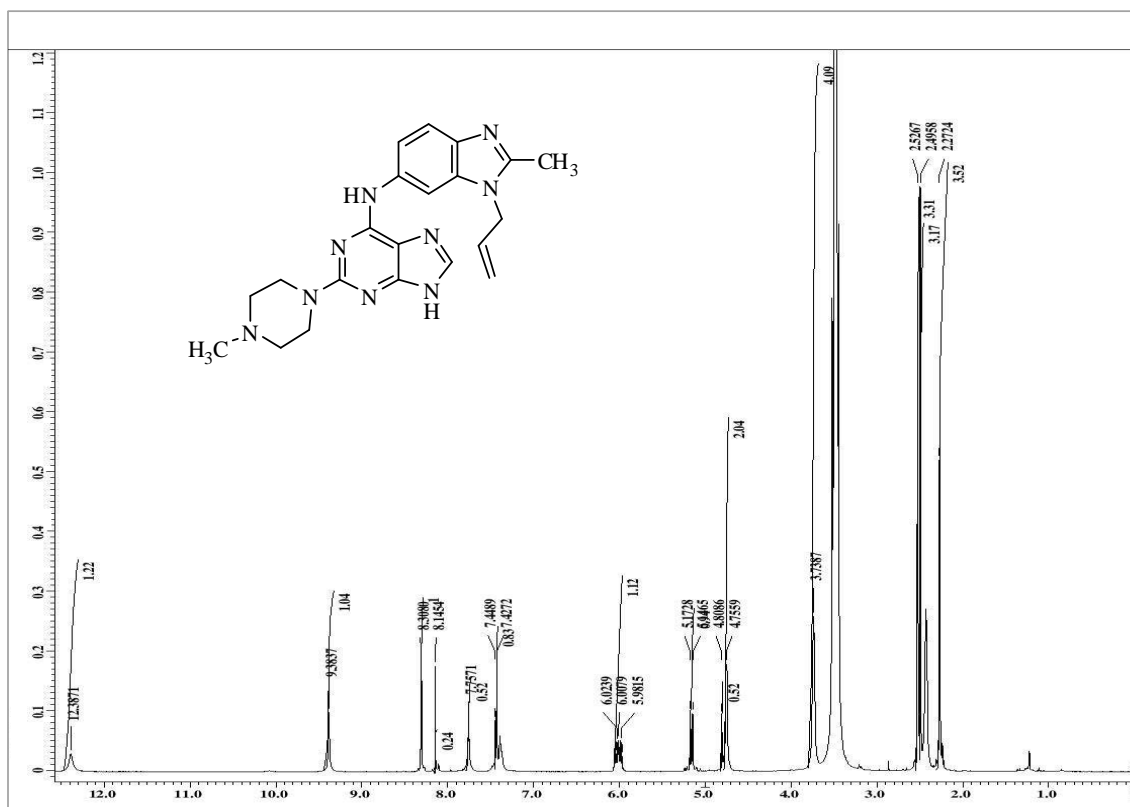


Figure S33. ^1H NMR spectrum of compound **15** in $\text{DMSO-}d_6$.

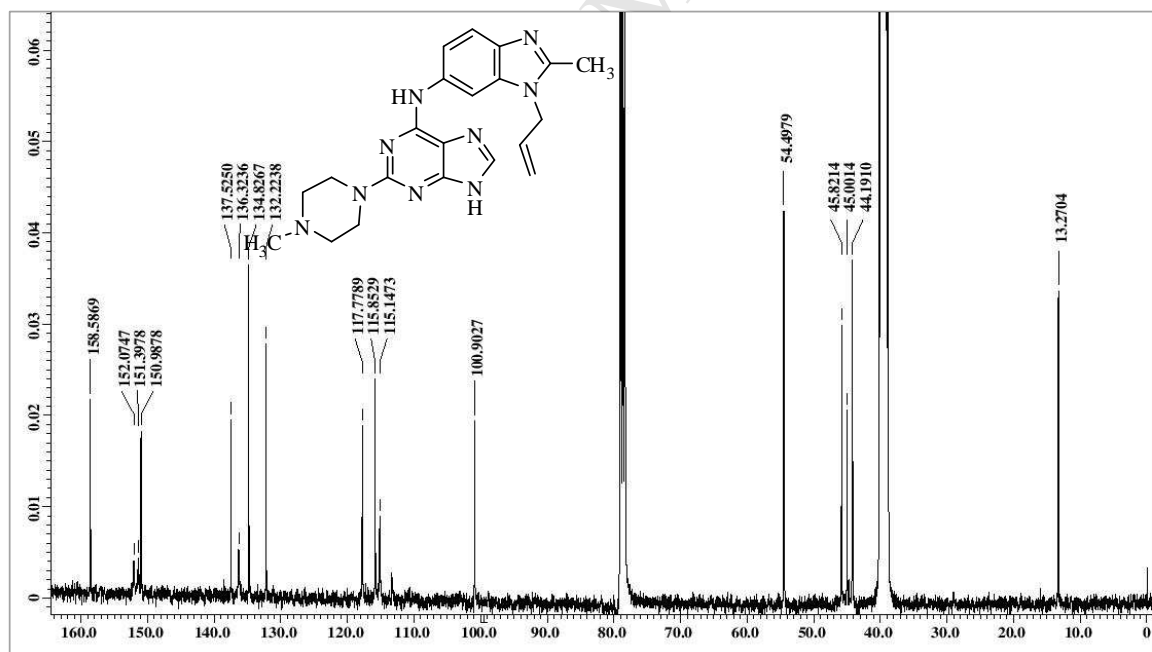


Figure S34. ^{13}C NMR spectrum of compound **15** in $\text{DMSO-}d_6$.

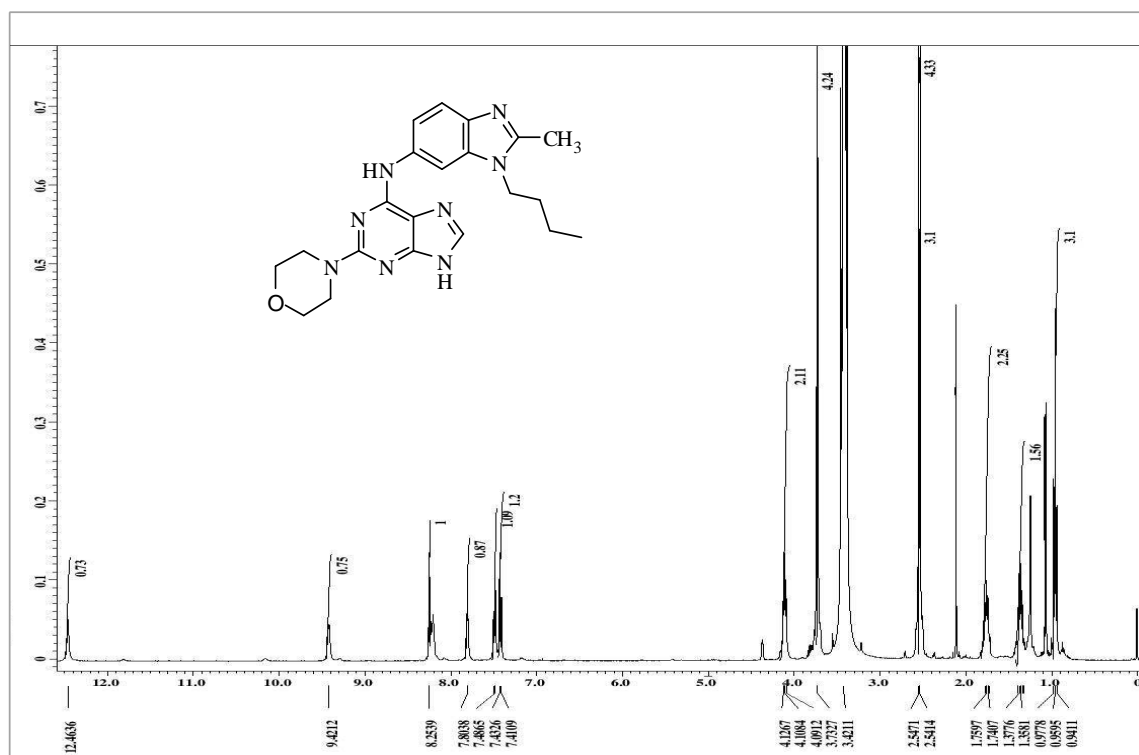


Figure S35. ^1H NMR spectrum of compound **16** in $\text{DMSO-}d_6$.

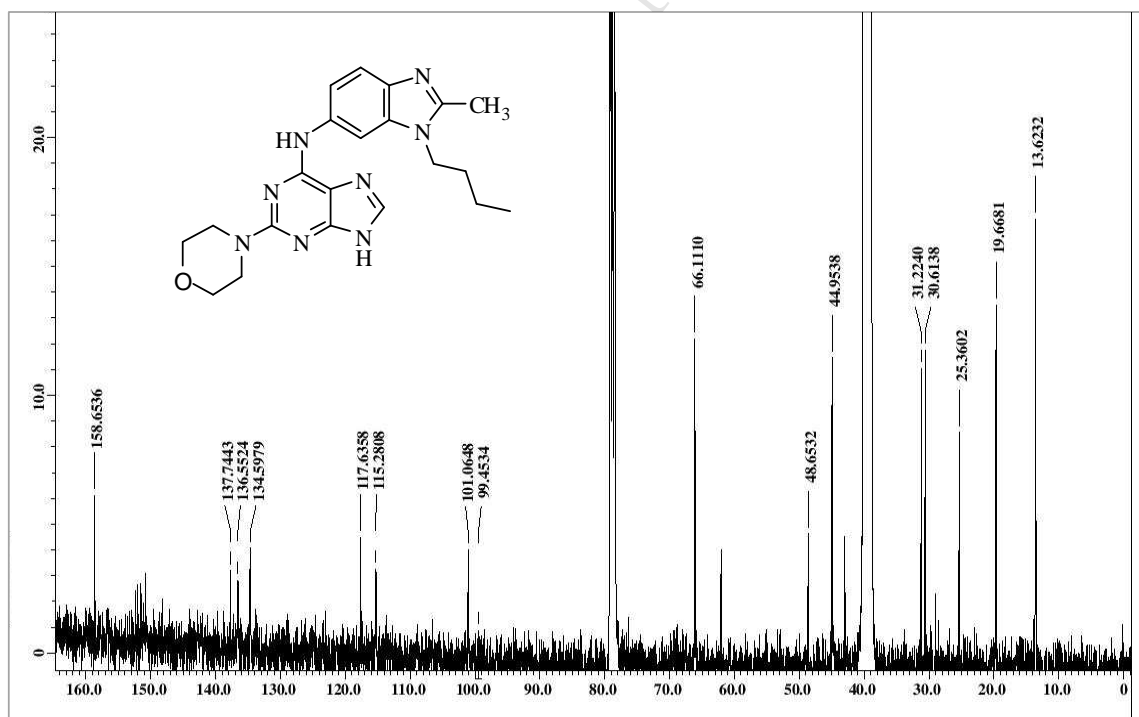


Figure S36. ^{13}C NMR spectrum of compound **16** in $\text{DMSO-}d_6$.

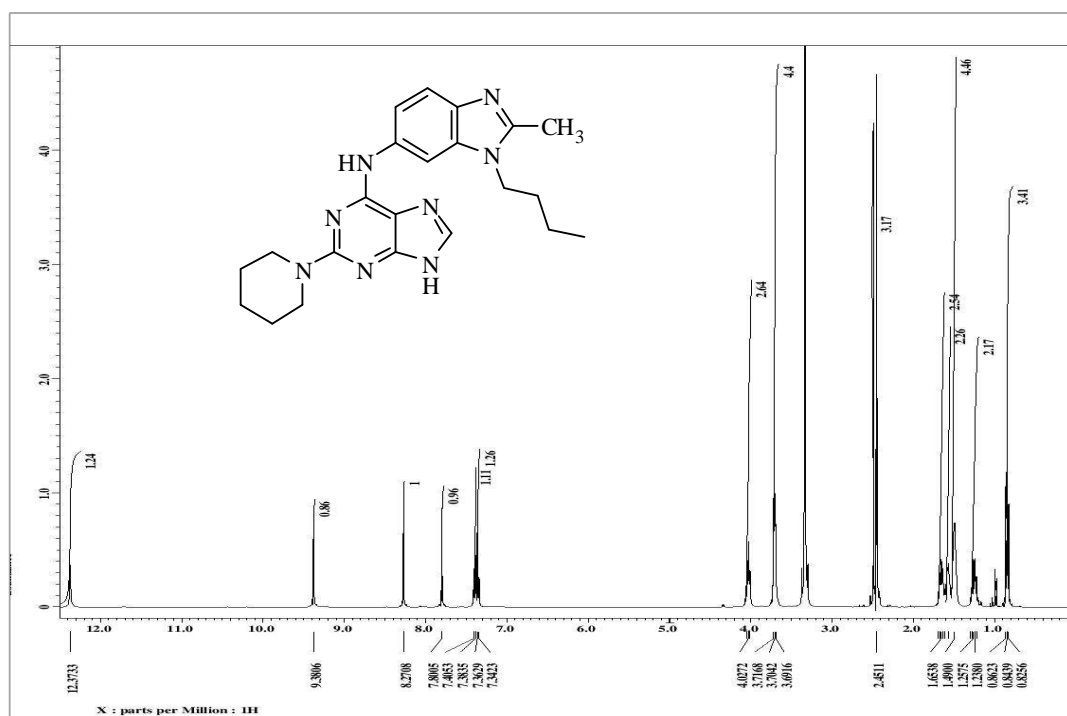


Figure S37. ^1H NMR spectrum of compound **17** in $\text{DMSO-}d_6$.

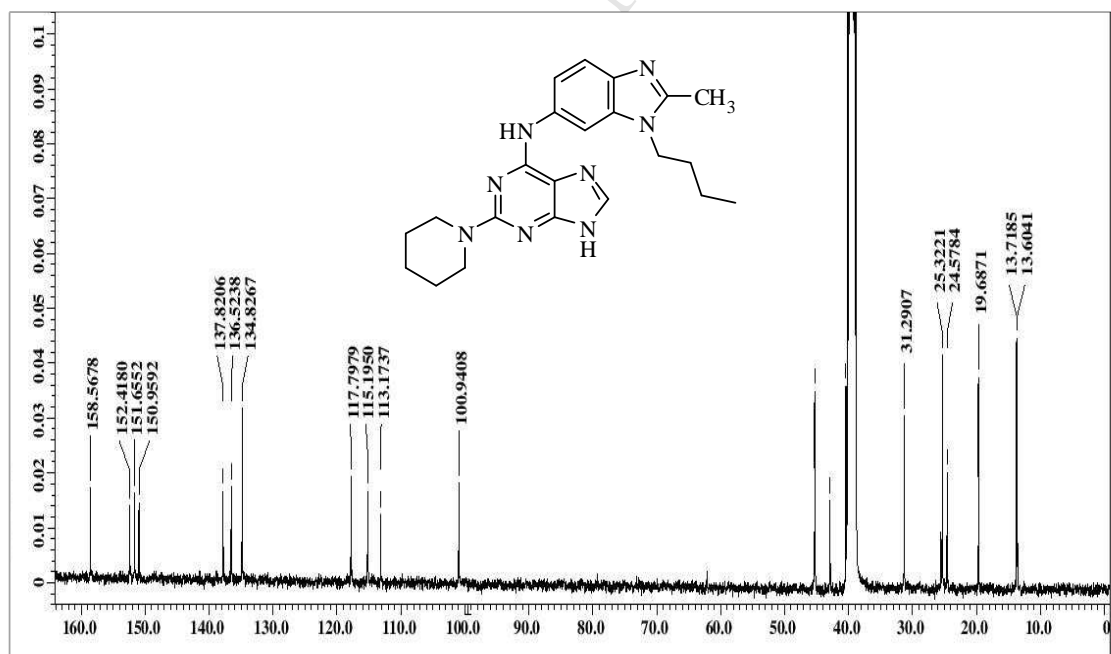


Figure S38. ^{13}C NMR spectrum of compound **17** in $\text{DMSO-}d_6$.

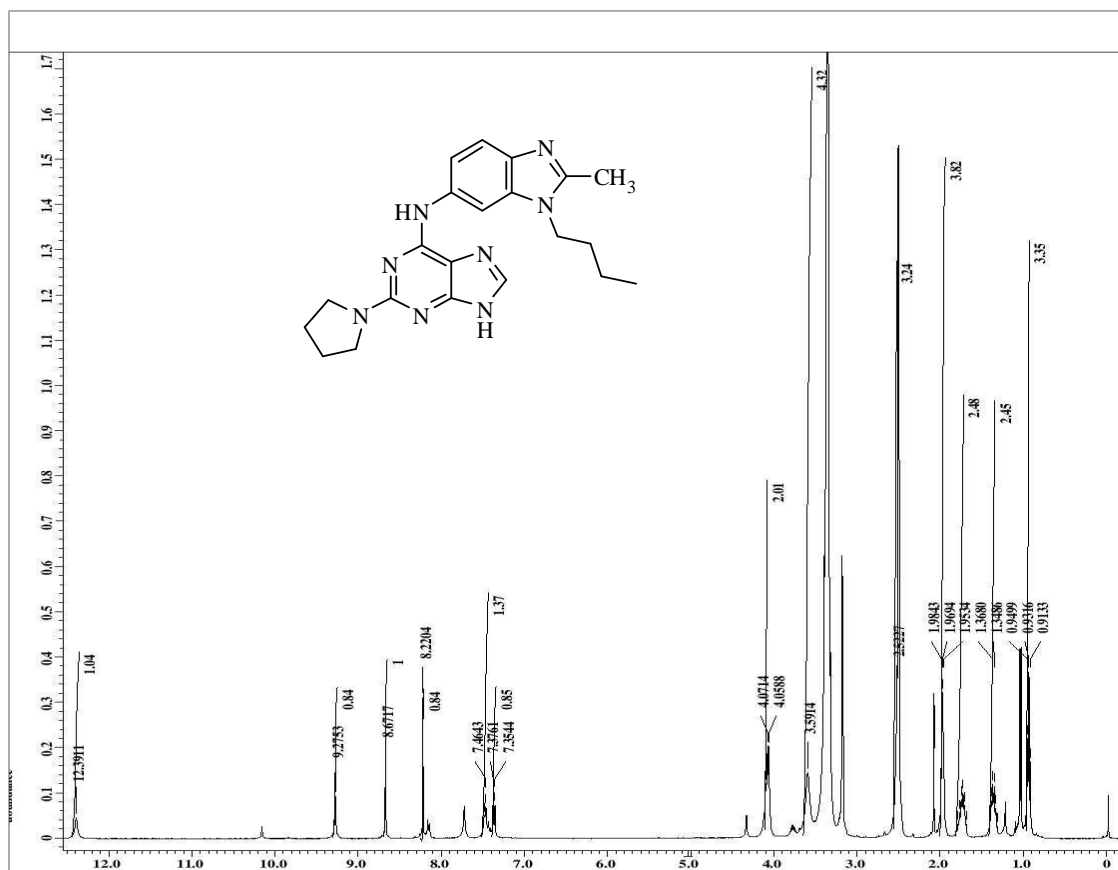


Figure S39. ¹H NMR spectrum of compound 18 in DMSO-*d*₆.

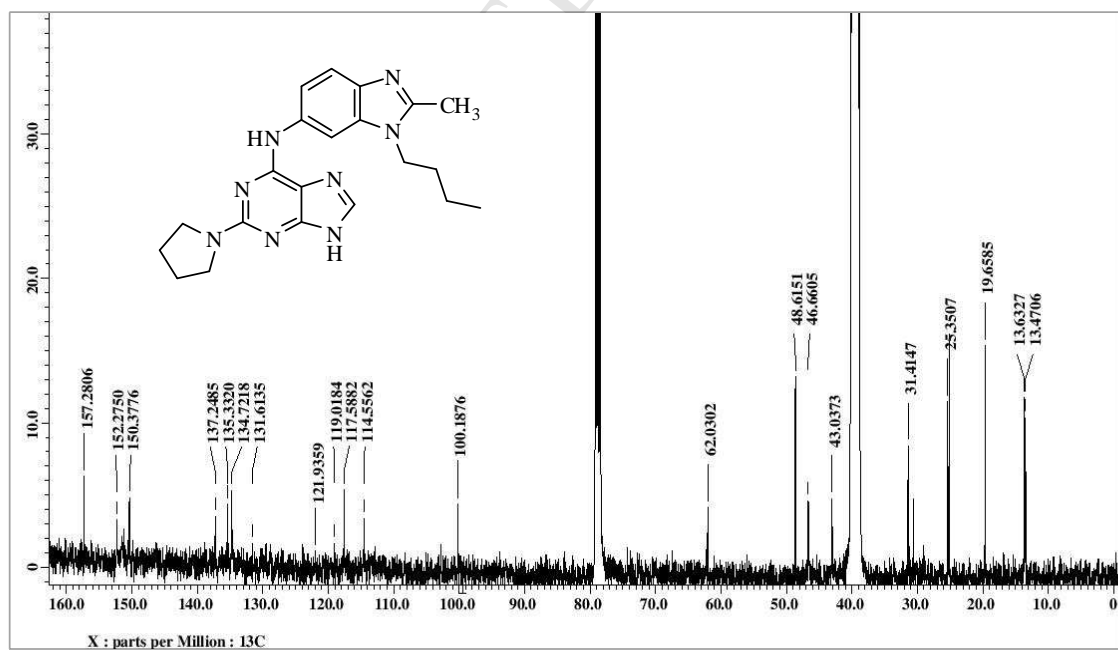


Figure S40. ¹³C NMR spectrum of compound 18 in DMSO-*d*₆.

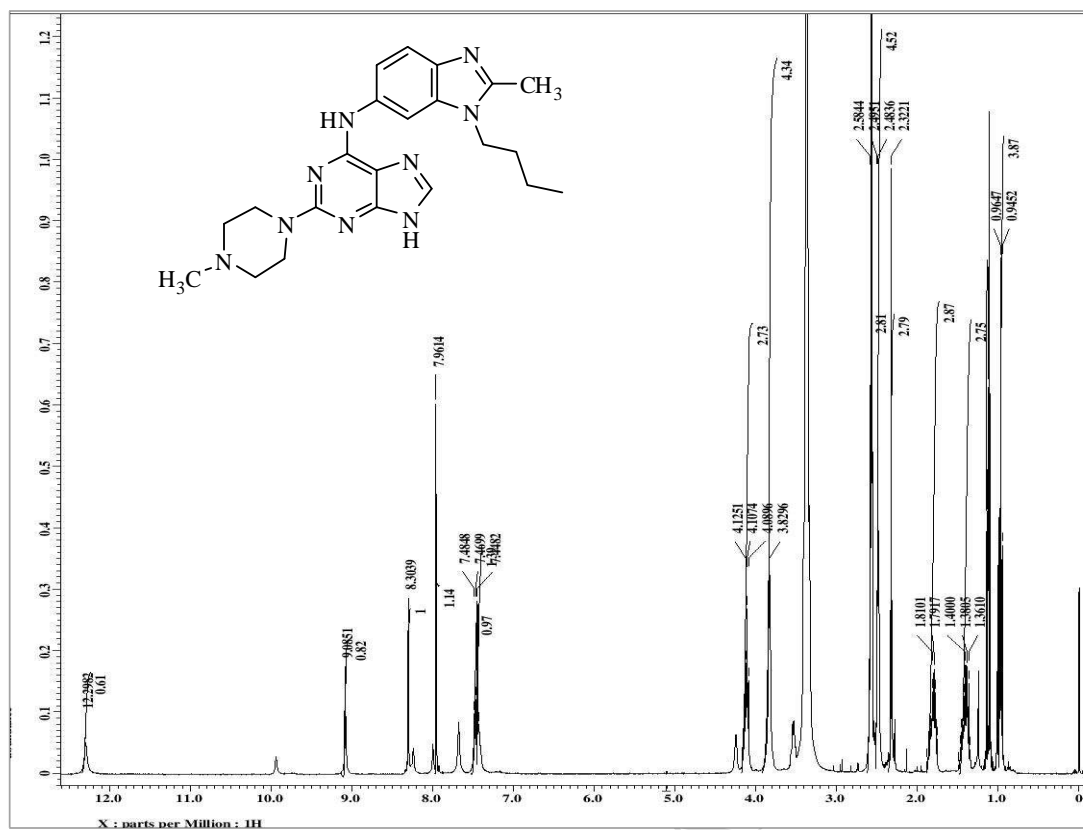


Figure S41. ¹H NMR spectrum of compound 19 in DMSO-*d*₆.

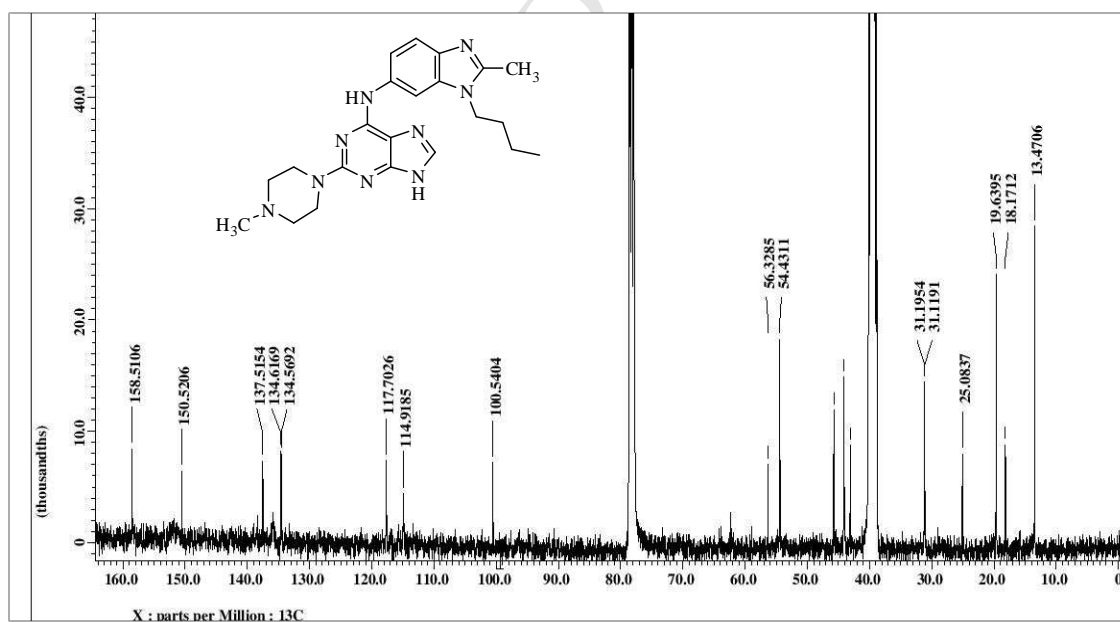


Figure S42. ¹³C NMR spectrum of compound 19 in DMSO-*d*₆.

Table S1 Percentage growth inhibition (GI%) of *in vitro* subpanel tumour cell lines at 10 μ M concentration of compounds **3a-d**, **4**, **6-11**, **16**, **18** and **19**

	3a	3b	3c	3d	4	6	7	8	9	10	11	16	18	19
Leukemia														
CCRF-CEM	-	21.97	-	47.02	-	-	-	30.34	53.43	-	-	50.66	-	-
HL-60(TB)	NT	NT	NT	NT	NT	NT	NT	-	21.58	NT	-	-	-	-
K-562	-	-	-	30.16	28.99	L	-	42.33	71.25	-	-	37.24	-	-
MOLT-4	-	35.99	-	62.09	25.57	-	-	30.68	90.95	-	-	45.85	-	-
RPMI-8226	-	34.63	-	56.32	-	70.09	-	37.88	59.66	21.39	-	47.17	-	-
SR	L	33.33	-	57.49	-	L	-	-	68.80	27.71	-	36.40	29.22	-
Non-Small Cell Lung Cancer														
A549/ATCC	-	-	-	-	-	53.68	-	-	51.55	-	-	22.58	-	-
EKVX	NT	NT	NT	NT	NT	NT	NT	-	47.46	NT	-	-	-	-
HOP-62	-	34.02	20.18	33.85	32.23	49.42	-	24.32	37.91	21.93	-	27.81	-	-
HOP-92	74.56	L	70.48	L	95.83	L	22.50	81.36	L	76.97	24.45	72.25	50.20	35.15
NCI-H226	-	24.96	-	37.58	-	41.13	-	28.20	55.57	-	-	43.41	28.95	-
NCI-H23	-	22.09	-	24.69	-	47.62	-	21.98	48.63	-	-	21.25	-	-
NCI-H322M	-	23.19	-	-	-	49.13	-	-	-	-	-	-	-	-
NCI-H460	-	-	-	29.08	-	99.63	-	-	34.46	-	-	-	-	-
NCI-H522	-	-	-	26.84	-	43.72	-	23.35	47.36	-	-	25.42	-	-
Colon Cancer														
COLO 205	-	-	-	-	-	26.58	-	-	71.08	-	-	20.45	-	-
HCC-2998	-	-	-	-	-	23.60	-	-	33.80	-	-	L	-	-
HCT-116	-	-	-	32.25	-	L	-	25.14	51.22	-	-	-	-	24.21
HCT-15	-	-	-	-	-	-	-	-	47.13	-	-	-	-	-
HT29	-	-	-	20.10	-	87.58	-	-	40.24	-	-	-	-	-
KM12	-	-	-	22.49	-	86.91	-	-	61.91	-	-	23.46	-	-
SW-620	-	-	-	21.42	-	59.17	-	-	21.00	-	-	-	-	-
CNS Cancer														
SF-268	-	-	-	23.96	-	70.69	-	26.38	39.58	-	-	30.84	-	26.76
SF-295	-	25.52	-	23.65	-	68.80	-	20.41	52.91	-	-	-	-	-
SF-539	-	23.73	-	20.14	-	L	-	-	28.82	-	-	-	-	-
SNB-19	-	-	-	-	-	55.06	-	-	26.75	-	-	-	-	-
SNB-75	-	21.64	-	37.21	-	L	-	67.69	88.56	-	-	46.88	28.36	36.53
U251	-	22.83	-	25.50	-	78.76	-	-	41.46	-	-	22.51	-	-
Melanoma														
LOX IMVI	-	-	-	-	-	44.20	-	44.20	66.30	-	-	34.86	-	-
MALME-3M	-	20.18	-	21.86	-	L	-	-	38.45	-	-	-	-	-
M14	-	-	-	31.66	-	71.21	-	-	67.16	-	-	-	-	-
MDA-MB-435	-	-	-	22.76	-	90.84	-	-	62.64	-	-	-	-	-
SK-MEL-28	-	-	-	-	-	69.75	-	-	23.99	-	-	-	-	-
SK-MEL-5	-	26.37	-	36.37	-	50.51	-	23.53	L	-	-	35.93	31.68	-
UACC-257	-	-	-	-	-	39.10	-	-	37.86	-	-	-	-	-

UACC-62	-	26.99	-	30.22	-	68.30	-	33.96	54.55	-	-	53.72	-	-
Ovarian Cancer														
IGROV1	-	29.29	-	31.76	27.15	44.20	-	52.86	70.00	-	-	-	-	-
OVCAR-3	-	-	-	37.31	-	L	-	27.08	62.30	-	-	23.24	-	-
OVCAR-4	-	21.09	-	31.65	-	L	-	-	80.98	-	-	29.23	-	-
OVCAR-5	-	-	-	25.50	25.87	69.4	-	25.97	49.85	-	-	-	-	-
OVCAR-8	-	-	-	21.80	-	25.26	-	38.60	70.00	-	-	50.47	-	-
NCI/ADR-RES	-	-	-	-	-	-	-	-	64.96	-	-	-	-	-
SK-OV-3	-	-	-	22.97	-	41.04	-	-	33.55	-	-	-	-	-
Renal Cancer														
786-0	-	23.64	-	44.61	36.94	L	-	28.37	50.87	-	-	27.68	-	-
A498	21.32	74.03	41.89	L	62.54	98.65	25.02	51.31	65.66	40.69	-	77.40	53.97	28.29
ACHN	-	-	-	21.01		82.19	-	45.91	63.17	-	-	21.42	-	-
CAKI-1	-	23.91	-	39.46		-	-	-	68.85	40.14	-	-	30.60	-
RXF 393	-	-	-	37.14		45.58	-	54.76	77.90	24.46	-	69.03	-	-
SN12C	-	21.08	-	25.40		63.21	-	28.97	50.44	-	-	28.00	-	-
TK-10	-	26.48	-	32.74		88.17	-	23.90	42.83	-	-	28.88	21.14	-
UO-31	-	35.43	21.76	42.24		38.76	-	51.53	71.94	32.52	-	63.63	44.13	-
Prostate Cancer														
PC-3	21.08	40.30	27.66	63.69	20.08	57.43	-	27.52	74.35	-	-	26.56	-	-
DU-145	-	-	-	-	-	51.75	-	22.05	39.83	-	-	24.32	-	-
Breast Cancer														
MCF7	-	24.59	-	23.50		26.45	-	-	67.53	-	-	-	-	-
MDA-MB-231/ATCC	20.88	25.00	33.88	35.15	22.28	L	-	26.93	60.75	26.78	-	34.49	-	-
HS 578T	-	47.32	34.75	93.87	42.68	L	-	33.98	56.25	-	-	31.72	-	-
BT-549	-	27.72	-	52.21	-	L	-	-	82.04	-	-	30.83	-	-
T-47D	-	60.70	21.94	66.07	24.63	54.96	-	48.08	93.22	-	-	55.08	41.88	-
MDA-MB-468	-	55.72	18.57	65.36	-	48.94	-	-	63.90	21.94	-	32.57	28.37	-

Prominent GI values are bolded.

- GI < 20%; L, compounds proved lethal to the cancer cell line; NT, not tested.

Table S2 Five dose assay of compound **6** (NSC 778814)

National Cancer Institute Developmental Therapeutics Program In-Vitro Testing Results															
NSC : 778814 / 1		Experiment ID : 1402NS30					Test Type : 08			Units : Molar					
Report Date : November 15, 2014		Test Date : February 18, 2014					QNS :			MC :					
COMI : AS-490 (136376)		Stain Reagent : SRB Dual-Pass Related					SSPL : 0YFW								
Panel/Cell Line	Time Zero	Log10 Concentration										GI50	TGI	LC50	
		Ctrl	-8.0	-7.0	-6.0	-5.0	-4.0	-8.0	-7.0	-6.0	-5.0				-4.0
Leukemia															
CCRF-CEM	0.364	1.789	1.781	1.717	1.662	1.551	0.907	99	95	91	83	38	5.45E-5	> 1.00E-4	> 1.00E-4
HL-60(TB)	0.610	1.779	1.773	1.849	1.980	1.951	1.931	99	106	117	115	113	> 1.00E-4	> 1.00E-4	> 1.00E-4
K-562	0.133	0.718	0.767	0.692	0.760	0.265	0.778	108	96	107	22	110	> 1.00E-4	> 1.00E-4	> 1.00E-4
MOLT-4	0.893	2.552	2.476	2.675	2.698	2.689	2.441	95	107	109	108	93	> 1.00E-4	> 1.00E-4	> 1.00E-4
RPMI-8226	0.676	2.060	2.103	2.117	2.167	1.658	2.007	103	104	108	71	96	> 1.00E-4	> 1.00E-4	> 1.00E-4
SR	0.273	0.887	0.867	0.867	0.900	0.328	0.767	97	97	102	9	80	> 1.00E-4	> 1.00E-4	> 1.00E-4
Non-Small Cell Lung Cancer															
A549/ATCC	0.450	1.836	1.884	1.881	1.787	0.880	1.934	103	103	96	31	107	> 1.00E-4	> 1.00E-4	> 1.00E-4
HOP-62	0.770	1.885	1.806	1.842	1.830	0.953	1.945	93	96	95	16	105	> 1.00E-4	> 1.00E-4	> 1.00E-4
HOP-92	1.093	1.705	1.650	1.660	1.497	1.414	1.593	91	93	66	52	82	> 1.00E-4	> 1.00E-4	> 1.00E-4
NCI-H226	0.854	1.563	1.512	1.517	1.411	1.485	1.588	93	93	78	89	103	> 1.00E-4	> 1.00E-4	> 1.00E-4
NCI-H23	0.556	1.697	1.635	1.658	1.719	1.165	1.832	95	97	102	53	112	> 1.00E-4	> 1.00E-4	> 1.00E-4
NCI-H322M	0.797	1.969	1.860	1.942	1.876	1.550	1.928	91	98	92	64	97	> 1.00E-4	> 1.00E-4	> 1.00E-4
NCI-H460	0.268	2.702	2.927	2.782	2.722	0.954	2.410	109	103	101	28	88	> 1.00E-4	> 1.00E-4	> 1.00E-4
NCI-H522	0.919	1.997	1.977	1.830	1.835	1.464	1.802	98	84	85	52	82	> 1.00E-4	> 1.00E-4	> 1.00E-4
Colon Cancer															
COLO 205	0.507	1.555	1.446	1.460	1.485	0.577	0.985	90	91	93	7	46	3.16E-6	> 1.00E-4	> 1.00E-4
HCC-2998	0.609	2.268	2.127	2.318	2.157	2.043	2.148	91	103	93	86	93	> 1.00E-4	> 1.00E-4	> 1.00E-4
HCT-116	0.237	1.508	1.568	1.403	1.420	0.290	1.222	105	92	93	4	77	> 1.00E-4	> 1.00E-4	> 1.00E-4
HCT-15	0.265	1.816	1.698	1.670	1.661	1.589	1.654	92	91	90	85	90	> 1.00E-4	> 1.00E-4	> 1.00E-4
HT29	0.212	1.282	1.323	1.253	1.198	0.424	1.165	104	97	92	20	89	> 1.00E-4	> 1.00E-4	> 1.00E-4
KM12	0.483	2.611	2.549	2.486	2.446	0.749	1.809	97	94	92	12	62	> 1.00E-4	> 1.00E-4	> 1.00E-4
SW-620	0.272	2.067	2.143	2.073	1.965	1.102	1.934	104	100	94	46	93	> 1.00E-4	> 1.00E-4	> 1.00E-4
CNS Cancer															
SF-268	0.543	1.896	1.874	1.808	1.803	0.883	1.730	98	93	93	25	88	> 1.00E-4	> 1.00E-4	> 1.00E-4
SF-295	0.850	3.016	2.930	2.801	2.882	2.293	3.116	96	90	94	67	105	> 1.00E-4	> 1.00E-4	> 1.00E-4
SF-539	0.924	2.627	2.613	2.429	2.635	1.083	2.575	99	88	100	9	97	> 1.00E-4	> 1.00E-4	> 1.00E-4
SNB-19	0.543	2.058	1.961	1.995	1.947	1.406	2.042	94	96	93	57	99	> 1.00E-4	> 1.00E-4	> 1.00E-4
SNB-75	0.696	1.315	1.269	1.179	1.186	0.616	0.980	93	78	79	-12	46	2.09E-6	> 1.00E-4	> 1.00E-4
U251	0.521	1.900	1.799	1.816	1.776	0.237	1.024	93	94	91	-55	36	1.91E-6	> 1.00E-4	> 1.00E-4
Melanoma															
LOX IMVI	0.229	1.756	1.706	1.678	1.746	1.472	1.957	97	95	99	81	113	> 1.00E-4	> 1.00E-4	> 1.00E-4
MALME-3M	0.571	1.163	1.136	1.157	1.232	0.639	1.220	95	99	112	11	110	> 1.00E-4	> 1.00E-4	> 1.00E-4
M14	0.441	1.302	1.272	1.191	1.161	0.995	0.734	96	87	84	64	34	2.96E-5	> 1.00E-4	> 1.00E-4
MDA-MB-435	0.452	2.131	2.129	1.991	2.104	1.115	2.107	100	92	98	39	99	> 1.00E-4	> 1.00E-4	> 1.00E-4
SK-MEL-2	1.184	2.399	2.379	2.315	2.411	2.381	2.483	98	93	101	98	107	> 1.00E-4	> 1.00E-4	> 1.00E-4
SK-MEL-28	0.605	1.827	1.818	1.769	1.754	1.033	1.947	99	95	94	35	110	> 1.00E-4	> 1.00E-4	> 1.00E-4
SK-MEL-5	0.842	2.935	2.861	2.825	2.780	2.361	2.548	96	95	93	73	81	> 1.00E-4	> 1.00E-4	> 1.00E-4
UACC-257	1.119	2.254	2.163	2.215	2.218	1.864	2.224	92	97	97	66	97	> 1.00E-4	> 1.00E-4	> 1.00E-4
UACC-62	0.838	2.714	2.694	2.734	2.505	2.271	2.674	99	101	89	76	98	> 1.00E-4	> 1.00E-4	> 1.00E-4
Ovarian Cancer															
IGROV1	0.641	2.223	2.166	2.150	2.151	1.874	1.973	96	95	95	78	84	> 1.00E-4	> 1.00E-4	> 1.00E-4
OVCAR-3	0.459	1.446	1.163	1.157	1.109	0.184	0.542	71	71	66	-60	8	1.34E-6	> 1.00E-4	> 1.00E-4
OVCAR-4	0.536	1.018	1.040	0.982	1.014	0.314	0.852	105	93	99	-41	66	> 1.00E-4	> 1.00E-4	> 1.00E-4
OVCAR-5	0.647	1.799	1.807	1.724	1.579	1.330	1.315	101	93	81	59	58	> 1.00E-4	> 1.00E-4	> 1.00E-4
OVCAR-8	0.612	2.289	2.294	2.329	2.328	1.004	2.249	100	102	102	23	98	> 1.00E-4	> 1.00E-4	> 1.00E-4
NCI/ADR-RES	0.643	2.095	2.050	2.072	2.123	2.067	2.383	97	98	102	98	120	> 1.00E-4	> 1.00E-4	> 1.00E-4
SK-OV-3	0.642	1.172	1.154	1.198	1.213	0.500	1.343	96	105	108	-22	132	> 1.00E-4	> 1.00E-4	> 1.00E-4
Renal Cancer															
786-0	0.602	1.750	1.762	1.701	1.759	0.546	1.981	101	96	101	-9	120	> 1.00E-4	> 1.00E-4	> 1.00E-4
A498	1.389	2.256	2.146	2.094	2.017	2.023	2.548	87	81	72	73	134	> 1.00E-4	> 1.00E-4	> 1.00E-4
ACHN	0.502	1.760	1.761	1.664	1.605	1.244	1.620	100	92	88	59	89	> 1.00E-4	> 1.00E-4	> 1.00E-4
CAKI-1	0.609	1.601	1.570	1.475	1.474	1.476	1.470	97	87	87	87	87	> 1.00E-4	> 1.00E-4	> 1.00E-4
RXF 393	0.786	1.345	1.310	1.339	1.274	1.121	1.609	94	99	87	60	147	> 1.00E-4	> 1.00E-4	> 1.00E-4
SN12C	0.861	2.729	2.628	2.686	2.539	1.766	2.707	95	98	90	48	99	> 1.00E-4	> 1.00E-4	> 1.00E-4
TK-10	0.870	1.989	1.983	1.966	1.930	1.088	1.763	99	98	95	19	80	> 1.00E-4	> 1.00E-4	> 1.00E-4
UO-31	0.884	2.775	2.617	2.601	2.574	2.601	2.767	92	91	89	91	100	> 1.00E-4	> 1.00E-4	> 1.00E-4
Prostate Cancer															
PC-3	0.565	2.354	2.278	2.293	2.249	2.098	2.392	96	97	94	86	102	> 1.00E-4	> 1.00E-4	> 1.00E-4
DU-145	0.409	1.766	1.828	1.772	1.854	1.148	1.463	105	100	106	54	78	> 1.00E-4	> 1.00E-4	> 1.00E-4
Breast Cancer															
MCF7	0.429	2.354	2.181	2.084	2.116	1.280	2.049	91	86	88	44	84	> 1.00E-4	> 1.00E-4	> 1.00E-4
HS 578T	0.885	1.849	1.895	1.882	1.824	1.346	1.852	105	103	97	48	100	> 1.00E-4	> 1.00E-4	> 1.00E-4
BT-549	0.934	1.644	1.565	1.539	1.596	0.978	1.425	89	85	93	6	69	> 1.00E-4	> 1.00E-4	> 1.00E-4
MDA-MB-468	0.773	1.643	1.566	1.673	1.541	1.316	1.686	91	103	88	62	105	> 1.00E-4	> 1.00E-4	> 1.00E-4

Procedure for Aurora-A kinase assay

The Aurora-A kinase Assay/Inhibitor Screening Kit was a single-site, non-quantitative immunoassay for Aurora-A activity. Plates were pre-coated with a substrate corresponding to recombinant Lats2, which contains serine83 residues that can be phosphorylated by Aurora-A. First of all, remove the appropriate number of microtiter 96 wells from the foil pouch and

place them into the well holder. The stock solutions of the entire compounds were prepared in dimethylsulfoxide (spectroscopy grade) at concentration of 10^{-3} M. Addition of 30 μL of compound into a substrate coated plate. Begin the kinase reaction by addition of 80 μL kinase reaction buffer per well, cover with plate sealer or lid, and incubate at 30°C for 30-60 minutes. Wash wells five times with wash buffer making sure each well is filled completely. Remove residual wash buffer by gentle tapping or aspiration. Pipette 100 μL of Anti-Phospho-Lats2-S83 Monoclonal Antibody ST-3B11 into each well, cover with plate sealer or lid, and incubate at room temperature for 1 h. Wash wells five times with wash buffer making sure each well is filled completely. Then pipette 100 μL of HRP-conjugated Anti-mouse IgG into each well, cover with plate sealer or lid, and incubate at room temperature for 1 h. Discard any unused conjugate after use. Wash wells five times with wash buffer making sure each well is filled completely. Add 100 μL of substrate reagent to each well and incubate at room temperature for 5–15 minutes. At last added 100 μL of Stop Solution to each well in the same order as the previously added substrate reagent. Measure absorbance in each well using a spectrophotometric plate reader at wavelengths of 450 nm. Wells must be read within 30 minutes of adding the Stop Solution.

Shake-flask method:

Partition coefficient for the target compounds were determined at room temperature using n-octanol–phosphate buffer (0.15 M, pH = 7.4). The experiments were performed in the system phosphate buffer : n-octanol at different volumes (10: 1, 50: 1). The stock solutions of the entire compounds were prepared in dimethylsulfoxide (spectroscopy grade) at concentration of 5×10^{-4} M. All solutions were pipette into glass vials; phosphate buffer and stock solution (125 μL , 250 μL) were added with a micropipette. The wavelength chosen according to the λ_{max} of the compounds i.e., 225, 226, 227, 229, 307, 309, 310, 311, 315, 316, 317, 318, 335 and 336 for **3a-d**, **4-19** respectively. Initial absorbance (A_i) of stock solution in the buffer phase was recorded for each compound. Followed this, n-Octanol was added into each vial. The phases were shaken together on a mechanical shaker (METREX, Cat No. MRS-50H) for 45 minutes, centrifuged (REMI R-24) at 2500 rpm for 30 min to afford complete phase separation, and n-octanol phase was removed. Absorbance of the buffer phase was measured spectrophotometrically using a CHAMPION UV-500 spectrophotometer.

P values were calculated from the following equation:-

$$P = \frac{A_i - A_f}{A_f} \times \frac{V_w}{V_o}$$

Where A_i and A_f represent the absorbance of compounds in the aqueous phase before and after partitioning, respectively. V_w and V_o represent the volume of the aqueous and organic phases used in the octanol/buffer system.

Single X-ray crystal for compound 19:

The structure of compound **19** was confirmed by measuring X-ray crystallography (Figure 2). In the crystal structure of the compound, it crystallizes with $Z = 4$ in the space group $P2_1/c$ (Table S3). The six-membered 4-methylpiperazine ring is positioned planar to the purine ring that exists in chair conformation. Atom system C13-N1-C2 is in regular tetrahedron sp^3 angle of 109.5° . Atom system C3-N2-C14 having some angle strain, deviated by 2.7° from the ideal value (angle strain is calculated as the difference between internal angle and the ideal sp^3 angle of 109.5°).

The benzimidazole ring C7-C6-N4 is deviated from the planar purine ring N4-C5-C15 by 2.2° . The bond lengths of two C-N bonds linking between benzimidazole and purine are differ, with the short N4-C5 [$1.364(4) \text{ \AA}$] bond having a double-bond character compared with the longer N4-C6 [$1.401(4) \text{ \AA}$] on benzimidazole side. It is indicated that the two carbon atoms (C5 and C6) in the molecule occupy anti-positions relative to the mean plane of the ring system. This anti-position of both carbon atoms in each molecule is one of the reason which makes the two rings are non planar. The bond length of N9-C21 [$1.337(5)$] of benzimidazole ring is shorter having double bond character than that longer bond length of C21-N5 [$1.365(4)$] indicate the presence of butyl group at N5 position. Comparing the bond distances of N6-C16 ($1.307(4) \text{ \AA}$) and N7-C16 ($1.372(4) \text{ \AA}$) of five membered purine ring, it has been clear that former has double bond character than later.

Table S3. Summary of crystal data, data collection and structure refinement for compound **19**

A. Crystal data		
Chemical formula	$C_{22}H_{29}N_9, H_2O$	
Formula weight	437.56	
Temperature	296(2) K	
Wavelength	0.71073 \AA	
Crystal habit	Colourless	
Crystal system	Monoclinic	
Space group	$P 2_1/c$	
Unit cell dimensions	$a = 8.6730(9) \text{ \AA}$	$\alpha = 90^\circ$
	$b = 12.6408(14) \text{ \AA}$	$\beta = 101.007(6)^\circ$
	$c = 21.721(3) \text{ \AA}$	$\gamma = 90^\circ$

Volume	2337.5(4) Å ³
Z	4
Density (calculated)	1.243 Mg/cm ³
Absorption coefficient	0.082 mm ⁻¹
F(000)	936
B. Data collection and structure refinement	
Theta range for data collection	1.87 to 25.05°
Index ranges	-10<=h<=10, -15<=k<=14, 25<=l<=25
Reflections collected	11271
Independent reflections	3545 [R(int) = 0.0897]
Coverage of independent reflections	
Absorption correction	Multi-scan
Structure solution technique	Direct methods
Structure solution program	SHELXS-97 (Sheldrick, 2008)
Refinement method	Full-matrix least-squares on F ²
Function minimized	Σ w(F _o ² - F _c ²) ²
Data / restraints / parameters	3545 / 0 / 301
Goodness-of-fit on F²	0.820
Δ/σ_{max}	0.001
Final R indices	1511 data; I > 2σ(I) R1 = 0.0668, wR2 = 0.1396 R1 = 0.1473, wR2 = 0.1643
Weighting scheme	w=1/[σ ² (F _o ²)+(0.0623P) ² +0.0000P] where P=(F _o ² +2F _c ²)/3
Extinction coefficient	0.0043(7)
Largest diff. peak and hole	0.279 and -0.306 eÅ ⁻³
R.M.S. deviation from mean	0.104 eÅ ⁻³

Table S4. Atomic coordinates and equivalent isotropic atomic displacement parameters (Å²) for SCE35

U(eq) is defined as one third of the trace of the orthogonalized U_{ij} tensor.

	x/a	y/b	z/c	U(eq)
O1S	0.5751(4)	0.1991(3)	0.26666(14)	0.0600(8)
N1	0.8696(4)	0.3027(2)	0.84819(14)	0.0583(9)
N2	0.8318(4)	0.3205(2)	0.97567(13)	0.0486(8)
N3	0.7543(4)	0.2428(2)	0.06185(13)	0.0457(8)
N4	0.6833(4)	0.15923(19)	0.14860(13)	0.0460(8)

	x/a	y/b	z/c	U(eq)
N5	0.6827(4)	0.8519(2)	0.00656(12)	0.0463(8)
N6	0.6253(4)	0.3825(2)	0.19411(13)	0.0534(8)
N7	0.6662(4)	0.5218(2)	0.13517(13)	0.0531(9)
N8	0.7572(4)	0.4318(2)	0.05005(14)	0.0524(8)
N9	0.6559(4)	0.7346(2)	0.08125(15)	0.0526(8)
C1	0.9624(6)	0.2905(4)	0.79959(19)	0.0757(13)
C2	0.8877(5)	0.2112(3)	0.88997(18)	0.0619(11)
C3	0.7891(5)	0.2230(3)	0.94034(18)	0.0579(11)
C4	0.7759(5)	0.3331(3)	0.03225(17)	0.0482(9)
C5	0.7077(4)	0.2494(2)	0.11736(16)	0.0411(9)
C6	0.6816(4)	0.0526(2)	0.13082(15)	0.0411(9)
C7	0.6910(4)	0.0186(2)	0.07068(15)	0.0425(9)
C8	0.6808(4)	0.9113(3)	0.05998(15)	0.0419(9)
C9	0.6980(4)	0.8921(3)	0.94502(15)	0.0505(10)
C10	0.8639(5)	0.8916(4)	0.93289(18)	0.0660(12)
C11	0.8691(6)	0.8995(4)	0.8624(2)	0.0912(16)
C12	0.8247(8)	0.7954(5)	0.8294(2)	0.124(2)
C13	0.9174(6)	0.3968(3)	0.88522(18)	0.0671(12)
C14	0.8213(6)	0.4136(3)	0.93472(17)	0.0682(12)
C15	0.6846(4)	0.3491(2)	0.14132(15)	0.0428(9)
C16	0.6168(5)	0.4853(3)	0.18764(17)	0.0569(11)
C17	0.7070(4)	0.4340(3)	0.10557(16)	0.0472(9)
C18	0.6641(5)	0.9783(3)	0.17706(16)	0.0484(9)
C19	0.6548(5)	0.8734(3)	0.16577(17)	0.0541(10)
C20	0.6618(4)	0.8367(2)	0.10602(17)	0.0454(9)
C21	0.6699(4)	0.7478(3)	0.02151(18)	0.0497(10)
C22	0.6702(5)	0.6614(3)	0.97656(18)	0.0642(12)

Table S5. Bond lengths (Å) for SCE35.

O1S-H5C	0.90(4)	O1S-H4C	0.91(4)
N1-C13	1.451(5)	N1-C1	1.453(5)
N1-C2	1.460(5)	N2-C4	1.414(5)
N2-C3	1.461(4)	N2-C14	1.468(4)
N3-C4	1.341(4)	N3-C5	1.345(4)
N4-C5	1.364(4)	N4-C6	1.401(4)
N4-H4	0.86	N5-C21	1.365(4)
N5-C8	1.385(4)	N5-C9	1.460(4)
N6-C16	1.307(4)	N6-C15	1.408(4)
N7-C17	1.363(4)	N7-C16	1.372(4)
N7-H7	0.86	N8-C4	1.325(4)
N8-C17	1.358(4)	N9-C21	1.337(5)
N9-C20	1.395(4)	C1-H1A	0.96
C1-H1B	0.96	C1-H1C	0.96
C2-C3	1.519(5)	C2-H2A	0.97
C2-H2B	0.97	C3-H3A	0.97
C3-H3B	0.97	C5-C15	1.393(4)
C6-C7	1.393(4)	C6-C18	1.404(4)
C7-C8	1.376(4)	C7-H7A	0.93
C8-C20	1.407(4)	C9-C10	1.511(6)
C9-H9A	0.97	C9-H9B	0.97
C10-C11	1.543(5)	C10-H10A	0.97
C10-H10B	0.97	C11-C12	1.513(7)
C11-H11A	0.97	C11-H11B	0.97
C12-H12A	0.96	C12-H12B	0.96
C12-H12C	0.96	C13-C14	1.496(6)
C13-H13A	0.97	C13-H13B	0.97
C14-H14A	0.97	C14-H14B	0.97

C15-C17	1.360(5)	C16-H16	0.93
C18-C19	1.348(5)	C18-H18	0.93
C19-C20	1.391(5)	C19-H19	0.93
C21-C22	1.465(5)	C22-H22A	0.96
C22-H22B	0.96	C22-H22C	0.96

Table S6. Bond angles (°) for SCE35.

H5C-O1S-H4C	97.(4)	C13-N1-C1	110.5(3)
C13-N1-C2	108.6(3)	C1-N1-C2	111.1(3)
C4-N2-C3	117.2(3)	C4-N2-C14	116.4(3)
C3-N2-C14	112.2(3)	C4-N3-C5	118.0(3)
C5-N4-C6	131.4(3)	C5-N4-H4	114.3
C6-N4-H4	114.3	C21-N5-C8	108.0(3)
C21-N5-C9	125.4(3)	C8-N5-C9	126.6(3)
C16-N6-C15	103.4(3)	C17-N7-C16	105.6(3)
C17-N7-H7	127.2	C16-N7-H7	127.2
C4-N8-C17	110.9(3)	C21-N9-C20	104.8(3)
N1-C1-H1A	109.5	N1-C1-H1B	109.5
H1A-C1-H1B	109.5	N1-C1-H1C	109.5
H1A-C1-H1C	109.5	H1B-C1-H1C	109.5
N1-C2-C3	111.2(3)	N1-C2-H2A	109.4
C3-C2-H2A	109.4	N1-C2-H2B	109.4
C3-C2-H2B	109.4	H2A-C2-H2B	108.0
N2-C3-C2	109.8(3)	N2-C3-H3A	109.7
C2-C3-H3A	109.7	N2-C3-H3B	109.7
C2-C3-H3B	109.7	H3A-C3-H3B	108.2
N8-C4-N3	128.7(3)	N8-C4-N2	116.2(3)
N3-C4-N2	115.0(3)	N3-C5-N4	119.7(3)
N3-C5-C15	118.7(3)	N4-C5-C15	121.6(3)

C7-C6-N4	123.8(3)	C7-C6-C18	119.9(3)
N4-C6-C18	116.3(3)	C8-C7-C6	116.7(3)
C8-C7-H7A	121.6	C6-C7-H7A	121.6
C7-C8-N5	131.7(3)	C7-C8-C20	123.6(3)
N5-C8-C20	104.7(3)	N5-C9-C10	114.4(3)
N5-C9-H9A	108.6	C10-C9-H9A	108.6
N5-C9-H9B	108.6	C10-C9-H9B	108.6
H9A-C9-H9B	107.6	C9-C10-C11	112.5(4)
C9-C10-H10A	109.1	C11-C10-H10A	109.1
C9-C10-H10B	109.1	C11-C10-H10B	109.1
H10A-C10-H10B	107.8	C12-C11-C10	111.2(4)
C12-C11-H11A	109.4	C10-C11-H11A	109.4
C12-C11-H11B	109.4	C10-C11-H11B	109.4
H11A-C11-H11B	108.0	C11-C12-H12A	109.5
C11-C12-H12B	109.5	H12A-C12-H12B	109.5
C11-C12-H12C	109.5	H12A-C12-H12C	109.5
H12B-C12-H12C	109.5	N1-C13-C14	112.1(4)
N1-C13-H13A	109.2	C14-C13-H13A	109.2
N1-C13-H13B	109.2	C14-C13-H13B	109.2
H13A-C13-H13B	107.9	N2-C14-C13	110.0(3)
N2-C14-H14A	109.7	C13-C14-H14A	109.7
N2-C14-H14B	109.7	C13-C14-H14B	109.7
H14A-C14-H14B	108.2	C17-C15-C5	117.0(3)
C17-C15-N6	110.0(3)	C5-C15-N6	132.6(3)
N6-C16-N7	113.8(3)	N6-C16-H16	123.1
N7-C16-H16	123.1	N8-C17-C15	126.6(3)
N8-C17-N7	126.3(3)	C15-C17-N7	107.1(3)
C19-C18-C6	122.6(3)	C19-C18-H18	118.7
C6-C18-H18	118.7	C18-C19-C20	119.1(3)

C18-C19-H19	120.4	C20-C19-H19	120.4
C19-C20-N9	131.6(3)	C19-C20-C8	118.1(3)
N9-C20-C8	110.2(3)	N9-C21-N5	112.2(3)
N9-C21-C22	124.5(3)	N5-C21-C22	123.3(4)
C21-C22-H22A	109.5	C21-C22-H22B	109.5
H22A-C22-H22B	109.5	C21-C22-H22C	109.5
H22A-C22-H22C	109.5	H22B-C22-H22C	109.5

Table S7. Anisotropic atomic displacement parameters (\AA^2) for SCE35.

The anisotropic atomic displacement factor exponent takes the form: $-2\pi^2 [h^2 a^{*2} U_{11} + \dots + 2 h k a^* b^* U_{12}]$

	U_{11}	U_{22}	U_{33}	U_{23}	U_{13}	U_{12}
O1S	0.071(2)	0.065(2)	0.0477(18)	-	0.0201(17)	-
				0.0006(15)		0.0014(16)
N1	0.070(2)	0.065(2)	0.0439(19)	0.0005(16)	0.0216(17)	0.0039(17)
N2	0.088(2)	0.0290(16)	0.0364(16)	-	0.0305(17)	-
				0.0003(12)		0.0008(14)
N3	0.062(2)	0.0390(17)	0.0421(17)	-	0.0247(16)	0.0012(14)
				0.0005(14)		
N4	0.070(2)	0.0373(17)	0.0360(16)	-	0.0229(15)	0.0009(14)
				0.0012(13)		
N5	0.057(2)	0.0432(18)	0.0408(17)	-	0.0143(15)	0.0024(14)
				0.0040(14)		
N6	0.076(2)	0.0435(19)	0.0482(19)	-	0.0296(17)	0.0024(15)
				0.0045(14)		
N7	0.077(2)	0.0338(16)	0.058(2)	-	0.0343(18)	-
				0.0023(14)		0.0008(15)
N8	0.076(2)	0.0371(17)	0.053(2)	-	0.0325(17)	-
				0.0002(14)		0.0020(15)
N9	0.063(2)	0.0350(17)	0.063(2)	-	0.0206(18)	-

	U_{11}	U_{22}	U_{33}	U_{23}	U_{13}	U_{12}
				0.0016(15)		0.0015(14)
C1	0.079(3)	0.104(4)	0.051(3)	0.002(2)	0.030(2)	0.006(3)
C2	0.078(3)	0.058(2)	0.054(3)	-0.003(2)	0.022(2)	0.007(2)
C3	0.072(3)	0.056(2)	0.052(2)	- 0.0012(18)	0.028(2)	-0.002(2)
C4	0.064(3)	0.032(2)	0.053(2)	- 0.0007(17)	0.022(2)	- 0.0019(17)
C5	0.050(2)	0.0324(19)	0.043(2)	0.0029(16)	0.0149(18)	0.0005(16)
C6	0.047(2)	0.0362(19)	0.043(2)	0.0036(16)	0.0167(18)	0.0019(15)
C7	0.057(2)	0.0350(19)	0.040(2)	0.0021(15)	0.0230(18)	0.0012(16)
C8	0.049(2)	0.041(2)	0.040(2)	0.0003(16)	0.0199(17)	0.0016(16)
C9	0.062(3)	0.055(2)	0.036(2)	- 0.0006(17)	0.013(2)	0.0023(19)
C10	0.061(3)	0.090(3)	0.050(2)	-0.008(2)	0.019(2)	-0.006(2)
C11	0.077(4)	0.140(5)	0.063(3)	-0.008(3)	0.032(3)	-0.011(3)
C12	0.123(5)	0.179(6)	0.079(4)	-0.058(4)	0.047(4)	-0.026(4)
C13	0.088(3)	0.062(3)	0.058(3)	0.002(2)	0.030(3)	-0.009(2)
C14	0.101(4)	0.052(2)	0.059(3)	0.003(2)	0.034(3)	0.000(2)
C15	0.055(2)	0.0353(19)	0.040(2)	0.0000(16)	0.0164(18)	0.0001(16)
C16	0.079(3)	0.048(2)	0.052(2)	- 0.0068(19)	0.032(2)	0.001(2)
C17	0.060(2)	0.035(2)	0.049(2)	- 0.0049(17)	0.018(2)	0.0000(17)
C18	0.067(3)	0.043(2)	0.041(2)	0.0028(17)	0.0257(19)	- 0.0004(18)
C19	0.073(3)	0.044(2)	0.053(2)	0.0098(18)	0.031(2)	0.0044(19)
C20	0.054(2)	0.0323(19)	0.054(2)	0.0058(17)	0.0207(19)	0.0020(16)
C21	0.055(2)	0.039(2)	0.056(3)	- 0.0043(18)	0.015(2)	0.0009(17)

	U_{11}	U_{22}	U_{33}	U_{23}	U_{13}	U_{12}
C22	0.083(3)	0.045(2)	0.062(3)	- 0.0086(19)	0.006(2)	0.004(2)

Table S8. Hydrogen atomic coordinates and isotropic atomic displacement parameters (\AA^2) for SCE35.

	x/a	y/b	z/c	$U(\text{eq})$
H4	0.6659	0.1696	1.1858	0.055
H7	0.6706	0.5865	1.1234	0.064
H1A	0.9450	0.3501	0.7717	0.114
H1B	0.9318	0.2268	0.7765	0.114
H1C	1.0717	0.2867	0.8185	0.114
H2A	0.9973	0.2036	0.9096	0.074
H2B	0.8560	0.1478	0.8657	0.074
H3A	0.6786	0.2249	0.9211	0.069
H3B	0.8063	0.1628	0.9685	0.069
H7A	0.7037	0.0660	1.0393	0.051
H9A	0.6584	-0.0359	0.9409	0.061
H9B	0.6325	-0.1502	0.9131	0.061
H10A	0.9158	-0.1731	0.9496	0.079
H10B	0.9213	-0.0494	0.9548	0.079
H11A	0.7972	-0.0458	0.8433	0.109
H11B	0.9741	-0.0806	0.8575	0.109
H12A	0.9052	-0.2560	0.8435	0.185
H12B	0.8140	-0.1949	0.7849	0.185
H12C	0.7269	-0.2289	0.8387	0.185
H13A	0.9068	0.4579	0.8578	0.08
H13B	1.0271	0.3904	0.9049	0.08
H14A	0.8592	0.4755	0.9594	0.082

	x/a	y/b	z/c	U(eq)
H14B	0.7126	0.4259	0.9152	0.082
H16	0.5805	0.5296	1.2160	0.068
H18	0.6587	0.0025	1.2170	0.058
H19	0.6439	-0.1737	1.1975	0.065
H22A	0.6433	-0.4037	0.9947	0.096
H22B	0.7727	-0.3448	0.9664	0.096
H22C	0.5946	-0.3239	0.9391	0.096
H5C	0.576(5)	0.268(4)	0.2577(19)	0.077(15)
H4C	0.663(5)	0.199(3)	0.297(2)	0.071(15)

Molecular Modelling (Docking):

Coordinates from the X-ray crystal structure of Aurora-A enzyme (PDB ID 2WTV and PDB ID 2XNE) were taken from the RCSB Protein Data Bank. Compounds were constructed with the builder toolkit of the software package ArgusLab 4.0.1 (www.arguslab.com) and energy minimized using the semiempirical quantum mechanical method PM3. The monomeric structure of the enzyme was chosen, and the active site was defined around the ligand. The molecule to be docked in the enzyme active site was inserted into the work space carrying the structure of the enzyme. The docking program implements an efficient grid-based docking algorithm, which approximates an exhaustive search within the free volume of the binding site cavity. The conformational space was surveyed by the geometry optimization of the flexible ligand (rings are treated as rigid) in combination with the incremental construction of the ligand torsions. Thus, docking occurred between the flexible ligand parts of the compound and enzyme. The ligand orientation was determined by a shape scoring function based on Ascore and the final positions were ranked by lowest interaction energy values. Hydrogen bond and hydrophobic interactions between the compound and enzyme were explored by distance measurements.